NUREG/CR-4165
EGG-2379
May 1987

Severe Accident Sequence Analysis Program—Anticipated Transient Without Scram Simulations for Browns Ferry Nuclear Plant Unit 1

R. Jack Dallman
Richard C. Gottula
Edward E. Holcomb
Wayne C. Jouse
Steve R. Wagoner
Philip D. Wheatley

F O R M A L R E P O R T

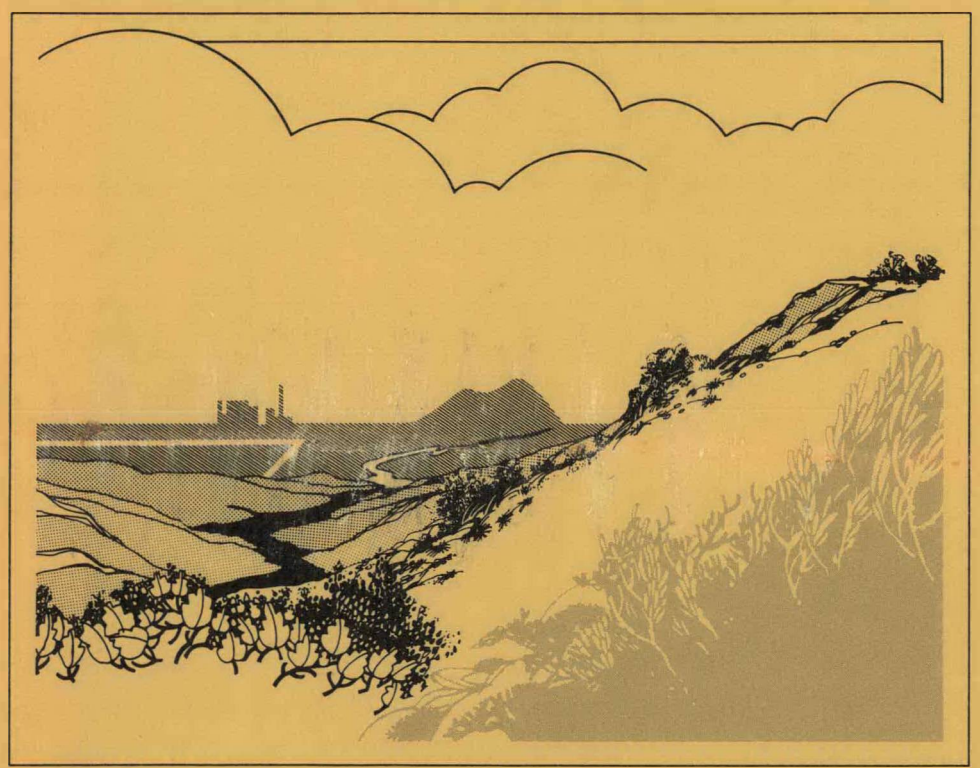

EG&G Idaho

Work performed under DOE Contract No. DE-AC07-76ID01570 for the ***U.S. Nuclear Regulatory Commission***

Idaho National Engineering Laboratory

Managed by the U.S. Department of Energy

Available from

Superintendent of Documents
U.S. Government Printing Office
Post Office Box 37082
Washington, D.C. 20013-7982

and

National Technical Information Service
Springfield, VA 22161

NUREG/CR-4165
EGG-2379
Distribution Category: R1

NUREG/CR--4165

TI87 010676

SEVERE ACCIDENT SEQUENCE ANALYSIS PROGRAM—ANTICIPATED TRANSIENT WITHOUT SCRAM SIMULATIONS FOR BROWNS FERRY NUCLEAR PLANT UNIT 1

R. Jack Dallman
Richard C. Gottula
Edward E. Holcomb
Wayne C. Jouse
Steve R. Wagoner
Philip D. Wheatley

Published May 1987

EG&G Idaho, Inc.
Idaho Falls, Idaho 83415

Prepared for the
Division of Reactor Accident Analysis
Office of Nuclear Regulatory Research
U.S. Nuclear Regulatory Commission
Washington, D.C. 20555
Under DOE Contract No. DE-AC07-76IDO1570
FIN No. A6354

ABSTRACT

An analysis of five anticipated transients without scram (ATWS) was conducted at the Idaho National Engineering Laboratory (INEL). The five detailed deterministic simulations of postulated ATWS sequences were initiated from a main steamline isolation valve (MSIV) closure. The subject of the analysis was the Browns Ferry Nuclear Plant Unit 1, a boiling water reactor (BWR) of the BWR/4 product line with a Mark I containment. The simulations yielded insights to the possible consequences resulting from a MSIV closure ATWS. An evaluation of the effects of plant safety systems and operator actions on accident progression and mitigation is presented.

EXECUTIVE SUMMARY

Under the auspices of the U.S. Nuclear Regulatory Commission (NRC), simulations of anticipated transients without scram (ATWS) were performed at the Idaho National Engineering Laboratory (INEL). The Browns Ferry Nuclear Plant Unit 1 (BFNP1) was selected as the specific subject of this work because of the cooperation of the Tennessee Valley Authority (TVA). Also, a probabilistic risk assessment (PRA) was available for BFNP1. BFNP1 is a boiling water reactor (BWR) representative of the BWR/4 product line with a Mark I containment. This work is part of a cooperative effort coordinated by the NRC's Severe Accident Sequence Analysis (SASA) Program. Work performed at the Oak Ridge National Laboratory (ORNL) and Brookhaven National Laboratory (BNL) is also part of the BWR SASA effort on ATWS.

Several objectives were identified in the present ATWS study. These include establishing the methodology for and performing comprehensive deterministic analyses of the postulated accident, determining accident event progression, and evaluating the effects of plant safety systems and operator actions on accident progression. An additional objective of the study was to define requirements for improved analytical methods or for experiments to resolve uncertainties. Proposed Emergency Procedure Guidelines (EPGs) were used as a basis for modeling operator actions. The ATWS simulations performed for this study thus served as a partial evaluation of the EPGs.

Probabilistic analyses have asserted that the ATWS at BFNP1 (and other BWRs) is included in a group of dominant transients relative to core damage frequency. Although low in probability, ATWS accidents are of concern because they could lead to core damage and fission product release to the environment. The transients analyzed were initiated with a main steamline isolation valve (MSIV) closure followed by a complete failure to scram. In all cases it was assumed that the recirculation pumps tripped automatically. This scenario results in the most severe duty to the containment because the main condenser is unavailable to condense vessel steam. Steam produced in the vessel is discharged to the pressure suppression pool (PSP), creating a threat to the containment unless reactor power can be reduced to decay heat levels. The simulations are limited to the response of the reactor pressure vessel (RPV) and primary containment (PSP and drywell). RELAP5/MOD1.6 was used to model the RPV and associated recirculation loops and plant systems. CONTEMPT/LT-028 was used to model the primary containment. An iterative approach was used to exchange information between the two codes. Fuel damage was analyzed using the FRAP-T6 and SCDAP computer codes. The fuel damage analysis included zircaloy oxidation and fission product release. However, it did not consider vessel melting or the transport of fission products outside of the RPV.

A probabilistic approach was first undertaken to isolate significant phenomena, events, and system interactions. A sequence event tree (SET) was developed, which formulated the relative frequency of occurrence of sequences and the expected consequences. Analysis of the SET revealed that even though sequence event timing can show variations, the transient signatures are limited and distinct. A plant automatic simulation (no operator actions) was chosen to illustrate the accident event progression. This simulation would also serve as a base case from which to determine the effects of certain operator actions. It was observed from the plant automatic simulation that mitigative operator actions are required to prevent containment failure and severe fuel damage. Primary containment failure was predicted from static overpressurization 45 min after transient initiation.

Four other simulations were performed that modeled various combinations of operator actions and assumed effectiveness of the standby liquid control system (SLCS). Each simulation modeled an operator action called level control, whereby the operator is instructed to lower downcomer water level to the top of the active fuel (TAF). Several conclusions resulted from the analysis of those simulations. The steps proposed in the EPGs, as they apply to the RPV and primary containment, would result in the mitigation of a MSIV closure ATWS if carried out successfully. The need for operator training in the use of the EPGs was observed because actions must be taken promptly to reduce the risk from the accident.

The SLCS was modeled using a bounding approach. Maximum SLCS effectiveness was modeled by assuming that the boron solution was transported isotropically with liquid in the RPV. Minimum SLCS effectiveness was modeled by assuming that the boron solution was completely stratified in the lower plenum, until a sufficient amount had been injected to effect a hot shutdown. Three simulations were performed assuming that the operator initiated SLCS (50 gpm capacity) and began level control at 120 s. With maximum SLCS effectiveness, the predicted PSP temperature at the time of reactor shutdown was 140°F. With minimum SLCS effectiveness, the PSP reached 195°F with RPV depressurization and 218°F without RPV depressurization when the reactor was shutdown. A fourth simulation was performed with the SLCS capacity increased

to 86 gpm. The 86 gpm corresponds to the published NRC final rule on ATWS. Assuming minimum SLCS effectiveness and no RPV depressurization, the increased capacity of 86 gpm reduced the PSP temperature at shutdown from 218 to 173°F. The simulation matrix and predicted PSP temperatures are illustrated in the following table.

Conclusions, results, and recommendations resulting from the study are summarized below.

1. Mitigative operator actions are required to prevent containment failure and severe fuel damage during a MSIV closure ATWS. During the plant automatic simulation, primary containment failure was predicted from static overpressurization 45 min after transient initiation. In less than four hours, over half of the core was predicted to have liquefied and relocated. Significant hydrogen production and fission product release from the fuel was predicted to occur.
2. It is predicted from these simulations that if all of the actions proposed by the EPGs are completed successfully, then a MSIV closure ATWS would be brought under control. Some of the actions, however, may be very difficult to accomplish.
3. Operator training should be an integral part of the implementation of the EPGs. These simulations indicate that the operator must act properly and promptly to reduce the risk from a MSIV closure ATWS. The process of following the EPGs through their various parts could be very time consuming unless the operators had a thorough understanding of them beforehand.
4. More guidance should be given in the EPGs relative to the injection of low pressure systems to the RPV. The operator is told to "slowly inject" when the RPV is depressurized. More definitive instruction is required, as are measures to prevent automatic injections.
5. Level control as advocated by Contingency #7 is an effective although limited means of reducing reactor power. Lowering RPV water level to TAF at 1000 psia was calculated to reduce reactor power from 30% to approximately 17% of rated. This reduces the PSP heatup rate from 6 to 4°F/min. Although several analyses have converged on the predicted power level range of 17-20%, uncertainties remain and the actual power could be higher.

Summary of MSIV closure ATWS simulations

Simulation Description	Boron Modeling	Level Control	RPV Depressurization	PSP Temperature at Shutdown (°F)
Plant automatic	None	No	Yes (automatic ADS)	Shutdown not achieved
EPG nominal—maximum SLCS effectiveness	50 gpm isotropic	Yes	No (pressure control, not depressurization)	140
EPG nominal—minimum SLCS effectiveness	50 gpm stratified	Yes	Yes (manual blowdown)	195
Minimum SLCS effectiveness without depressurization	50 gpm stratified	Yes	No	218
EPG nominal—increased SLCS capacity and minimum effectiveness	86 gpm stratified	Yes	No	173

6. The action of depressurizing the RPV to avoid violation of the heat capacity temperature limit (HCTL) should be evaluated further. RPV depressurization should result in a power reduction during an ATWS, and it may also preclude the need to blowdown the RPV when the PSP has no condensing capacity. However, the potential for low pressure power oscillations and unthrottled low pressure ECC system injections could cause fuel damage.

7. Even with minimum SLCS effectiveness, it is predicted that PSP temperature would be less than 200°F at the time of shutdown. Using 50 gpm of 13% sodium pentaborate solution in conjunction with level and pressure control results in a PSP temperature of 195°F at shutdown. Assuming maximum SLCS effectiveness results in a PSP temperature of 140°F.

8. Increasing SLCS capacity to 86 gpm reduces the predicted PSP temperature at shutdown from 218 to 173°F for minimum effectiveness assumptions and no RPV depressurization. The reduction in temperature is significant in that complete condensation in the PSP should ensure that no steam breakthrough would occur, thus preventing drywell pressurization.

9. The uncertainty of assuming uniform control rod worth is currently too large to allow reliable modeling. It is recommended that the effect of individual rod insertion be quantified in terms of negative reactivity versus time.

10. Use of the torus cooling mode of the residual heat removal (RHR) system is not assured during a level control transient. Once RPV level is raised back up, torus cooling should be readily accomplished. The importance of torus cooling lies not only in reducing PSP heatup rate but also helping ensure that the torus remains well mixed.

ACKNOWLEDGMENTS

The support of the U.S. Nuclear Regulatory Commission is gratefully acknowledged, particularly that of Dr. Bharat Agrawal. The cooperation and valuable discussions of several others also contributed significantly to this study: L. Claassen (General Electric Co.), B. Chexal (EPRI), S. Hodge and M. Harrington (ORNL), M. Miller and K. Keith (TVA), and P. Saha and G. Slovik (BNL).

The authors thank Gary E. Wilson for his technical review and management support of this work. The efforts of Louise Judy and Joan Mosher in text processing are greatly appreciated. Special thanks go to Nancy Thornley for generating drawings and plots throughout this analysis.

CONTENTS

FIGURES

TABLES

NOMENCLATURE

ADS	Automatic depressurization system
ATWS	Anticipated transient without scram
BFNP1	Browns Ferry Nuclear Plant Unit 1
BNL	Brookhaven National Laboratory
BWR	Boiling water reactor
CRD	Control rod drive
CST	Condensate storage tank
DW/T	Drywell temperature
ECC	Emergency core cooling
EPGs	Emergency Procedure Guidelines
EPRI	Electric Power Research Institute
FIST	Full Integral Simulation Test
HCTL	Heat capacity temperature limit
HDWP	High drywell pressure
HPCI	High pressure coolant injection
INEL	Idaho National Engineering Laboratory
LLLWL	Triple lo level water level
LOCA	Loss-of-coolant accident
LPCI	Low pressure coolant injection
LPCS	Low pressure core spray
MSIV	Main steamline isolation valve
NRC	Nuclear Regulatory Commission
NSSS	Nuclear steam supply system
ORNL	Oak Ridge National Laboratory
PC	Primary containment
PC/P	Primary containment pressure
PRA	Probabilistic risk assessment
PSP	Pressure suppression pool
RCIC	Reactor core isolation cooling
RC/L	RPV control/level
RC/P	RPV control/pressure
RC/Q	RPV control/power
RHR	Residual heat removal
RPV	Reactor pressure vessel
SASA	Severe Accident Sequence Analysis
SCDAP	Severe Core Damage Analysis Package
SET	Sequence event tree
SLCS	Standby liquid control system
SP/L	Suppression pool water level
SP/T	Suppression pool temperature
SRV	Safety relief valve
TAF	Top of active fuel
TVA	Tennessee Valley Authority

SEVERE ACCIDENT SEQUENCE ANALYSIS PROGRAM—ANTICIPATED TRANSIENT WITHOUT SCRAM SIMULATIONS FOR BROWNS FERRY NUCLEAR PLANT UNIT 1

1. INTRODUCTION

The subject of this report is the analysis of an anticipated transient without scram (ATWS) in a boiling water reactor (BWR). With the cooperation of the Tennessee Valley Authority (TVA), the specific subject of this effort is the Browns Ferry Nuclear Plant Unit 1 (BFNP1). The work is sponsored by the U.S. Nuclear Regulatory Commission (NRC) through the Severe Accident Sequence Analysis (SASA) Program. SASA objectives include establishing the methodology for and performing comprehensive deterministic analyses of severe accidents, determining accident event progression, evaluating the effects of plant safety systems and operator actions on accident progression, and defining requirements for improved analytical methods or for experiments to resolve uncertainties.

An ATWS occurs when an expected operational occurrence is followed by a failure to scram the reactor. Previous probabilistic analyses[1] have asserted that the ATWS at BFNP1 is included in a group of dominant risk transients. Although low in probability, ATWS accidents are of concern because they could lead to core damage and fission product release to the environment. The ATWS studied here is initiated by a main steamline isolation valve (MSIV) closure. This event leads to the most severe ATWS sequence,[2,3] because the power conversion system is lost from the start of the transient. Steam produced in the vessel is discharged to the pressure suppression pool (PSP), creating a threat to containment unless power can be reduced to decay levels. The outcome of the transient is governed by the ability of plant systems and operator actions to maintain core cooling and containment integrity until the accident can be controlled.

In line with SASA objectives, the MSIV closure ATWS at BFNP1 was studied by developing an analysis methodology. Using probabilistic methods, a sequence event tree (SET)[4] was developed which described the various paths (or sequences) that an ATWS could follow in terms of plant systems and operator actions. Four dominant (higher probability of core or containment damage) sequences were identified. Analysis of the dominant sequences yielded insight to the possible consequences from a MSIV closure ATWS. Even though timings of events can show considerable variation, the transient signatures are limited and distinct.

Section 2 of this report describes the BFNP1 with regard to systems that are important during an ATWS. Operator actions are also discussed as they relate to Emergency Procedure Guidelines (EPGs) in Section 3. Plant systems and operator actions are tied together by describing their interaction during the tranient.

The analysis methodology is outlined in Section 4. Section 5 presents key calculational results as they relate to the reactor pressure vessel (RPV) and primary containment. Fuel damage analysis of the plant automatic transient (no operator actions) is given in Section 6. Uncertainties with the deterministic analyses are outlined in Section 7, and conclusions and recommendations resulting from the analysis are given in Section 8. A list of references is provided in Section 9.

Appendix A describes the RELAP5/MOD1.6 computer model of the reactor pressure vessel of BFNP1. Appendix B describes the primary containment and CONTEMPT/LT-028 model. Appendix C describes the SCDAP code and the BFNP1 SCDAP model, and Appendix D describes the FRAP-T6 code and model.

2. EARLY PLANT RESPONSE TO A MSIV CLOSURE ATWS

In this section, the plant response to a MSIV closure ATWS is described. First, the system alignment during normal operation is discussed. Next, the automatic plant response for the first 100 s of the ATWS event is presented. Because operator actions are assumed to begin at 120 s, presentation of the early event timings applies to simulations with and without operator actions. Results from the complete simulations are presented in Sections 5 and 6.

2.1 Normal Operation

A schematic of the pressure vessel, main steam system, and condensate and feedwater system is shown in Figure 1. Flow paths indicate the alignment during normal operation of the BWR direct steam cycle. Steam generated in the core exits the pressure vessel through four main steamlines. Most of the steam is used to drive the main turbines for electricity generation. After leaving the turbines, the steam is condensed and becomes makeup for the feedwater system. Steam that is not used by the main turbines is diverted from the main steamlines and used to drive the feedwater turbines.

A drawing of the RPV is shown in Figure 2. During normal operation, two recirculation pumps provide the driving potential for the core inlet flow. Taking suction from the lower downcomer, ~1/3 of the total core flow passes through the recirculation loops, discharging through the jet pump drive nozzles. The remaining 2/3 enters the jet pump suction from the downcomer. This combined flow is discharged through the jet pumps (10 per loop) into the lower plenum region. Entering the core inlet, ~10% of the flow is diverted through the interstitial bypass region (the region inside the core shroud, but outside the fuel channels). Recombining in the upper plenum region with flow through the fuel channels, the saturated two-phase mixture passes through the steam separators. Water is separated and returned to the downcomer. Steam continues upward through the dryers and leaves the pressure vessel via the main steamlines. The mass of steam leaving through the steamlines is replenished by the main feedwater system.

Also shown in Figure 2 are elevations corresponding to downcomer level trips. These will be referred to in subsequent discussions. Also shown are injection points for the control rod drive (CRD) and standby liquid control system (SLCS). When activated, the SLCS injects sodium pentaborate through a single sparger below the core support plate.

2.2 System Alignment During MSIV Closure ATWS

Closure of the MSIVs isolates the turbines and condenser from the pressure vessel. The main condenser is no longer available to condense vessel steam, and the feedwater pumps will not function because steam for feedwater turbines is not available. Figure 3 illustrates pertinent flow paths during the early portion of a MSIV closure ATWS.

Vessel steam is directed through the safety relief valves (SRVs) to the PSP, where it is condensed. Part of the steam is diverted from the main steamline to drive the high pressure coolant injection (HPCI) and reactor core isolation cooling (RCIC) turbines, which provide high pressure makeup water to the vessel. The HPCI and RCIC pumps, as well as the CRD pump, take suction from the condensate storage tank (CST). PSP cooling (~2-1/2% of rated power) can be provided with the residual heat removal (RHR) system following manual alignment.[a] Low pressure coolant injection (LPCI), core spray, and condensate booster pumps would also take suction from the CST.

During a transient involving MSIV closure, containment interactions are important. Figure 4 illustrates the primary containment at BFNP1. The primary containment encloses the reactor pressure vessel, recirculation loops, and other components including the SRVs. The primary containment consists primarily of a drywell and pressure suppression pool. Connecting vent systems, isolation valves, cooling systems, and other service equipment are also included. Appendix B includes a more complete description of the BFNP1 Mark I containment.

The main function of the primary containment system is to provide radiological shielding, first between the nuclear boiler and the reactor building, and ultimately the environment. The drywell is a steel pressure vessel encased in concrete. Its internal design pressure is 56 psig at 281°F. Cooled by 10 large fan cooling units, it normally operates at an internal temperature of less than 135°F. The drywell is nitrogen filled, the containment being inerted to prevent burning of hydrogen in the event of its release from the vessel during an accident. Via eight large vent pipes, the drywell is connected to the torus, which includes

a. As pointed out by S. A. Hodge (ORNL), the PSP cooling capacity is a function of pool temperature and can reach 4-1/2% of rated power at very high pool temperatures.

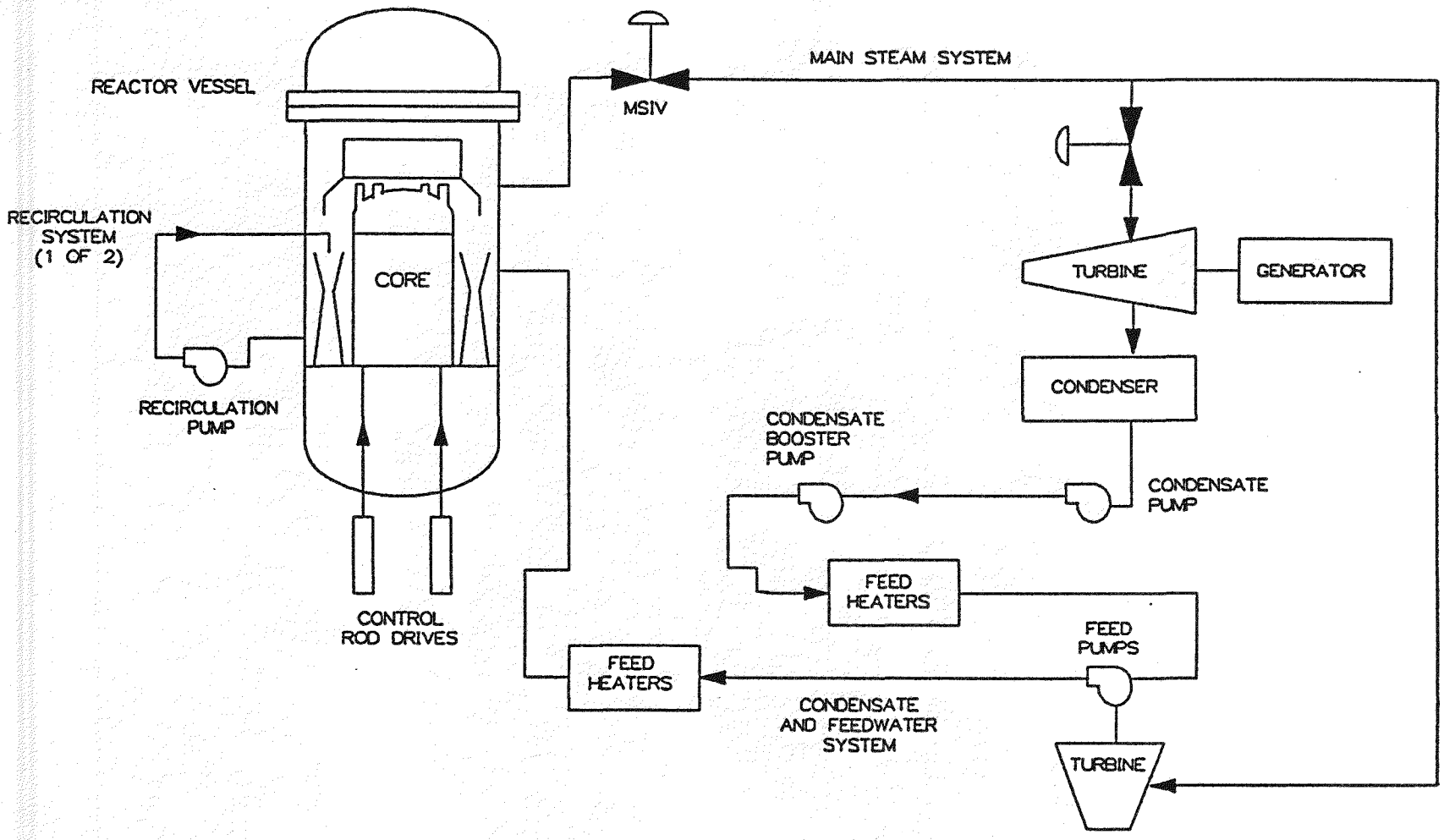

Figure 1. BFNP normal operation schematic.

NST00405

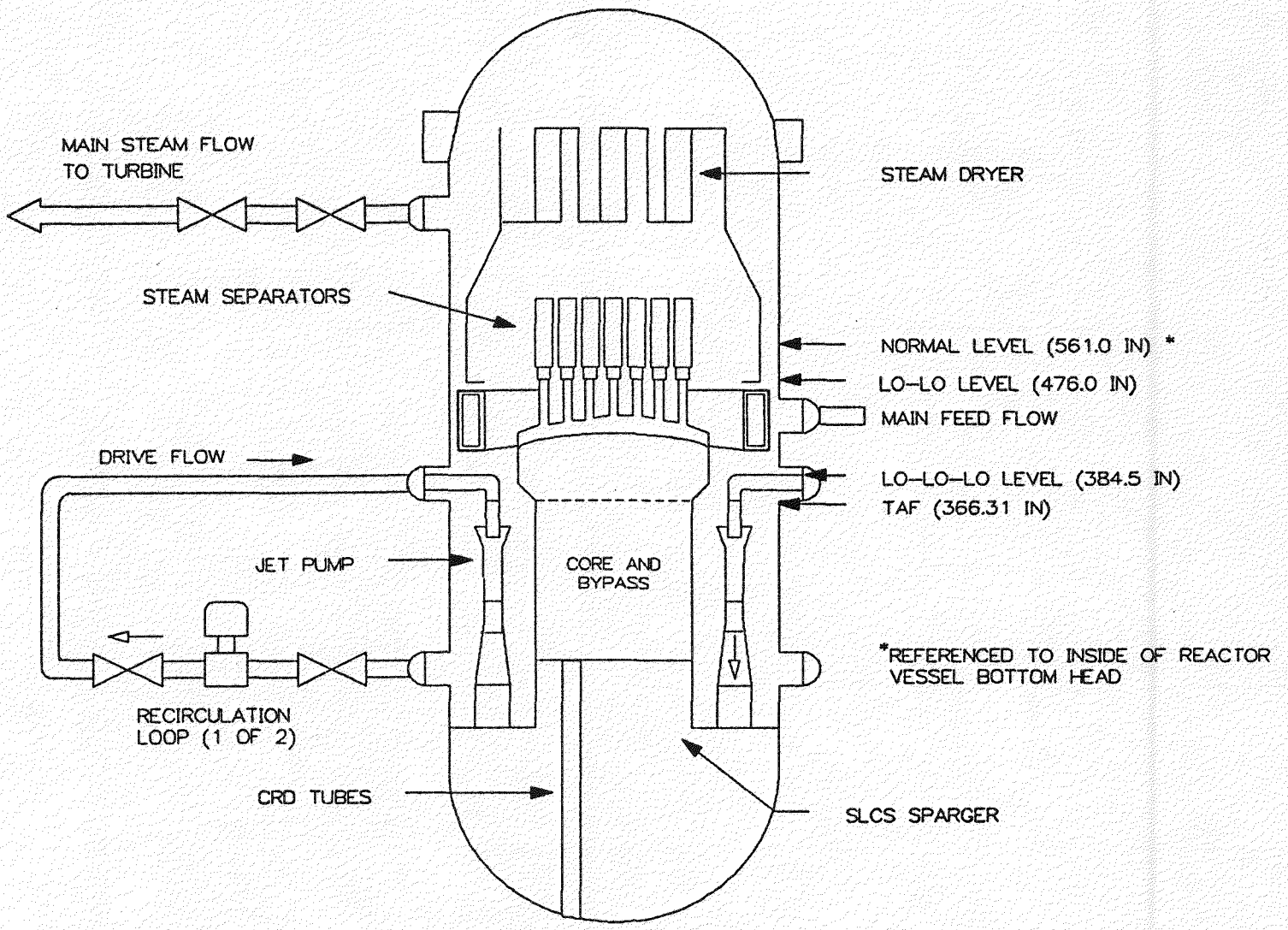

Figure 2. Reactor pressure vessel.

NST00406

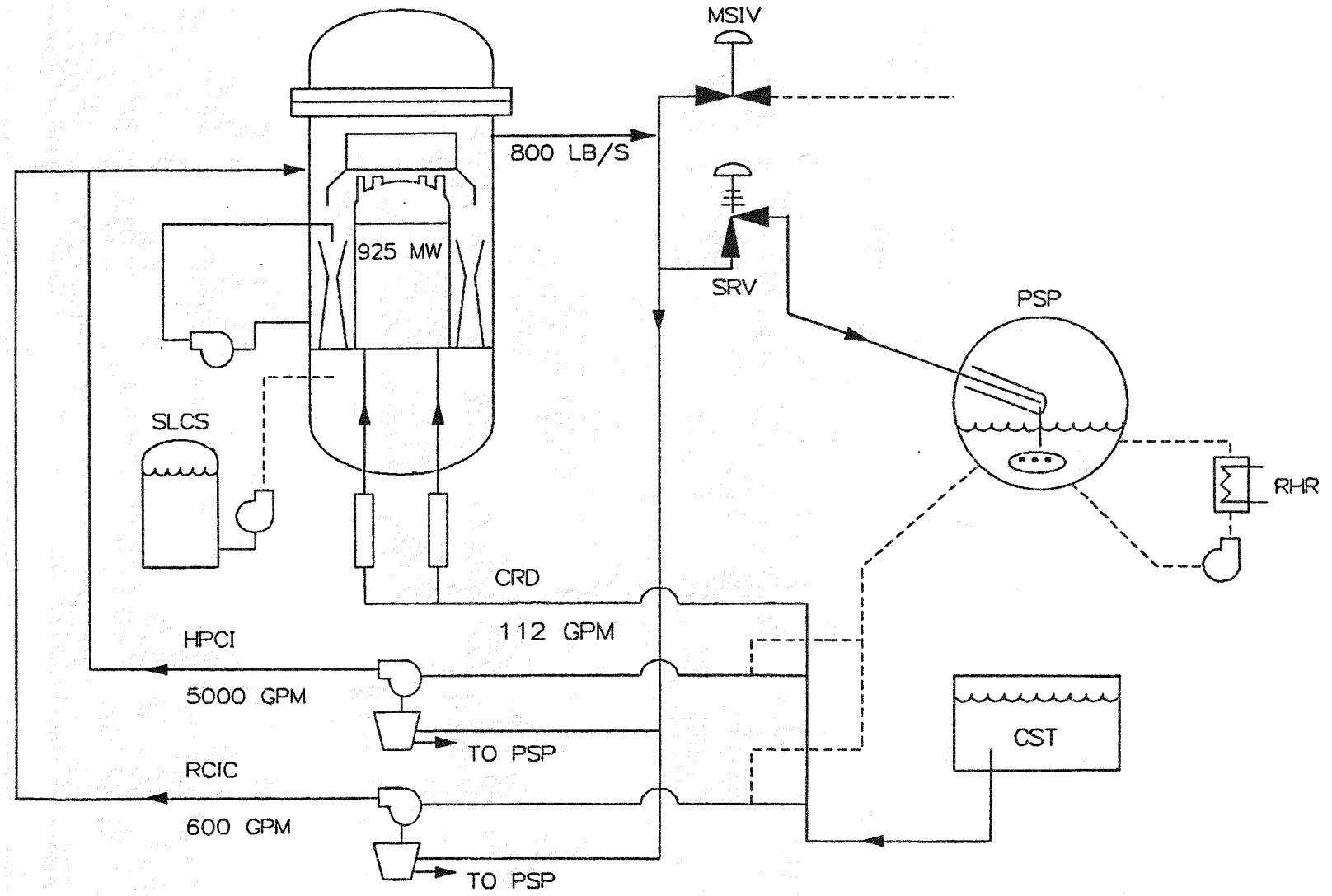

Figure 3. Flow path schematic during early stages of MSIV closure ATWS.

NST00404

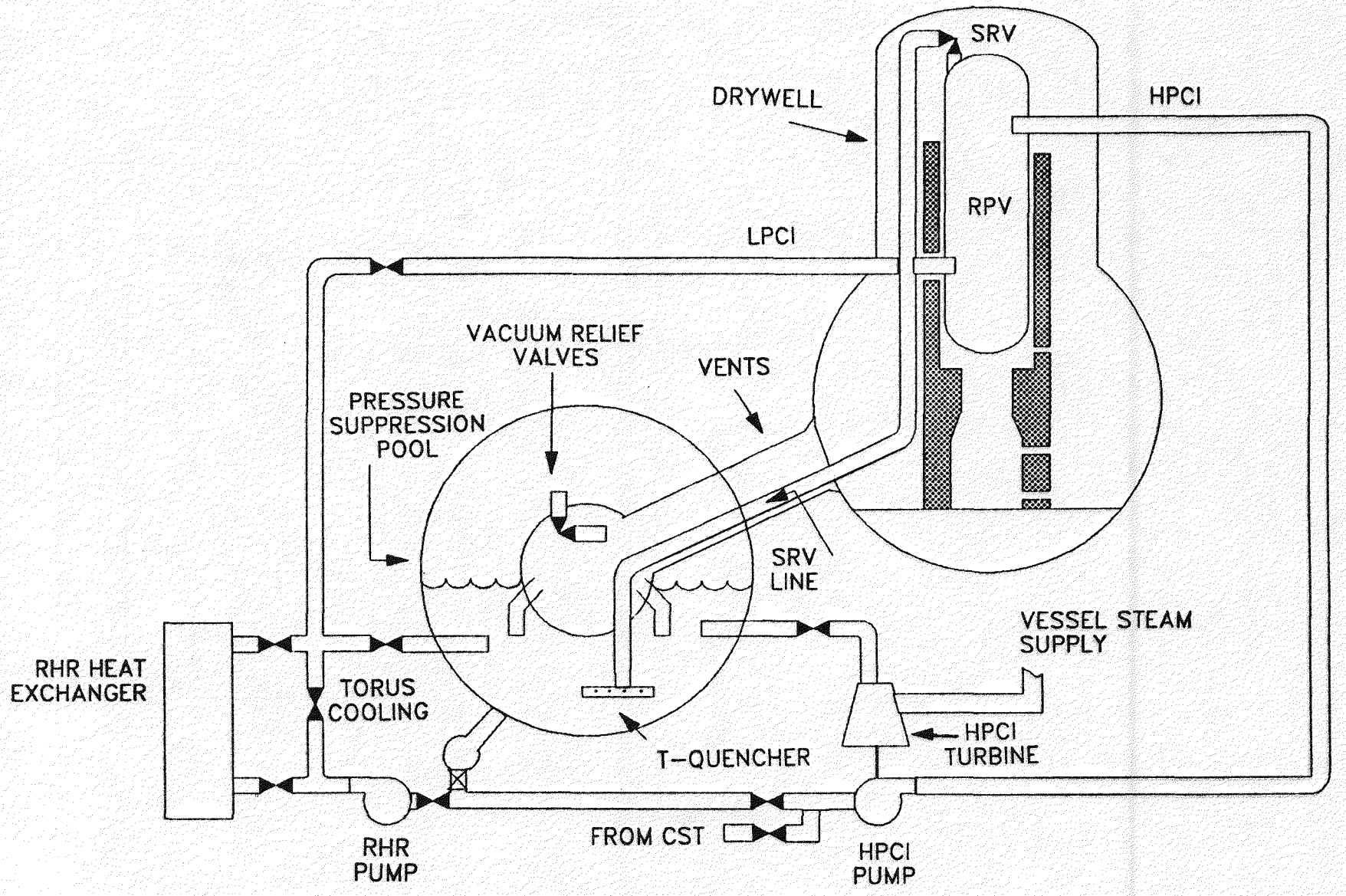

Figure 4. Primary containment schematic.

NST00407

the PSP holding nearly 1 million gallons of water. The function of the PSP is to provide a heat sink for energy released from the vessel during a design basis loss-of-coolant accident (LOCA). The PSP also provides a source of makeup water for the low pressure emergency core cooling systems (ECCS).

Reactor vessel SRVs discharge to the PSP when required. Steam generated in the vessel during a MSIV closure ATWS is relieved entirely through the SRVs to the PSP. Steam is discharged to the suppression pool via spargers called T-quenchers. The T-quenchers are designed to promote complete condensation in the pool.

2.3 Sequence of Events During MSIV Closure ATWS

Vendor analysis (see Reference 2) of ATWS occurrence concluded that the MSIV closure without scram "transient results in higher vessel pressure, more severe fuel duty, and a larger amount of steam being dumped into the (pressure) suppression pool than any other moderately frequent transient." Thus, analysis of MSIV closure without scram provides a bounding case for ATWS events in BWRs, and the scope of the present analysis was restricted accordingly. A description of the subject transient follows.

MSIV closure causes a rapid pressurization of the RPV because the core continues to produce steam at near rated conditions. Increased pressure collapses voids in the core, which introduces positive reactivity causing increased power and steam generation. The increasing pressure causes the recirculation pumps to trip automatically (at 1135 psia), and the SRVs to lift. These two actions relieve overpressurization by venting steam and reducing core inlet flow, which reduces power by decreasing core void content and introducing negative reactivity into the core.

The MSIV closure isolates the steam supply to the three feedwater turbines. As the turbines and feedwater pumps rapidly coast down, turbine-driven feedwater is lost. Continued core steaming and loss of feedwater causes the vessel downcomer level to decrease. When lo-lo level (see Figure 2) is reached, HPCI and RCIC pumps start automatically. The HPCI and RCIC take suction from the CST, and pump water into the RPV via the feedwater line. HPCI flow accounts for 5000 gpm and RCIC for 600 gpm of high pressure makeup.

A scram would be signaled on four situations: MSIV closure, high RPV pressure, high neutron flux, and lo downcomer level (539.0 in. above the inside of the RPV bottom head). It is assumed for this ATWS study that all of the control rods fail to insert. Following the scram signal, 112 gpm of water is pumped into the RPV by the CRD system.[a]

Table 1 lists timing of key events during the early portion of a MSIV closure ATWS. Note that all events have occurred without operator action.

After recirculation pump coastdown, the RPV is in a natural circulation mode of operation. With makeup provided by the HPCI, RCIC, and CRD systems, a pseudo steady state condition exists in the RPV. Reactor power stabilizes at ~30%, which results in a steaming rate to the PSP of ~21% of normal steamline flow. The difference in power and steaming rate is accounted for by heating of the subcooled ECC fluid to saturation temperature in the core.

The subsequent transient can progress through many different sequences, depending on plant system and operator action interactions. Operator actions as they relate to an ATWS are discussed in the following section.

---

a. The CRD hydraulic system pumps water continuously into the RPV. Before a scram signal, that water flow is 60 gpm. Following a scram signal, the flow is increased and taken to be a constant value of 112 gpm in this study.

Table 1. MSIV closure ATWS sequence of events—first 80 s[a]

Time (s)	Value	Event
0.0	—	Transient initiation, MSIVs begin to close.
0.4	10%	MSIV fractional area has decreased 10% causing scram signal.
2.67	104.7%	Jet pump discharge mass flow peaks.
2.71	253.0%	Peak reactor power.
3.03	110.0 psi/s	Maximum rate of change of steam dome pressure, SRVs begin to open.
3.26	1135.0 psia	Recirculation pump trip signal on high steam dome pressure.
3.79	—	Recirculation pumps trip, begin flow coastdown.
5.0	—	MSIV completely closed.
6.7	2582°F	Peak fuel temperature.
6.7	82%	SRV flow peaks at 82% of normal steaming.
7.3	608.9°F	Peak cladding temperature.
10.5	1272 psia	Peak steam dome pressure.
34	476.0 in.	Downcomer level reaches lo-lo level, HPCI and RCIC actuate.
78	110°F	PSP temperature reaches 110°F, SLCS injection called for by EPGs.
79	5600 gpm	HPCI and RCIC at full flow.

a. Event timings as predicted by RELAP5/MOD1.6.

3. EMERGENCY PROCEDURE GUIDELINES

As described in the previous section, a quasi steady state condition would be automatically reached in less than two minutes following MSIV closure and control rod scram failure. With high pressure makeup provided by the HPCI, RCIC, and CRD systems, the RPV would be steaming at approximately 21% of its full power rate. The steam is condensed in the PSP, which contains highly subcooled water. Without operator action, this scenario would continue until either high pressure makeup or PSP condensing capacity was lost. A detailed analysis of the plant automatic transient is contained in Section 4. The purpose of this section is to present probable operator actions within the context of proposed EPGs.[5]

The proposed EPGs were developed by the Emergency Procedures Committee of the BWR Owners Group to provide detailed guidance for plant operators during abnormal or accident conditions. They are designed to be symptom oriented, and as such are quite elaborate in order to address all postulated plant conditions. Those parts of the EPGs that relate to the predicted plant status during a MSIV closure ATWS were extracted accordingly for this analysis. Specifically, the EPGs were used as a basis for modeling operator actions during the postulated ATWS scenario.

A flowchart of RPV control guidelines is shown in Figure 5. It is emphasized that the actual EPGs are much more detailed. Only those parts that are pertinent to the present analysis are discussed in this section. Referring Figure 5, it is seen that entry to the EPGs is gained following MSIV isolation. The operator is first told to ensure reactor scram, which would be automatically initiated. For these simulations, however, it is assumed that reactor scram is unsuccessful. Proceeding down the figure, the operator is told to monitor and control (concurrently) RPV water level, RPV pressure, and reactor power. These three paths will be discussed individually.

While following the path entitled RPV water level [RPV control/level (RC/L)], the operator is told to ensure automatic actions. Specifically, this entails confirming MSIV isolation and high pressure system (HPCI and RCIC) initiations. To ensure RPV level control, the water level must be restored and maintained above the top of the active fuel (TAF). This is accomplished automatically with the recirculation pump trip and initiation of the HPCI and RCIC systems. Combined with CRD flow, HPCI and RCIC flows result in a reactor power of approximately 30% and a vessel water level above TAF. An alternate decision branch is provided which tells the operator to proceed to Contingency #7 if boron injection is required. Contingency #7 is discussed in more detail at the end of this section.

While executing RPV water level control, the operator is also told to monitor and control reactor power [RPV control/power (RC/Q)]. Two decision points are passed immediately (see Figure 5) because reactor power is not less than 3% and the MSIVs are closed. The operator is told to trip the recirculation pumps to reduce power,[a] and then to proceed down two parallel branches. One branch consists of procedures intended for the insertion of control rods. These procedures manifest themselves as attempts to manually scram the reactor. If the manual scram attempts are unsuccessful (which is assumed for these simulations), the procedures call for manually inserting individual control rods. The second branch, which is executed concurrently, tells the operator to monitor the PSP temperature. If the PSP temperature exceeds 110°F, he is told to initiate SLCS and prevent automatic actuation of the automatic depressurization system (ADS). When the PSP temperature exceeds 110°F (approximately 80 s after transient initiation), boron injection is required and the operator is directed to enter Contingency #7.

The third path (see Figure 6), which is executed concurrently with RC/L and RC/Q, is entitled RPV pressure [RPV control/pressure (RC/P)]. If any SRV is cycling, the operator is told to minimize cycling by reducing RPV pressure below the minimum SRV opening setpoint. It is preferable to relieve pressure through the turbine bypass valves (blowdown to main condenser) rather than the SRVs. However, it is assumed here that the main condenser is not available because of MSIV isolation. Although not accounted for in this analysis, the EPGs imply that the operator should attempt to reestablish the main condenser as a heat sink. This would be accomplished by opening the MSIVs, which requires that there is no indication of gross fuel failure and no indication of a steamline break. In addition, boron injection must be required, and the main condenser available, before isolation interlocks should be overridden to open MSIVs.

During pressure control, the operator may find that either the heat capacity temperature limit (HCTL) or the suppression pool load limit is reached. These limits are plots of PSP temperature and level respectively, as functions of RPV pressure. Figure 7 illustrates a plot of the HCTL as applied to the Browns

a. The recirculation pumps would have tripped automatically on high RPV pressure.

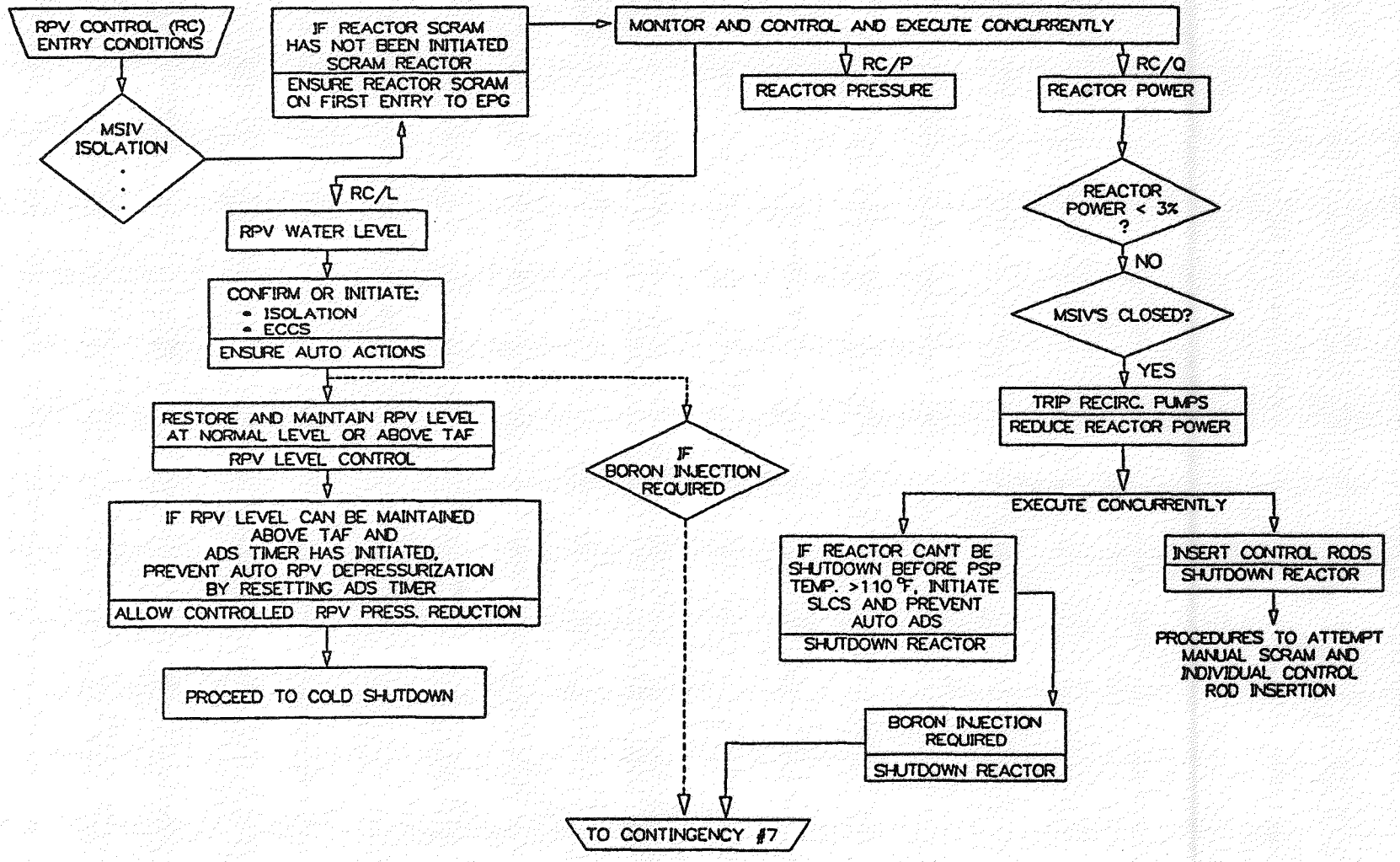

Figure 5. EPG level and power control flowchart.

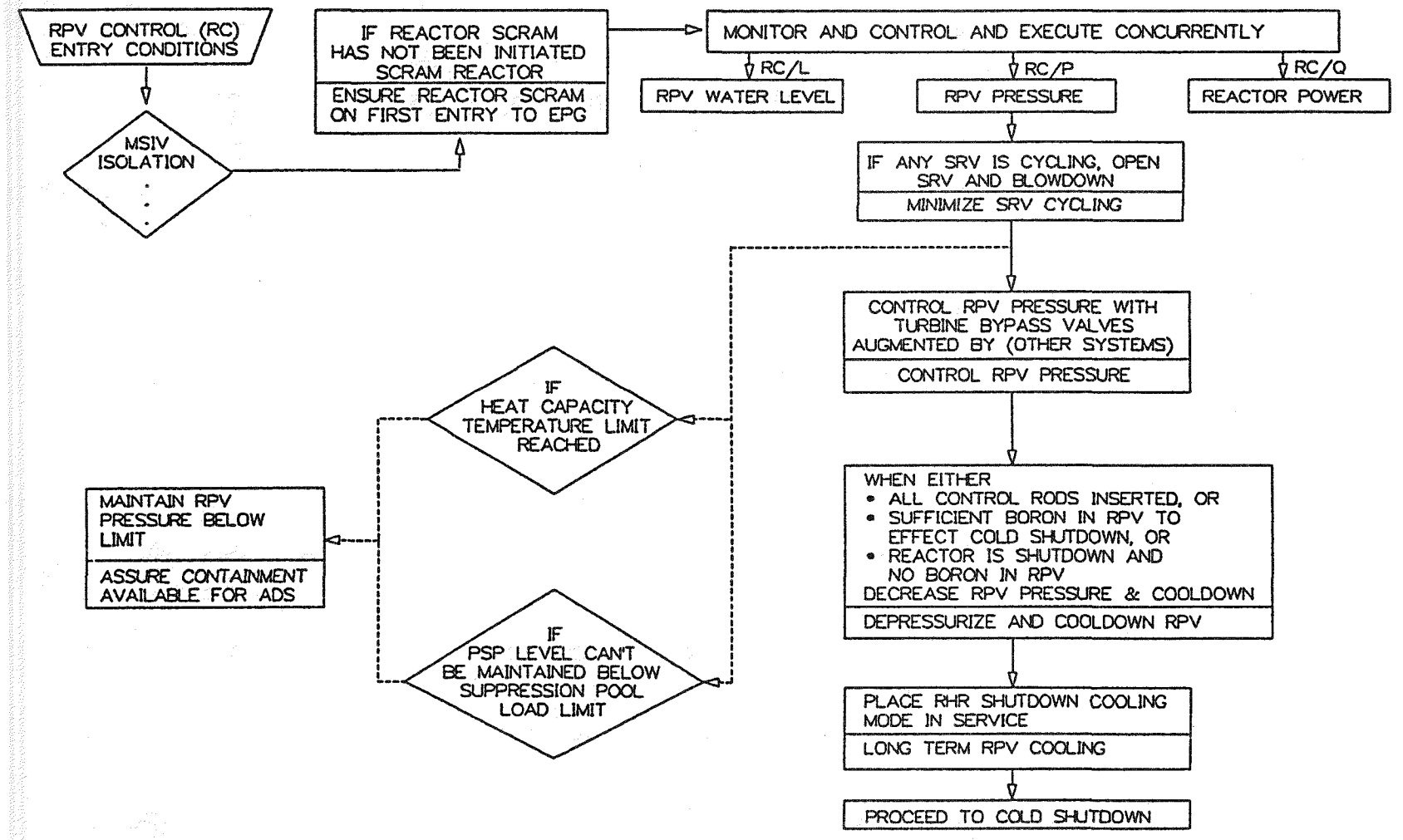

Figure 6. EPG pressure control extracted flowchart.

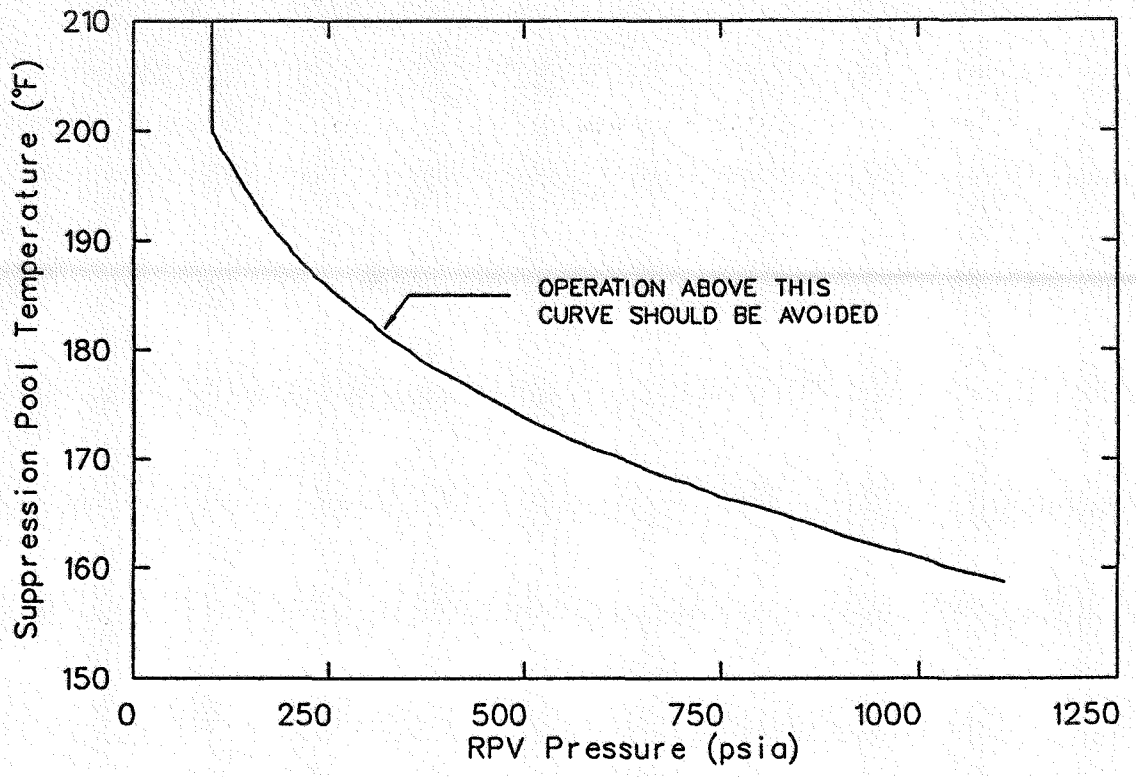

Figure 7. Heat capacity temperature limit.

Ferry containment. If either limit is reached, the operator is told to reduce RPV pressure to stay below the limit.

For the simulations presented here, the operator would be monitoring and controlling RPV water level, RPV pressure, and reactor power. When the PSP temperature reached 110°F,[a] the operator would be instructed to initiate SLCS and proceed to Contingency #7 of the EPGs. From the previous discussion, Contingency #7 is entered from paths RC/L and RC/Q. RPV pressure would continue to be monitored and controlled according to RC/P.

The expressed objective of Contingency #7 is to "minimize heatup of the suppression pool during the time of boron injection, thus avoiding the need for emergency RPV depressurization." Figure 8 illustrates pertinent actions and decision steps extracted from Contingency #7. Following the entry conditions, with power >3%, the operator is told to terminate and prevent all injection into the RPV except CRD and SLCS. This action will cause the RPV water level to drop because steam lost through the SRVs will exceed makeup from CRD and SLCS. When the water level reaches TAF, it is to be maintained there with available high pressure systems. This action is intended to reduce reactor power by reducing core inlet flow. If the water level cannot be maintained at TAF, an alternate branch indicates that depressurization is required. This would allow the use of low pressure systems to maintain level at TAF.

So far, the actions discussed have been concerned with RPV control. In addition to RPV control, the operator would also be concerned with primary containment (PC) control. Figure 9 illustrates actions from the primary containment guidelines, which are pertinent to the transients documented in this report. As with the RPV guidelines, the PC guidelines presented here are considerably reduced from the actual EPGs.

For the ATWS, entry to the PC control would occur when the PSP temperature exceeds 95°F. At that time, the operator is told to monitor and control concurrently drywell temperature (DW/T), suppression pool temperature (SP/T), primary containment pressure (PC/P), and suppression pool water level (SP/L). Only the SP/T path requires attention past the first action step, and as such is the only path detailed in Figure 9.

For the DW/T path, the drywell coolers are assumed operable. Because there is no containment pressurization calculated during the operator action transients,

a. This temperature is predicted to be reached approximately 78 s after transient initiation.

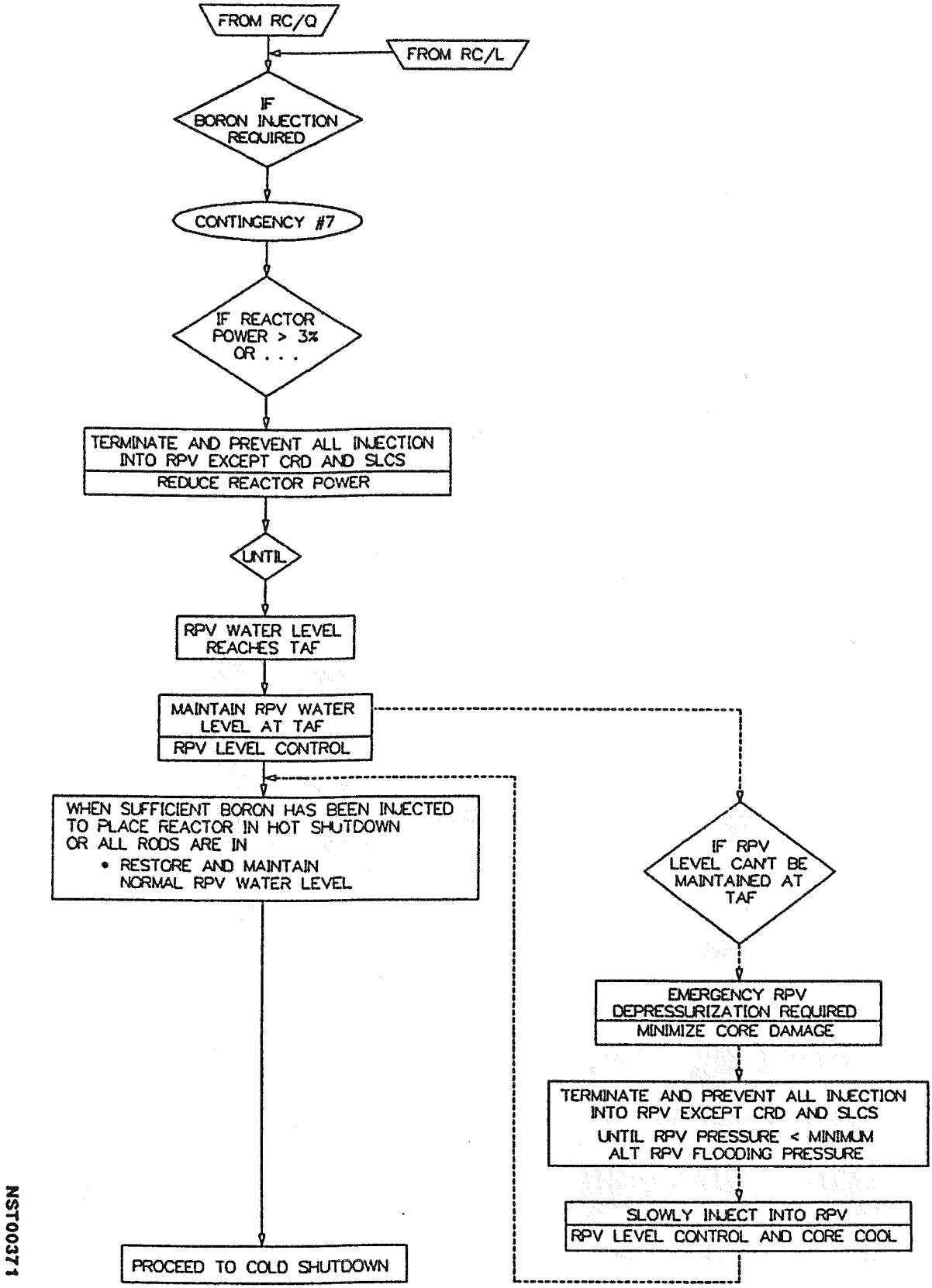

Figure 8. Contingency #7 extracted flowchart.

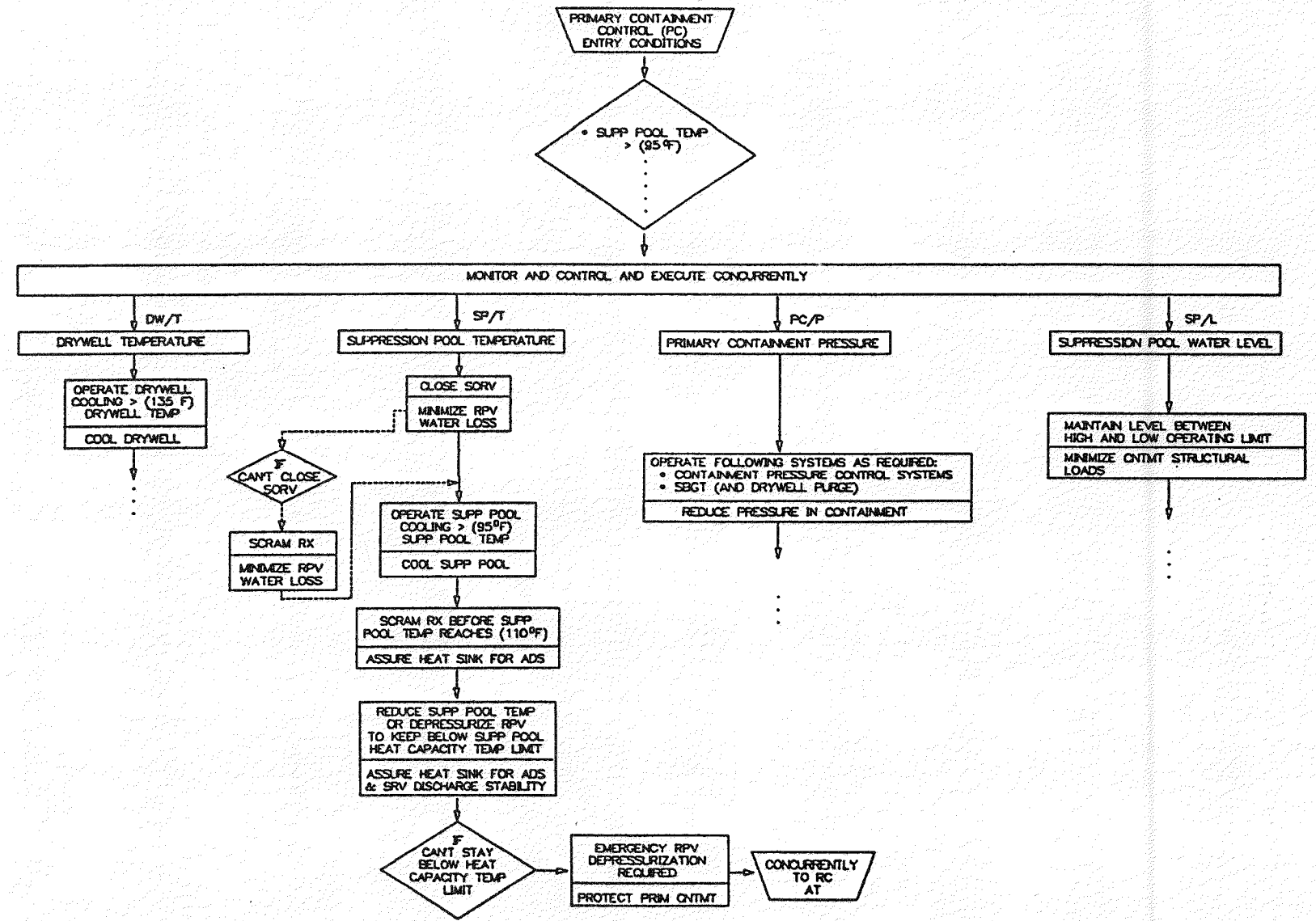

Figure 9. EPG primary containment flowchart.

NST00379

path PC/P requires only monitoring. Similarly, path SP/L is only monitored because the PSP water level is calculated to remain within normal operating limits.

Following the SP/T path, the operator is told to operate suppression pool cooling when the PSP temperature exceeds 95°F. With the PSP initial temperature assumed to be 90°F, this occurs early (<25 s) in the ATWS. It is unlikely that the operator would have time to establish suppression pool cooling (torus cooling mode of the RHR system) during the first few minutes of an ATWS as explained below. At approximately 220 s, the RPV level would be lowered to TAF in accordance with level control procedures in Contingency #7. When the RPV level passes through the triple lo level water level (LLLWL) setpoint (Figure 2), the RHR pumps (Figure 4) are automatically aligned for LPCI injection and interlocked on a five minute timer. This prohibits realignment to pool cooling even though LPCI is not needed. The timer is a LOCA consideration to ensure that LPCI is available to provide makeup to the RPV if necessary. After five minutes the operator may realign for pool cooling. However, if the RPV water level rises above LLLWL, the timer will reactivate each time it passes below the setpoint and prohibit pool cooling. Because this level movement is predicted to occur, no credit for pool cooling was taken in these simulations. The possibility for RHR alignment to pool cooling is illustrated in Figure 10.

Continuing down path SP/T, the operator must monitor PSP temperature and keep it below the HCTL. This is the same action required as in the RC/P path discussed earlier (see Figure 6). Guidelines for secondary containment and radioactivity release control are also provided by the EPGs. However, their evaluation is beyond the scope of this analysis.

The effectiveness of these guidelines in mitigating an ATWS is discussed in Section 5 of this report.

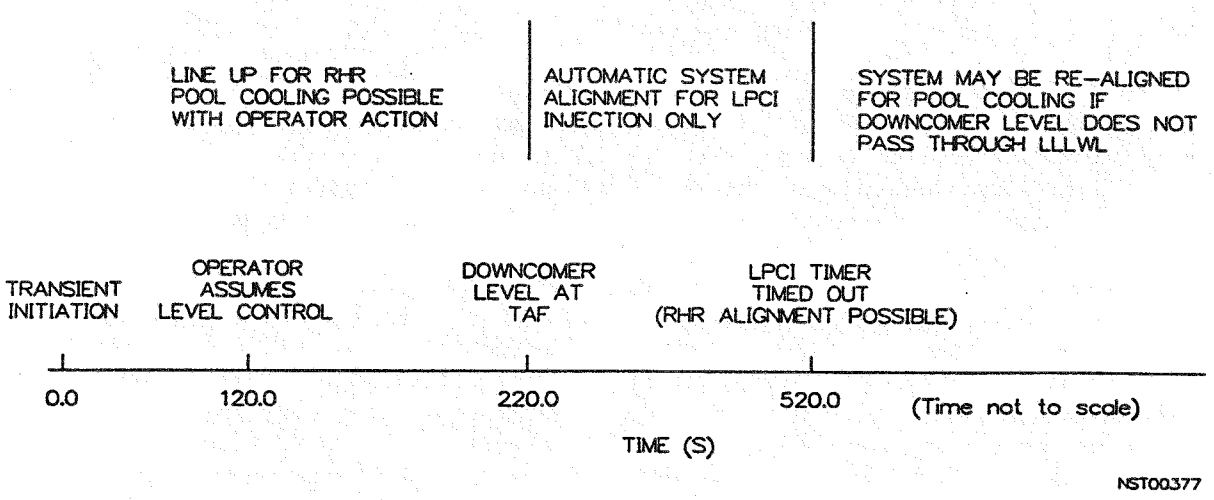

Figure 10. RHR alignment.

4. ANALYSIS APPROACH

This section describes how significant parameters, operator actions, and accident sequences were isolated for analysis. This isolation procedure was necessary because of the many and varied combinations of operator actions and accident sequences that could possibly result during a MSIV closure ATWS.

4.1 Operator Actions and System Interactions

During a MSIV closure ATWS, the primary responsibility of the operator is to effect a safe shutdown. To be successful, the operator must either insert control rods into the core or poison the core with the SLCS. The ability of the operator to fulfill this responsibility is dependent on the availability and reliability of the various plant systems, and on the state of the reactor. The effectiveness of the systems depend on the ability of the operator to recognize the signature of the transient and take appropriate mitigative actions in a timely manner.

Initially, the operator would attempt to scram the reactor. The EPGs provide guidance for alternate scram procedures. Depending on the cause of the original scram failure, the operator may very well be successful and shutdown the reactor. However, for the purposes of this analysis, it is assumed that reactor scram cannot be achieved. The operator would then be expected to attempt other means of inserting control rods. One such procedure is termed manual rod insertion, and involves inserting control rods individually from the control room. This procedure was not accounted for because of the uncertainty in modeling individual rod reactivity. A discussion of its potential effectiveness is included in Section 7.3.

Scramming the reactor is the simplest and most reliable means of transient mitigation. In the absence of control rod insertion, the operator must initiate the SLCS to effect a shutdown. The success of this system is, however, contingent upon system effectiveness and the presence of other, complementary operator actions. These actions are directed to maintaining core cooling and containment integrity while the operator borates the core. For example, enough core flow to transport the boron into the core must be provided. If that is not accomplished, the boron could stagnate in the lower plenum and have little or no affect on reducing power.

At Browns Ferry, the SLCS must be manually activated. It is designed to inject ~13% by weight of sodium pentaborate solution into the lower plenum of the RPV through a single sparger at the rate of 50 to 56 gpm. Assuming that 265 pounds of boron solution is required for hot shutdown (see Reference 3), the SLCS would have to inject for ~24 minutes. While injecting boron, the operator would be following procedures outlined in Contingency #7 of the EPGs.

The objective of Contingency #7 is "to minimize heatup of the suppression pool during the time of boron injection, thus avoiding the need for emergency RPV depressurization." This is because "reactor instabilities are likely to be associated with a blowdown at power, (and) it is desirable to have the reactor shutdown prior to depressurization."[5] The reactor system is not necessarily stable because low pressure vessel water inventory systems can flood the RPV if depressurized, thus inducing reactor power excursions and increased steaming rates to the PSP. According to the plant automatic chronology presented in Section 5.1, the vessel could be automatically depressurized as early as 18 minutes after transient initiation.

Contingency #7 proposes to avoid RPV depressurization while borating by reducing the level in the downcomer to the lowest practical level, TAF. Accompanied with a corresponding HPCI throttling technique, this action should reduce the reactor power. This action of level control is very important. Normal HPCI system flow alone induces a vessel steaming rate of approximately 20% of normal steamline flow to the PSP. Level control should reduce this rate, and delay the PSP heatup rate. If the PSP gets hot enough, eventually the HPCI will fail on high turbine lube oil temperature.[a] Thus, by reducing the PSP heatup rate with level control, HPCI failure due to high PSP temperature would be delayed or avoided. The importance of preserving HPCI integrity is related to boron effectiveness. If HPCI should fail before shutdown from boron occurs, it is unlikely that the remaining high pressure systems (RCIC and CRD) would be sufficient to efficiently transport boron into the core. The combined flows of HPCI, RCIC, and CRD result in a core inlet flow that is approximately 10% of normal flow. RCIC and CRD result in a core inlet flow that is approximately 1% of normal flow. Following HPCI failure, RPV water level would drop below TAF, necessitating emergency RPV depressurization per EPG direction.

a. Once HPCI shifts suction to the PSP on high PSP water level, its turbine lube oil is cooled with PSP water. An estimate of 190°F in the PSP was used to predict HPCI failure. While this value is believed to be conservative, HPCI failure would occur at some elevated PSP temperature.

While controlling level at TAF, the operator would also be monitoring PSP temperature. If the HCTL (Figure 7) is reached, the operator would be directed by the EPGs to depressurize to stay below the limit. If depressurization is required before the reactor is shutdown, reactor instabilities are possible. In addition, unless the low pressure injection systems are throttled or their injection prevented, large power excursions could occur when they flood the RPV.

The objective of the simulations presented in Section 5 is to answer questions about the plant response to a MSIV closure ATWS. In particular, how effective is the SLCS in accomplishing shutdown? How effective is level control in reducing reactor power? Can an emergency depressurization be avoided? How much time does the operator have before taking action? What are the consequences of emergency depressurization?

The progression of an ATWS sequence is complicated by the interdependence of operator actions, plant systems, and phenomena. Operator actions are contingent on the operator's perception of the state of the reactor system which, conversely, depends on operator actions. Because of this complexity, a probabilistic rather than a deterministic analysis approach was adopted to isolate significant phenomena, events, and systems.

4.2 Sequence Event Tree

From the preceding subsection, it is apparent that a MSIV closure ATWS could proceed through many different paths. For that reason, a structured approach to the analysis of ATWS sequence progression was required. Specifically, it was desired to formulate probabilistically the frequency of occurrence of sequences and the expected consequences. To that end, a SET was developed.

The SET used traditional event tree analysis to depict logically the sequence of events that must occur to recover the plant or to induce a severe accident. In all cases, entry to the SET involved four assumptions: the MSIVs close and are not reopened, the control rods fail to insert, the SRVs function as designed, and the recirculation pumps trip automatically. Subsequently, the SET encompassed plant phenomena, plant systems, operator actions, and EPGs. Reference 4 describes each event tree heading and corresponding success criteria.

Four sequences were identified in the SET as being most likely to result in core and/or containment damage. All four satisfied the entry conditions described in the previous paragraph, and all four included failure of boration and failure of manual rod insertion. Unique features of the four most likely sequences are outlined below.

1. Sequence 483[a] is essentially a plant automatic transient. The high pressure ECC systems maintain core cooling; however, continual large steaming rates eventually threaten containment integrity.
2. Sequence 551 describes a transient with early failure of HPCI and no RPV depressurization. A high pressure boiloff ensues, leading to core damage. (Subsequent analyses have indicated that RCIC and CRD flow together may be sufficient to limit fuel rod heatup.)
3. Sequence 465 is similar to Sequence 483 except that the operator takes level control by throttling the HPCI. Core steaming is reduced; however, containment integrity is threatened.
4. Sequence 482 is similar to Sequence 483 except the operator takes pressure control. Again, core steaming is sufficient to pose a threat to containment integrity

4.3 Application of the SET

Evaluation of the four most likely sequences from the SET revealed a striking similarity between three of them. The similarity is best described in terms of consequence level. A qualitative discussion of the plant automatic transient follows, which delineates this point.

The plant automatic transient (Sequence 483, described quantitatively in Section 5.1) begins with the common transient initiator, i.e. MSIV closure, scram failure, SRVs operate as designed, and recirculation pumps trip. In the absence of boration, the RPV steams through the SRVs to the PSP at ~21% of rated flow. Makeup is provided by the HPCI, RCIC, and CRD systems. HPCI will shift suction from the CST to the PSP on an indicated PSP high water level. HPCI eventually fails due to high PSP water temperature, which is used to cool lube oil for the HPCI turbine bearings. Following HPCI failure, reactor power is reduced to less than 5% as RCIC and CRD provide the only makeup.

PSP heatup continues, which pressurizes the PSP, and pressure is relieved to the drywell. The high drywell pressure combined with the already low downcomer level trips the ADS. Following a 120 s delay, the RPV depressurizes through the ADS valves[b] to the PSP. Low pressure ECC systems flood the RPV resulting in power excursions, which increase the

a. Sequence numbers are provided for consistency with Reference 4.
b. When the automatic depressurization system is activated, six pressure relief valves open automatically, relieving RPV pressure to the PSP.

steaming rate to the PSP. The ADS valves will close on high containment pressure (115 psia). The RPV then pressurizes above the low pressure ECCS shutoff heads. HPCI has failed, RCIC has isolated (at 40 psia drywell pressure), and containment failure is imminent. Core damage is expected from the assumed loss of all ECCS injections following containment failure.

The level control transient (Sequence 465) differs from the plant automatic transient only in the timing of events. It is assumed that at some time the operator lowers downcomer water level by throttling HPCI. This action reduces the RPV steaming rate, and delays the time of HPCI failure. Following HPCI failure, the events are identical for the two transients albeit shifted in time.

During the pressure control transient (Sequence 482), the operator depressurizes the RPV in accordance with the heat capacity temperature limit. The depressurization results in a power reduction during HPCI operation. However, with pressure control, the low pressure ECC systems will start injection when RPV pressure drops below the shutoff head of the pumps.

Although shifted in time, the three transients exhibit the same consequence level. This consequence level is characterized by containment failure, and subsequent expected core damage (see Reference 4).

The SET formulation of the high pressure boiloff transient (Sequence 551) assumed that HPCI failure was sufficient for entry into a potential boiloff situation. Subsequent analyses showed that RCIC and CRD flows were sufficient to delay and limit core heatups. Four situations were postulated, which would result in RCIC unavailability and a resulting core boiloff.

1. Because the RCIC system is nonsafety grade, there is a remote possibility that it would be out of service at the time that the MSIV closure ATWS occurred.

2. During combined HPCI, RCIC, and CRD flow situations, the downcomer level may recover such that HPCI and RCIC are tripped off. A manual reset is required to restart RCIC injection.

3. During simulator sessions conducted by the Oak Ridge National Laboratory (ORNL) at the Tennessee Valley Authority (TVA), it was observed in some situations that the operator would shift RCIC suction to the PSP following the automatic HPCI shift. This would lead to RCIC failure on high lube oil temperature.

4. If the primary containment pressurizes above 40 psia, high turbine exhaust pressure will isolate the RCIC turbine.

The plant automatic transient provides a description of a MSIV closure ATWS without operator action. It exhibits the same consequence level as transients with level or pressure control only. In addition, it was found that the transient degraded into a high pressure boiloff when the ADS valves close because of high containment pressure.[a] The RPV then pressurized above the low pressure system shutoff heads. Since HPCI and RCIC were no longer available, a high pressure boiloff ensued. For that reason, the plant automatic transient was chosen as the vehicle for describing the dominant sequences identified by the SET. Results from the plant automatic transient simulation are presented in Section 5.1 (RPV and primary containment) and Section 6 (fuel damage).

---

a. In the relief mode of SRV operation (including ADS), air pressure is applied to the air actuator by energizing a solenoid-operated control air valve. The resultant pressure differential across the bellows of the remote air actuator causes the SRV to open. Because the compressor supplying control air lies outside the primary containment, when the pressure inside the containment rises to the pressure of the control air, the remote air actuator will no longer be capable of maintaining the SRV in an open position.

5. RPV AND PRIMARY CONTAINMENT RESULTS

Results from several MSIV closure ATWS simulations are presented in this section. The simulations were performed with RELAP5/MOD1.6[6] and CONTEMPT/LT-028.[7] RELAP5 was used to model the RPV and associated internals, the feedwater line, and the main steamlines. Also modeled were the SLCS, CRD system, and ECC systems. Appendix A contains details of the RELAP5 modeling. CONTEMPT modeled the primary containment, specifically the drywell and PSP. Also modeled were associated heat structures and flow paths. The CONTEMPT model is discussed in more detail in Appendix B.

The simulations were performed in an iterative manner. RELAP5 provided boundary conditions to CONTEMPT in the form of mass and energy rates through the SRVs. CONTEMPT in turn provided event timings back to RELAP5. Figure 11 illustrates the information exchanged between the two codes.

Five MSIV closure ATWS simulations are presented. The plant automatic transient is discussed in Section 5.1. Section 5.2.1 discusses an EPG nominal simulation with maximum SLCS effectiveness, and Section 5.2.2 considers the case with minimum SLCS effectiveness. Section 5.2.3 looks at the effect of not depressurizing the RPV when the HCTL is reached. The effect of increasing SLCS capacity to 86 gpm (per NRC final rule on ATWS)[8] is discussed in Section 5.2.4. Table 2 summarizes the simulations presented.

5.1 Plant Automatic Simulation

The plant automatic simulation illustrates the automatic progression of a postulated ATWS in the absence of operator actions. Without mitigating actions, the containment could fail by overpressurization and it has been common practice in PRAs to assume that this would lead to the loss of the ECC systems. Loss of injection to the RPV leads to core uncovery and subsequent fuel damage. This simulation is bounding in that it provides a realistic estimate of the minimum time to containment and fuel damage.

Events occurring during the early portion of a MSIV closure ATWS (Table 1) are well defined. MSIV closure causes a rapid pressurization of the RPV because the core continues to produce steam at near rated conditions. Increased pressure collapses voids in the core which provides positive reactivity feedback. Increased power results, which increases the core steaming rate. The increasing pressure causes the recirculation pumps to trip (at 1135.0 psia), and the SRVs to open.

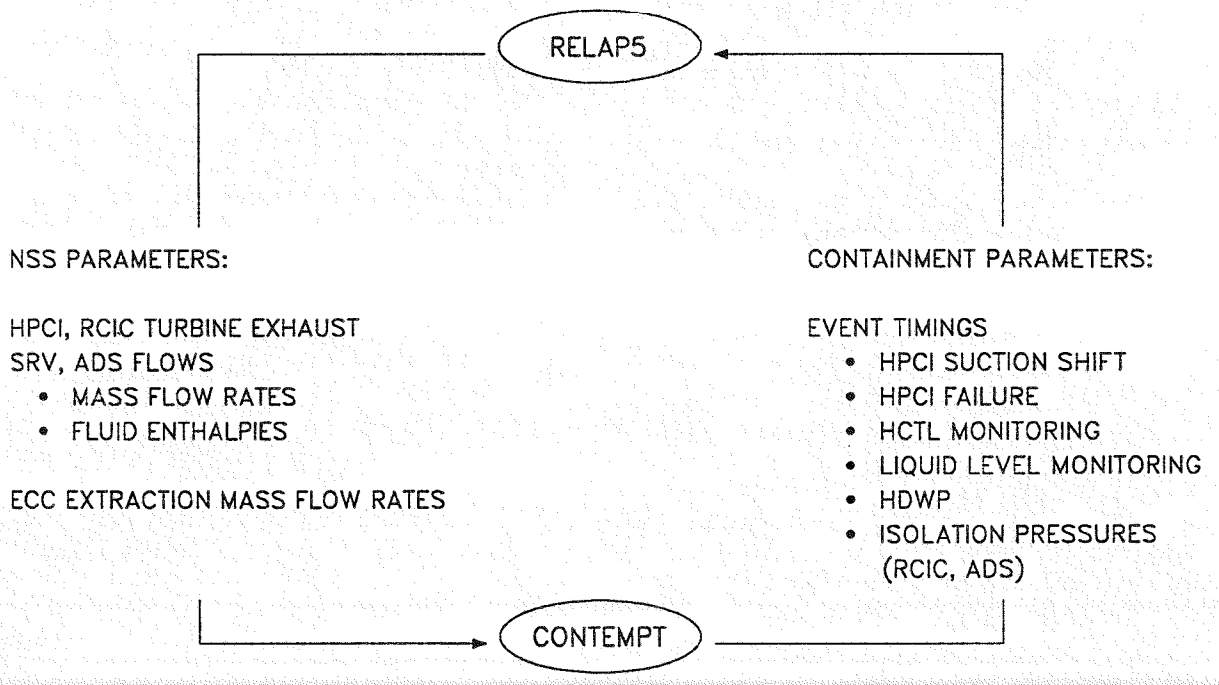

Figure 11. Information exchange between RELAP5 and CONTEMPT.

Table 2. MSIV closure ATWS simulations

Simulation	Description	Boron Modeling	Level Control	Depressurization
1	Plant automatic	None	No	Yes (automatic ADS)
2	EPG nominal—maximum SLCS effectiveness	50 gpm isotropic	Yes	No (pressure control, not depressurization)
3	EPG nominal—minimum SLCS effectiveness	50 gpm stratified	Yes	Yes (manual blowdown)
4	Minimum SLCS effectiveness without depressurization	50 gpm stratified	Yes	No
5	EPG nominal—increased SLCS capacity and minimum effectiveness	86 gpm stratified	Yes	No

MSIV closure isolates the steam supply of the feedwater turbines from the RPV. As the feedwater turbines and pumps rapidly coast down, turbine-driven feedwater is lost. Continued core steaming causes the vessel downcomer level to decrease. When lo-lo level (476.0 in.) is reached, HPCI and RCIC systems are activated. Taking suction from the CST, HPCI pumps 5000 gpm and RCIC pumps 600 gpm of high pressure makeup into the RPV via the feedwater line. For the purposes of these analyses, it was assumed that a scram signal was generated but no control rods were inserted. Following the scram signal, 112 gpm of water was pumped into the RPV by the CRD system. Figure 3 illustrates the flow alignment described above.

Following recirculation pump trip, the reactor stabilizes in a natural circulation mode. Core power is determined from the mass flow rates and enthalpies of the injected water. The resulting power with HPCI, RCIC, and CRD injection is ~30% of rated. This causes a steaming rate of ~21% of normal steamline flow to be relieved to the PSP. The difference in core power and RPV steaming rate is accounted for by the heating of the highly subcooled ECC fluid.

The RPV stabilizes to a quasi steady state condition in less than 100 s after transient initiation. Steam produced in the core is relieved to the PSP through the cycling of two to four SRVs (SRV setpoints are listed in Table A-5). As the steam is condensed in the PSP, the PSP heats up at the rate of ~6F°/min. At 255 s, the PSP water level has risen to the upper limit of its normal operating range (181.25 in.). This causes the HPCI suction to automatically and irreversibly shift from the CST to the PSP. After the shift, PSP water is used to cool the lube oil for the HPCI turbine bearings. These bearings will eventually fail as the PSP water temperature continues to increase, resulting in the loss of HPCI flow. For the purposes of this simulation, it was assumed that HPCI failed when the PSP temperature reached 190°F (at 830 s).

Following HPCI failure, the core power decreases as only RCIC and CRD flow enter the RPV and downcomer level decreases. Together, they provide sufficient core flow to maintain power at 3-4% of rated. Even though the downcomer water level drops below TAF, sufficient core cooling is provided to delay rod cladding heatup from occurring.

The PSP pool temperature continues to increase, but at a slower rate following HPCI failure. The bulk PSP temperature is calculated to reach 200°F at 924 s, and at that time complete condensation is no longer ensured. When the RPV steam is no longer completely condensed in the pool, some of it will flow through the pool directly to the PSP atmosphere. The pressure in the PSP increases and is relieved to the drywell. The drywell in turn is pressurized, with a high drywell pressure (HDWP) signal occurring when the drywell reaches 2.45 psig. This is predicted to occur at 985 s based on linear departure from complete condensation at 200°F.[a]

Two signals are required for initiation of the ADS: lo-lo-lo water level (Figure 2) in the RPV and HDWP.

a. For this model, complete condensation is calculated in the pool until it reaches 200°F. Condensation efficiency is then calculated to decrease linearly to zero as the pool approaches saturation temperature (~218°F).

Low water level is predicted to occur early in the transient (<100 s). Later, the HDWP signal initiates the ADS timer, and the ADS valves open following a time delay of 120 s. At 1105 s, the six relief valves dedicated to the ADS open and rapidly depressurize the RPV. When RPV pressure reaches the shutoff heads of the low pressure ECC systems and condensate booster pumps, they flood the RPV with cold water (210°F). Shutoff heads for LPCI, core spray, and condensate systems are 346, 355, and 418 psia, respectively. The design capacities of LPCI, core spray, and the condensate booster pumps are 40,000, 12,500, and 30,000 gpm, respectively. RPV flooding results in a large positive reactivity insertion. Core power increases rapidly, producing steam faster than it can be relieved through the ADS relief valves. The increased steam production raises RPV pressure above the shutoff heads of the low pressure injection systems, terminating their injection. The pressure increases until the remaining SRVs lift. With low pressure injection to the RPV stopped, moderator voiding in the core terminates the power excursion. RPV water level drops, and pressure is relieved through the ADS valves which are automatically held open by control air. When RPV pressure drops below the low pressure injection system shutoff heads, they again begin injection. The cycle of core flooding, power excursion, and pressure relief thus repeats itself.

Primary containment pressure increases rapidly as a result of the power excursions. At 1800 s, containment pressure reaches 40 psia, which isolates RCIC on high turbine exhaust pressure. At 2100 s, containment design pressure (71 psia) is reached. After seven power cycles, the ADS valves close when containment pressure reaches 115 psia at 2470 s.

With the ADS valves closed, the RPV remains at high pressure (~1100 psia) with SRV cycling. This prevents the injection of water by low pressure makeup systems. Because HPCI has failed and RCIC has isolated, the CRD system provides the only injection to the RPV. The downcomer water level drops to the jet pump suction elevation as water is boiled off in the core. Pressure is maintained around 1100 psia by the cycling of one SRV. The continued core steaming is relieved to the primary containment, which is predicted to reach failure pressure (132 psia) at 2700 s. CRD flow alone is not sufficient to maintain core cooling even at very low decay power levels. As a result, rod heatups are predicted to begin at approximately 4000 s.

RPV pressure during the plant automatic simulation is shown in Figure 12. The predicted peak pressure of 1272 psia occurs at 11 s. Pressure is maintained near

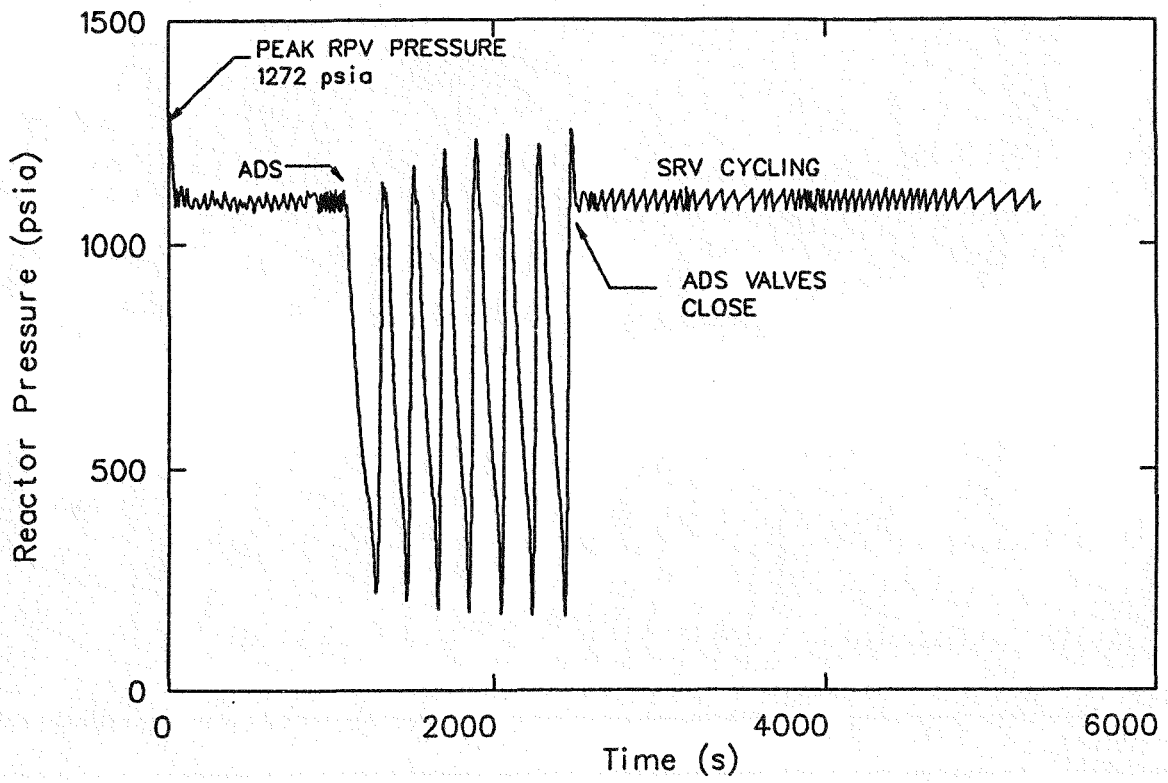

Figure 12. Plant automatic transient—RPV pressure.

1100 psia by SRV cycling until ADS blowdown begins at 1105 s. The pressure drops to almost 200 psia before it turns around from increased core steaming caused by low pressure injection to the RPV. Following repressurization, the cycle of blowdown, RPV flooding, and repressurization repeats. In all, seven cycles were predicted until 2470 s when the ADS valves closed. Following ADS valve closure, pressure was again maintained near 1100 psia by SRV cycling.

The predicted core power is shown in Figure 13. MSIV closure causes a peak power of 253% at 3 s (subsequent pressure spikes are caused by low pressure injections). The power levels off following recirculation pump trip to 30% as the high pressure systems maintain injection. HPCI failure at 830 s causes a power reduction until low pressure injections begin at 1240 s. The seven predicted injection cycles are clearly illustrated with the corresponding power excursions. Following ADS valve closure at 2470 s, the power decreases to decay levels with only CRD flow injecting to the RPV.

PSP pool temperature steadily increases as shown in Figure 14. The temperature reaches 200°F at 924 s, and saturation temperature (218°F) at 1220 s. Figure 15 illustrates the predicted drywell pressure response. The pressure increases rapidly as a result of the power excursions, with failure pressure (132 psia) predicted to occur at 2700 s.

With the fuel rod cladding heating up due to lack of coolant, the simulation was terminated at 5600 s. At that time peak cladding temperature was ~1600°F, which is above the threshold temperature for cladding oxidation. At that temperature, zircaloy fuel rod cladding will react with steam to oxidize the cladding and produce hydrogen. Core inlet conditions were taken from the RELAP5 calculation and input to the Severe Core Damage Analysis Package (SCDAP). SCDAP was then used to predict fuel damage during the high pressure boiloff. Results from the fuel damage analysis are presented in Section 6.2.

In addition, the possibility of fuel damage during the power excursions caused by low pressure injections was examined. A best estimate fuel rod analysis program (FRAP-T6) was used for that analysis, and results are included in Section 6.1.

Table 3 lists predicted event timings after 100 s for the plant automatic transient. It is realized that the latter stages of the plant automatic transient could very well proceed differently than in this simulation. For instance, containment failure could possibly affect RPV penetrations, resulting in RPV depressurization. These possibilities, however, are beyond the scope of this

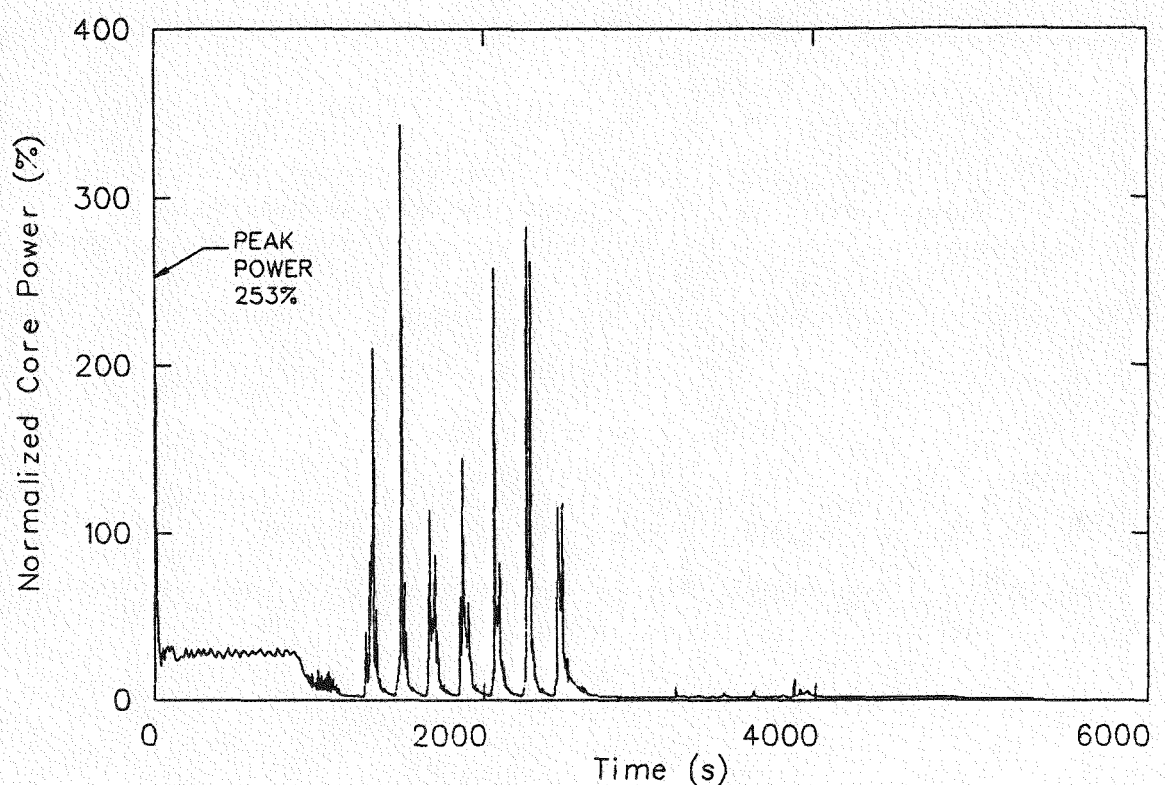

Figure 13. Plant automatic transient - normalized core power.

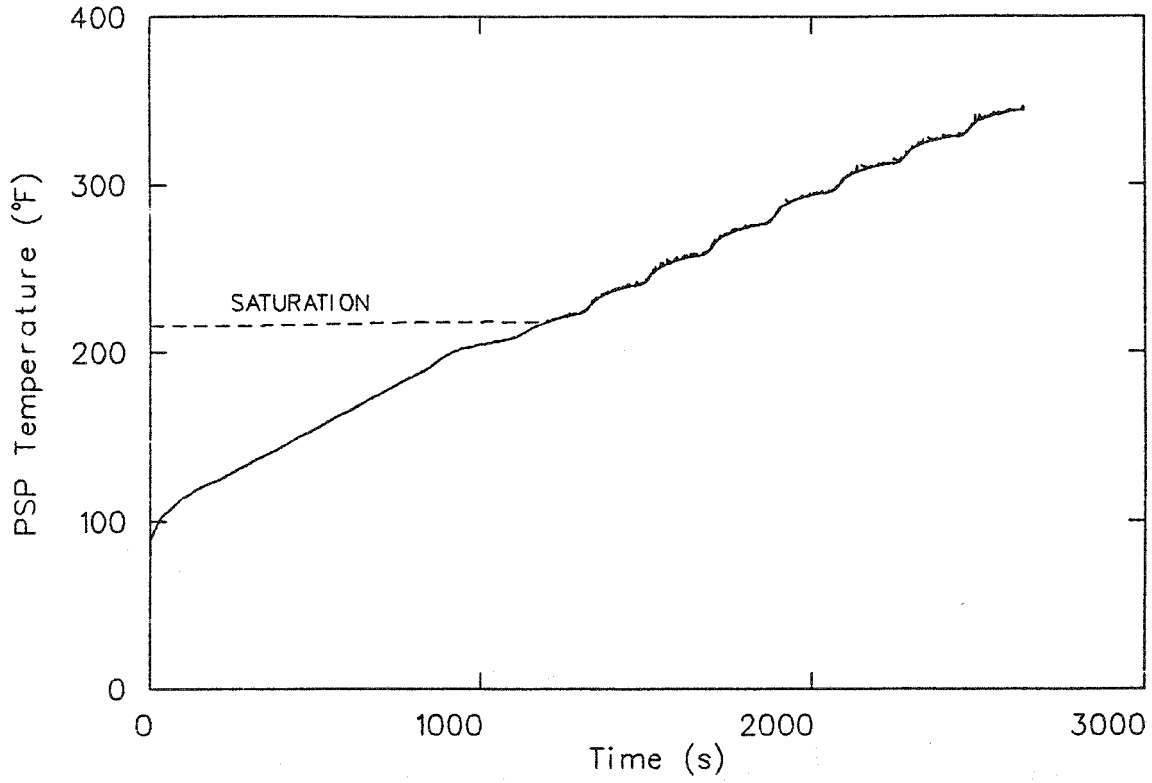

Figure 14. Plant automatic transient - pressure suppression pool temperature.

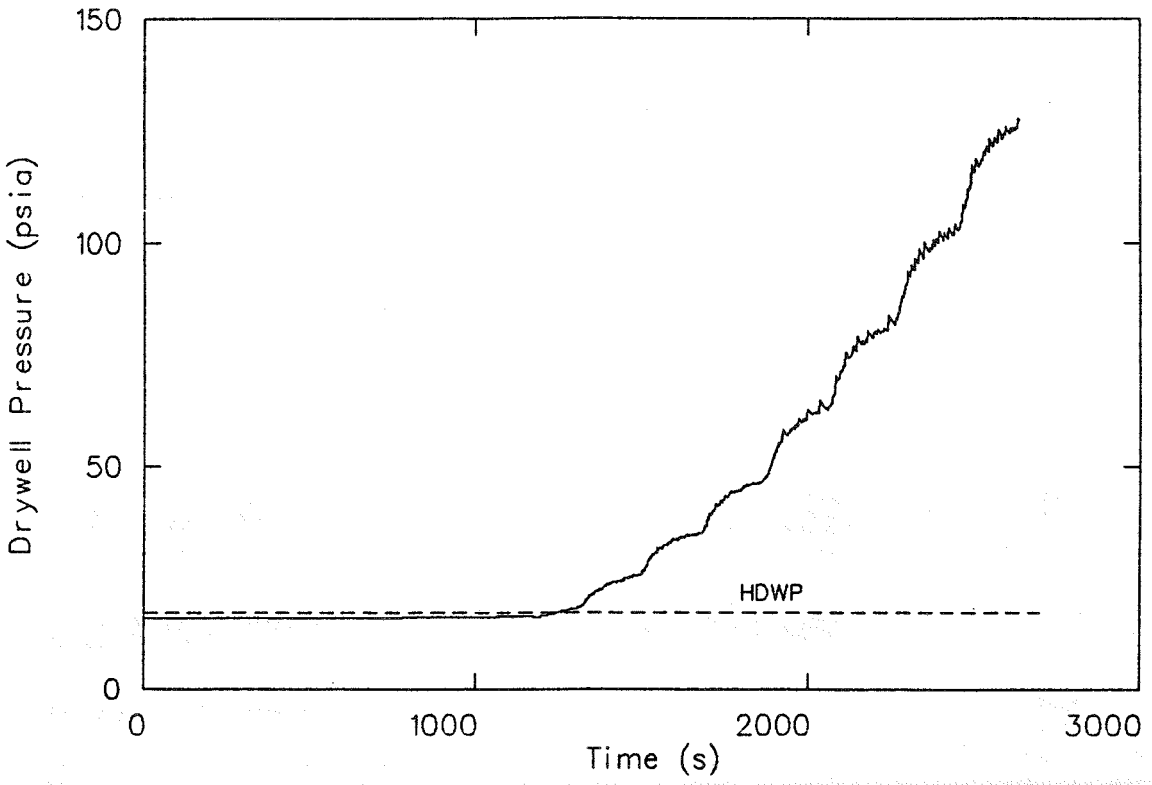

Figure 15. Plant automatic transient - drywell pressure.

Table 3. Plant automatic transient event timings after 100 s[a]

(s)	Event
0	Transient initiation
255	HPCI suction shift to PSP
830	Assumed HPCI failure (PSP pool at 190°F)
985	High drywell pressure (2.45 psig)
1105	Automatic depressurization (ADS)
1220	PSP at saturation temperature
1240	First low pressure injection
1270	First power excursion
1800	Drywell pressure at 40 psia (RCIC isolation)
2100	Primary containment at 71 psia (design pressure)
2470	ADS valves close
2700	Primary containment at 132 psia (predicted failure pressure)
4000	Rod heatup from boiloff begins

a. Event timings as predicted by RELAP5/MOD1.6 and CONTEMPT/LT-028.

analysis because of uncertainties inherent in the sequence progression. For the purposes of this study it was assumed that the CRD hydraulic system remained operational throughout, but all other injection systems fail when the containment fails.

5.2 Simulation of Operator Actions

The plant automatic transient described in Section 5.1 illustrated that containment and fuel damage are expected to occur during a MSIV closure ATWS without operator actions. Describing the automatic response to an ATWS is valuable in understanding possible event progressions. It also provides an estimate of the minimum time to damage. It is, however, more realistic to assume that the operator would take actions to mitigate the accident. The effectiveness of the operator to shutdown the reactor in a timely manner is the subject of this section. It is recognized that the timings and extent of operator actions are infinite. For the purpose of these simulations, a series of actions were modeled. That series was termed "EPG nominal," and is described in the following paragraphs.

5.2.1 EPG Nominal-Maximum SLCS Effectiveness. As described earlier, a quasi steady state condition would be reached automatically in less than 100 s following transient initiation. During this time, the operator has entered the EPGs (upon MSIV isolation) and is monitoring the status of the plant. While monitoring reactor power (RC/Q path on Figure 5), the operator would be directed to initiate SLCS when the PSP temperature reached 110°F, which occurs 78 s after transient initiation. It is assumed, however, that operator actions will not begin before 120 s. This is believed to be a reasonable estimate of the minimum time required to assess the situation and act appropriately.

This simulation assumes maximum SLCS effectiveness. When the boron solution begins injection, the 50 gpm flow is modeled to be distributed isotropically in the RPV. This is accomplished by assuming that the boron solution is transported with the liquid in the RPV. It is acknowledged that this modeling is idealistic and will result in the maximum possible effect of the boron injection. Section 5.2.2 presents a simulation of the same transient, but the boron injection is modeled in such a way as to minimize its effectiveness.

At 120 s, when the operator first takes action, the core power is ~30%. HPCI, RCIC, and CRD flows are providing 5712 gpm of high pressure makeup from the CST to the RPV. Steam is being relieved through the SRVs to the PSP, which has a pool temperature

of 117°F and is heating up at ~6F°/min. As directed by the EPGs, the operator initiates SLCS and enters Contingency #7. It is also assumed that at 120 s the operator terminates HPCI and RCIC flow as directed by Contingency #7. In line with the RC/P control path (Figure 6), pressure control by the operator is also assumed. Pressure control means to reduce pressure to eliminate SRV cycling; it does not mean depressurization.

Figure 16 illustrates the effects of these actions on the downcomer water level. When HPCI and RCIC are shut off, the level rapidly falls, reaching TAF (366 in.) at ~220 s. The operator, following Contingency #7, would then start HPCI and RCIC injection (at reduced rates) to maintain level at TAF. The overshoot at 450 s and subsequent decrease to the TAF level are indicative of the expected time response of the level to changes in injection rates. At 1585 s, 265 lb of sodium pentaborate has been injected in the RPV, an amount sufficient to place the reactor in hot shutdown.[a] At that time, the operator is directed (by Contingency #7) to restore and maintain normal water level. This is simulated by injecting HPCI and RCIC at full flow. The level recovers to normal level at ~2000 s. Figure 17 shows the combined injection rates of the high pressure systems.

The effect of boron injection combined with level control is dramatic. Core power (Figure 18) decreases to less than 10% by 200 s, and approaches decay levels by 600 s. The PSP heatup rate is reduced considerably as a result of the low power levels. As shown in Figure 19, the PSP pool reaches a maximum temperature of 144°F when the simulation was terminated at 2800 s. After RPV level recovery at 2000 s, it is anticipated that the operator would be able to initiate the torus cooling mode of the RHR system. This would terminate the PSP heatup and begin cooling down the pool.

5.2.2 EPG Nominal-Minimum SLCS Effectiveness. When SLCS is initiated at 120 s and the boron solution moves isotropically in the RPV, the reactor is calculated to be shutdown with a PSP temperature of 140°F. In reality, the boron solution may not be well mixed and could stratify in the lower plenum

a. A conservative estimate of the boron mass in the RPV required for hot shutdown is 265 lb. At 50 gpm, this would require approximately 1465 s of injection. Thus, with SLCS initiation at 120 s, the required amount would be injected 1585 s after transient initiation.

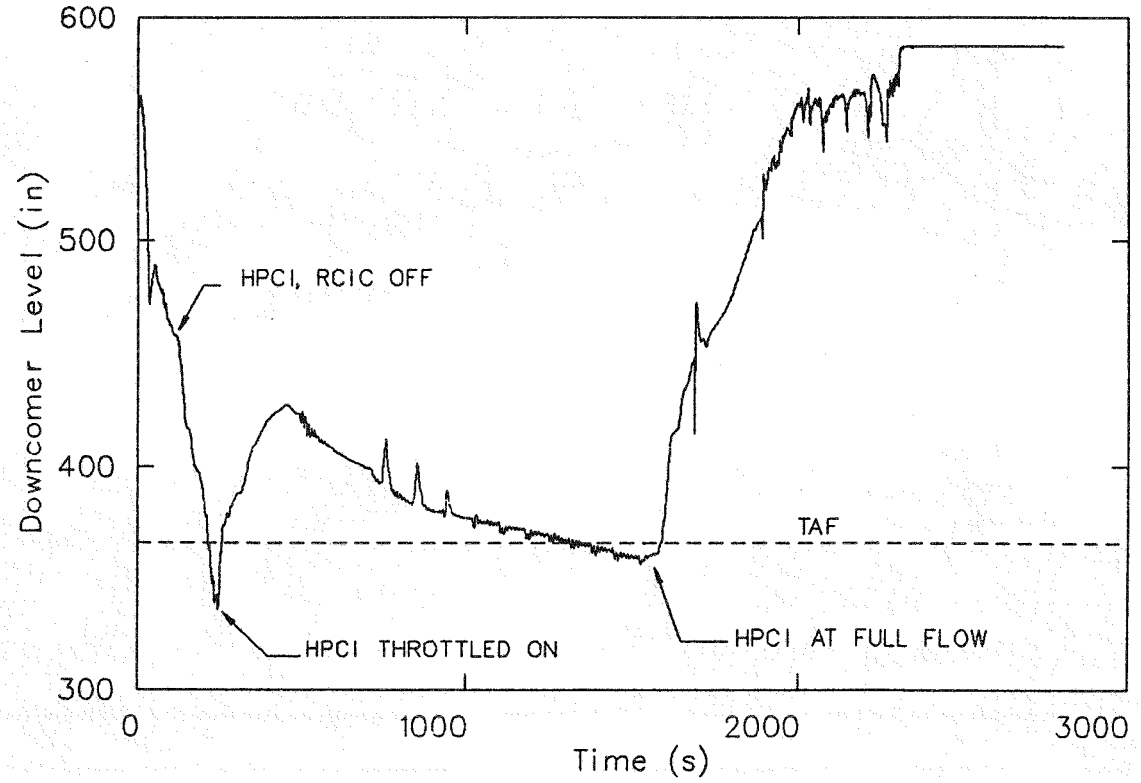

Figure 16. Isotropic boron - downcomer water level.

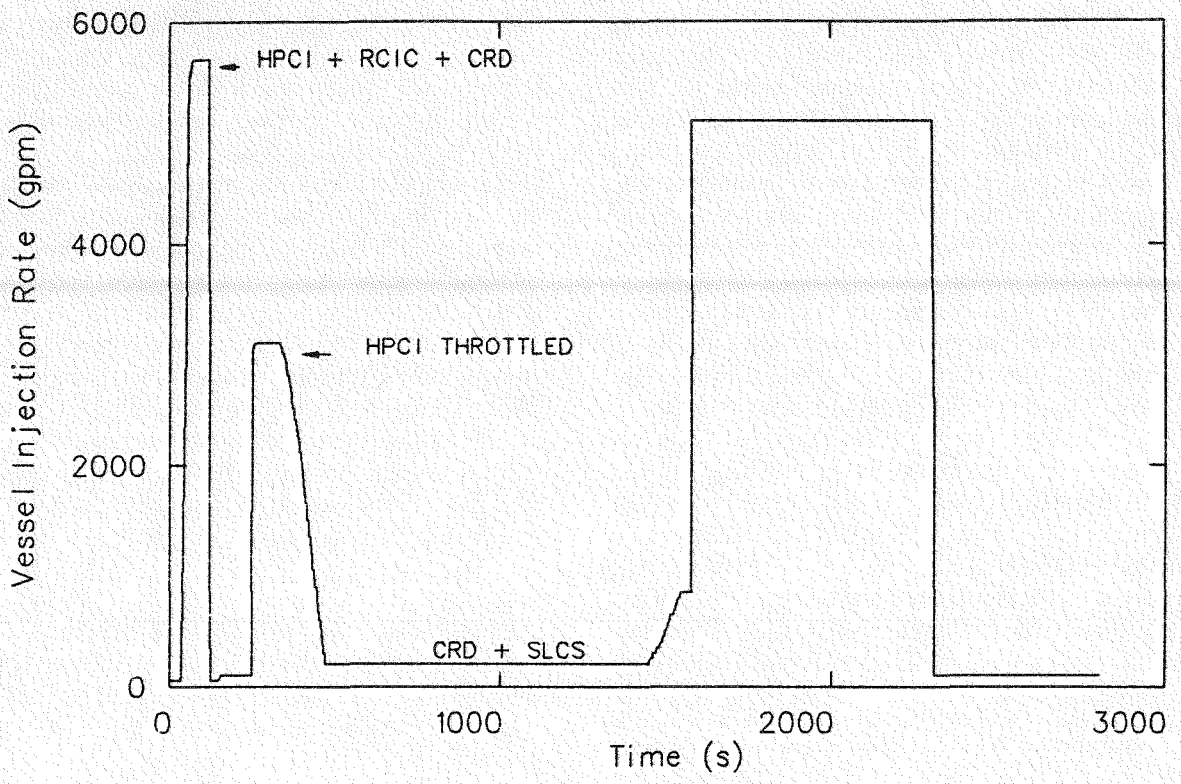

Figure 17. Isotropic boron - injection rate to the RPV.

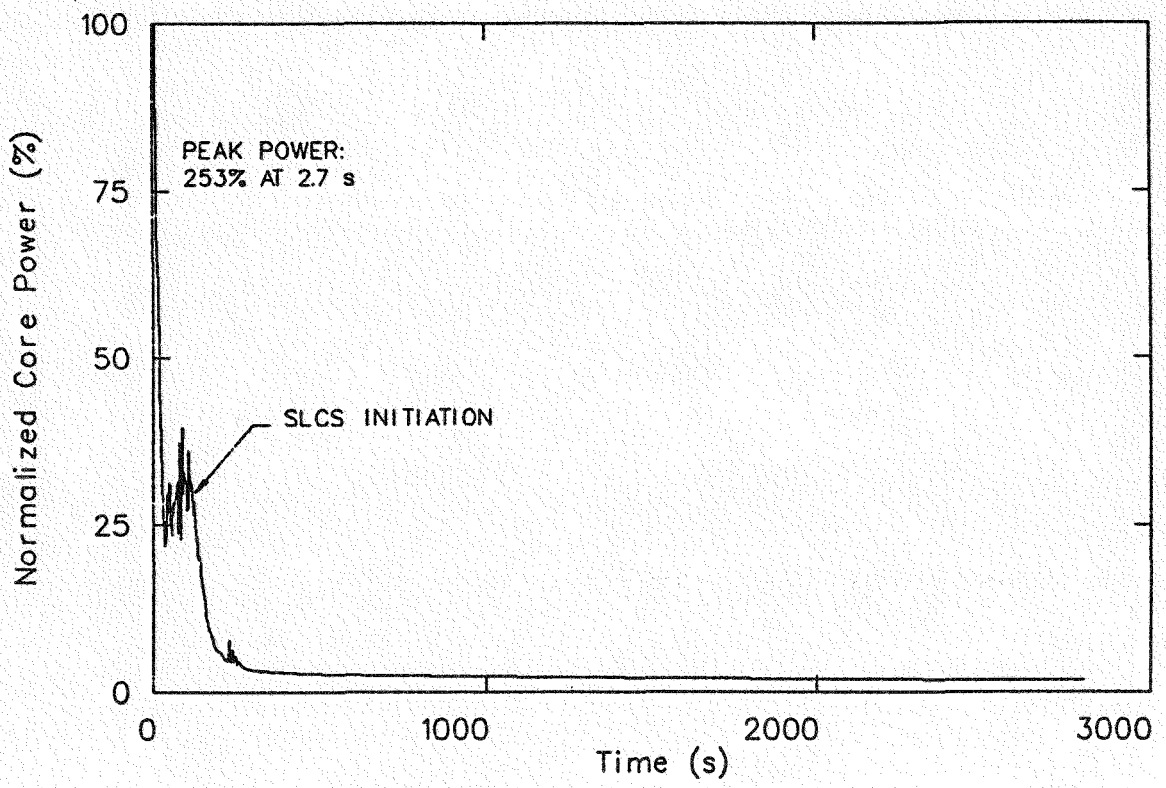

Figure 18. Isotropic boron - normalized core power.

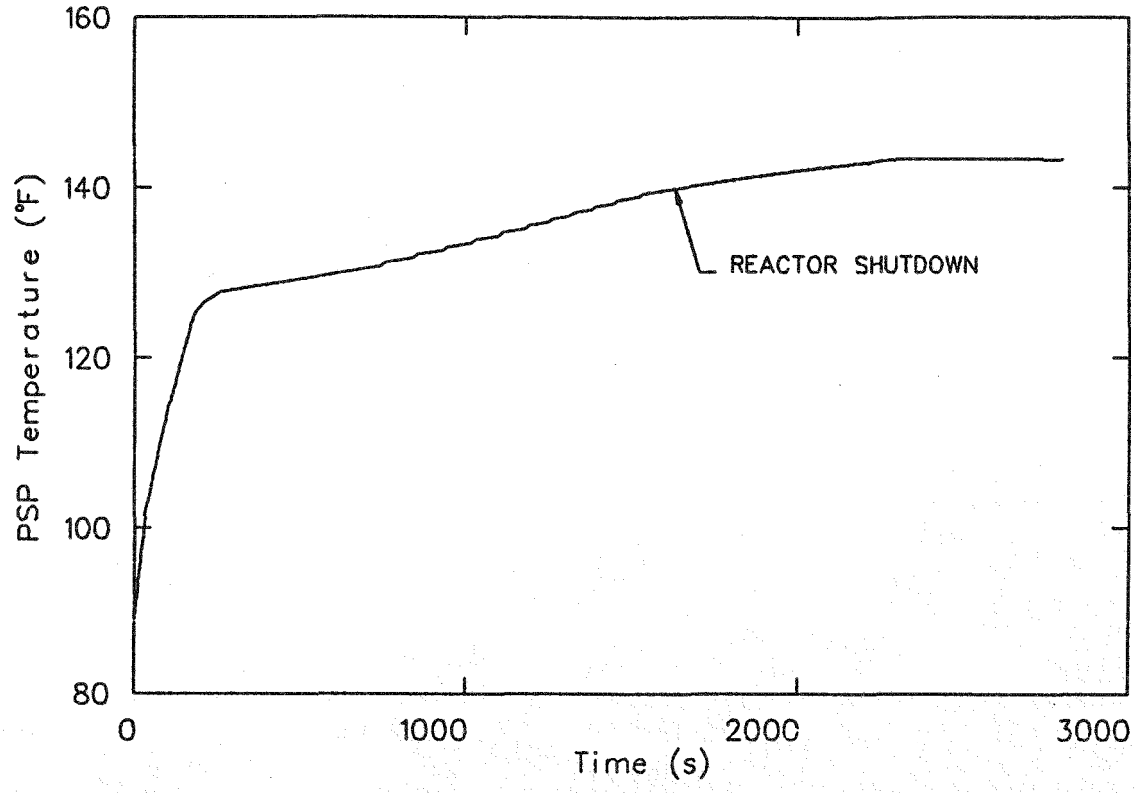

Figure 19. Isotropic boron - pressure suppression pool temperature.

during level control. When the downcomer water level is raised back to normal level, the stratified boron would be transported into the core. To bound the system response, a simulation was performed with minimum SLCS effectiveness. This was modeled by assuming that the boron would be entirely stratified in the lower plenum until 1585 s. At that time the 265 lb of boron solution in the lower plenum would be transported into the core when the water level was raised in the downcomer. Thus, no effect of boron on core power was seen before 1585 s. The remainder of the simulation was modeled identical to the previous case (Section 5.2.1).

The simulation proceeds automatically until 120 s, when HPCI and RCIC injections are terminated. At the same time the SLCS is initiated and begins injecting 50 gpm into the lower plenum. The boron worth, however, is assumed to be zero until 1585 s. The RPV water level (Figure 20) drops rapidly until throttled HPCI flow recovers and maintains it slightly above TAF. An injection flow rate of 3800 gpm is required to maintain level at TAF. This results in a core power of ~17%, as shown in Figure 21. The effect of reduced core power on PSP heatup is shown in Figure 22. With HPCI and RCIC at full flow, the core power of ~30% resulted in a heatup rate of 6F°/min. With level control (HPCI throttled), the 17% core power resulted in a 4F°/min. heatup rate.

Level control is effective in reducing core power and hence PSP heatup. However, without negative reactivity insertion from control rods or boron, the PSP continues to heatup. At 875 s, the HCTL (Figure 7) is reached with the PSP at 165°F. The operator, monitoring this temperature, is instructed by the EPGs to maintain RPV pressure below the limit. It is assumed that the operator would open the six relief valves dedicated to the ADS and blowdown the RPV. The resulting RPV pressure response is shown in Figure 23. Opening the ADS valves rapidly depressurized the RPV to below 400 psia. While depressurizing the RPV, Caution #14 of the EPGs "warns the operator not to reduce RPV pressure below the isolation setpoints of steam-driven makeup systems unless motor-driven pumps are available." Since HPCI would isolate when the RPV reached 100 psig, the operator could well be expected to terminate the depressurization before then. For this simulation, the operator was assumed to hold RPV pressure between 300 and 400 psia. That range keeps the pressure below the HCTL and also ensures HPCI operation. It should be noted that there is some uncertainty in modeling the manual depressurization. ORNL has discussed in detail the problems involved with staying below the HCTL

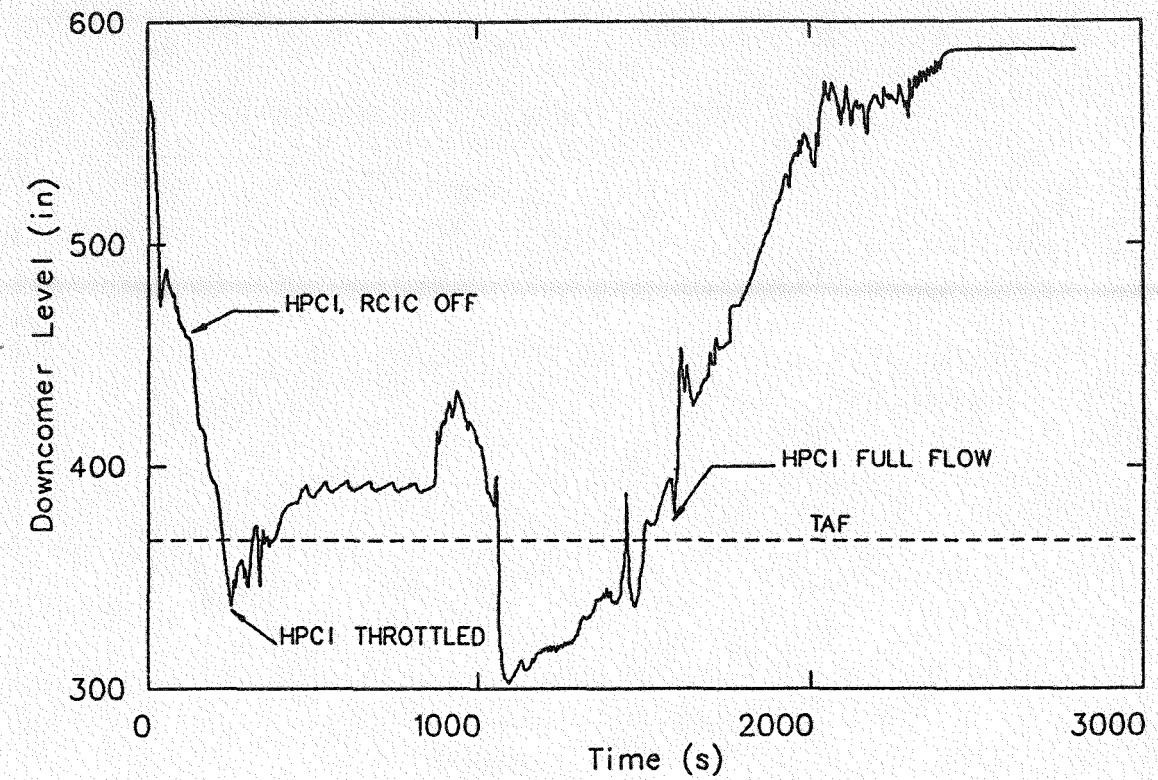

Figure 20. Stratified boron - downcomer water level.

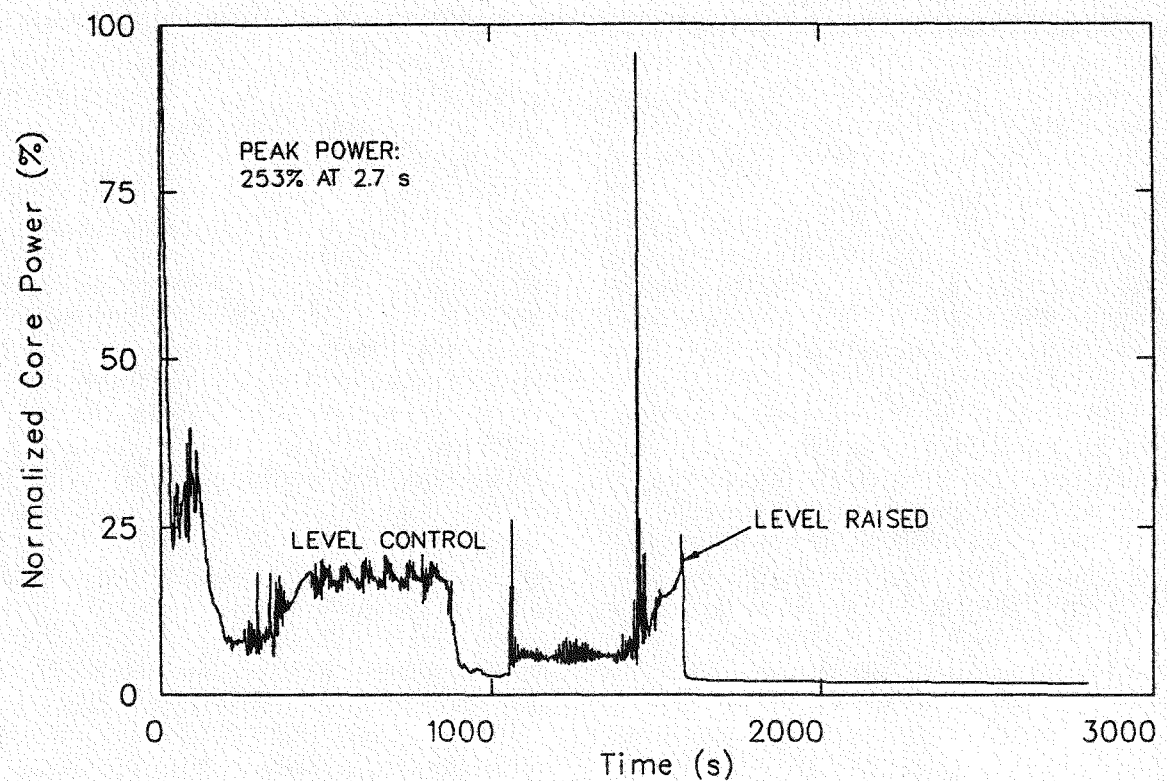

Figure 21. Stratified boron - normalized core power.

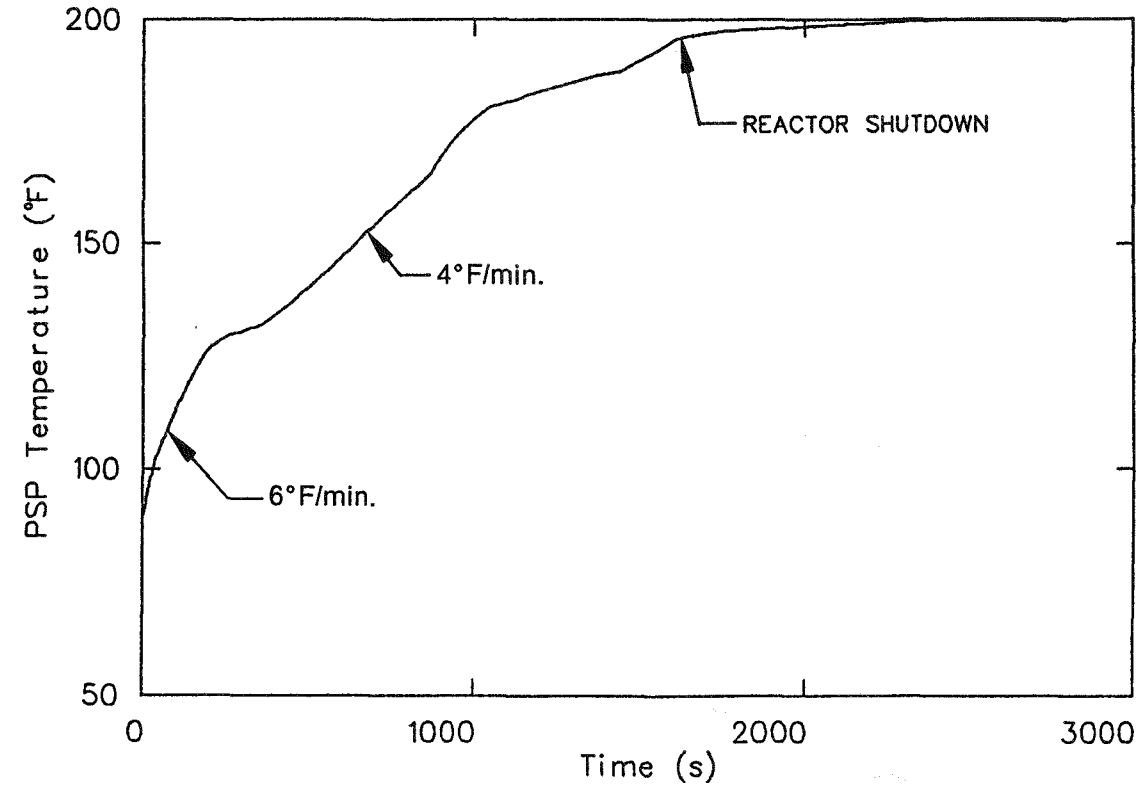

Figure 22. Stratified boron - pressure suppression pool temperature.

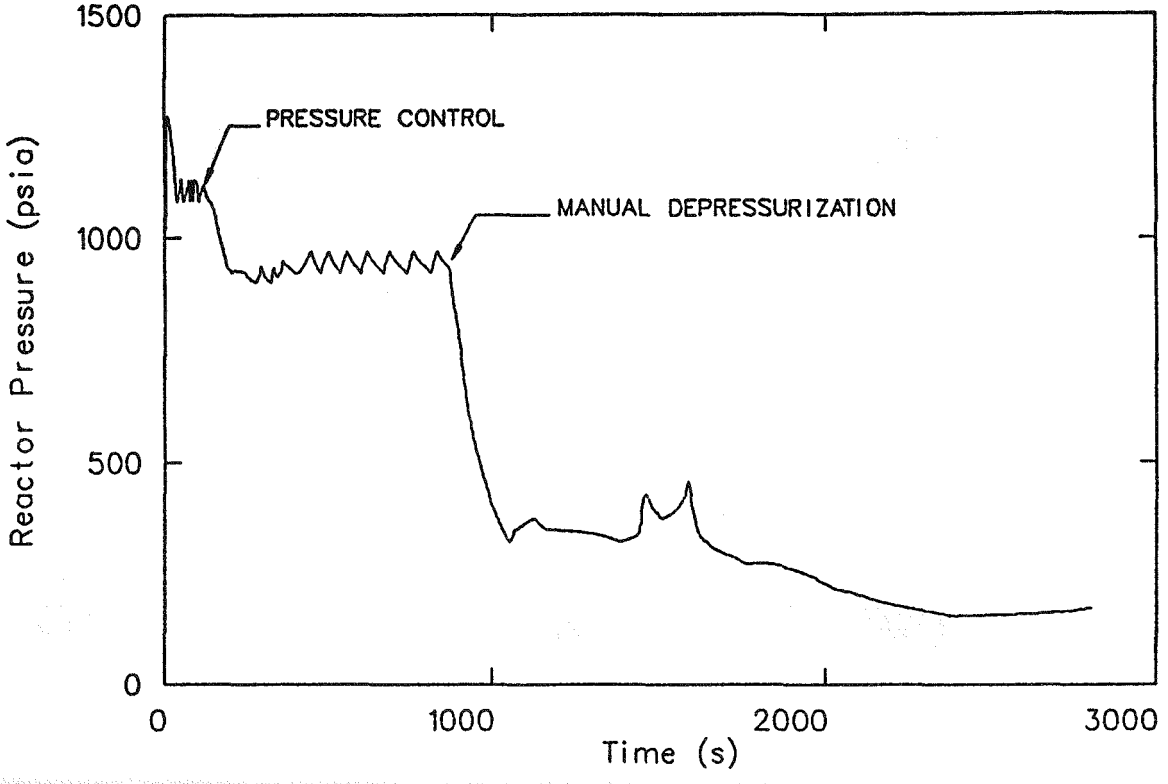

Figure 23. Stratified boron - RPV pressure.

(see Reference 3). The approach taken here is reasonable, but certainly not the only way to model a manual depressurization.

During the depressurization, the PSP experiences increased heatup (Figure 22). However, at 1050 s the heatup rate is lower than before the depressurization. This is because significant void is introduced in the core during the depressurization, reducing core power.

The downcomer water level is raised at 1585 s when 265 lb of boron have been injected. This rapidly shuts down the reactor as the boron enters the core. The PSP pool temperature has reached 195°F at the time of shutdown.

5.2.3 Minimum SLCS Effectiveness—Without Depressurization. As stated previously, the objective of Contingency #7 is to minimize PSP heatup during the time of boron injection, thus avoiding the need for emergency RPV depressurization. Reactor instabilities are possible during a blowdown if the reactor has not been shutdown. The EPGs offer some flexibility, and state that "the operator need not resort to emergency depressurization immediately upon reaching the HCTL." A simulation was performed to assess the effect of not depressurizing the RPV even though the HCTL was reached.

This simulation was modeled identically to that in Section 5.2.2, except no depressurization was modeled. At 120 s, the operator initiated SLCS and began the level control procedure. The boron was assumed to be totally stratified in the lower plenum until 1585 s. The HCTL was reached at 875 s, however, it was assumed that the operator did not depressurize the RPV.

Core power is shown in Figure 24. Following level control, the power steadies out at around 17%. At 1585 s, 265 lb of boron is placed in the lower plenum, and the downcomer water level is raised. Boron is rapidly transported into the core, effecting a hot shutdown.

During level control, the PSP pool heats up (Figure 25) at ~4F°/min. Again the HCTL (165°F in pool) is reached at 875 s, however, no depressurization was modeled. The pool reaches 200°F at 1380 s and saturation temperature (218°F) at 1585 s. At 1600 s, the reactor is shutdown and producing steam at decay power levels. At this time, torus cooling could halt the PSP heatup and gradually cool it down. Assuming complete condensation in the pool, the drywell pressurized slightly but HDWP was not reached.

For this simulation, it was assumed that HPCI was available throughout the transient. At 1220 s, the PSP

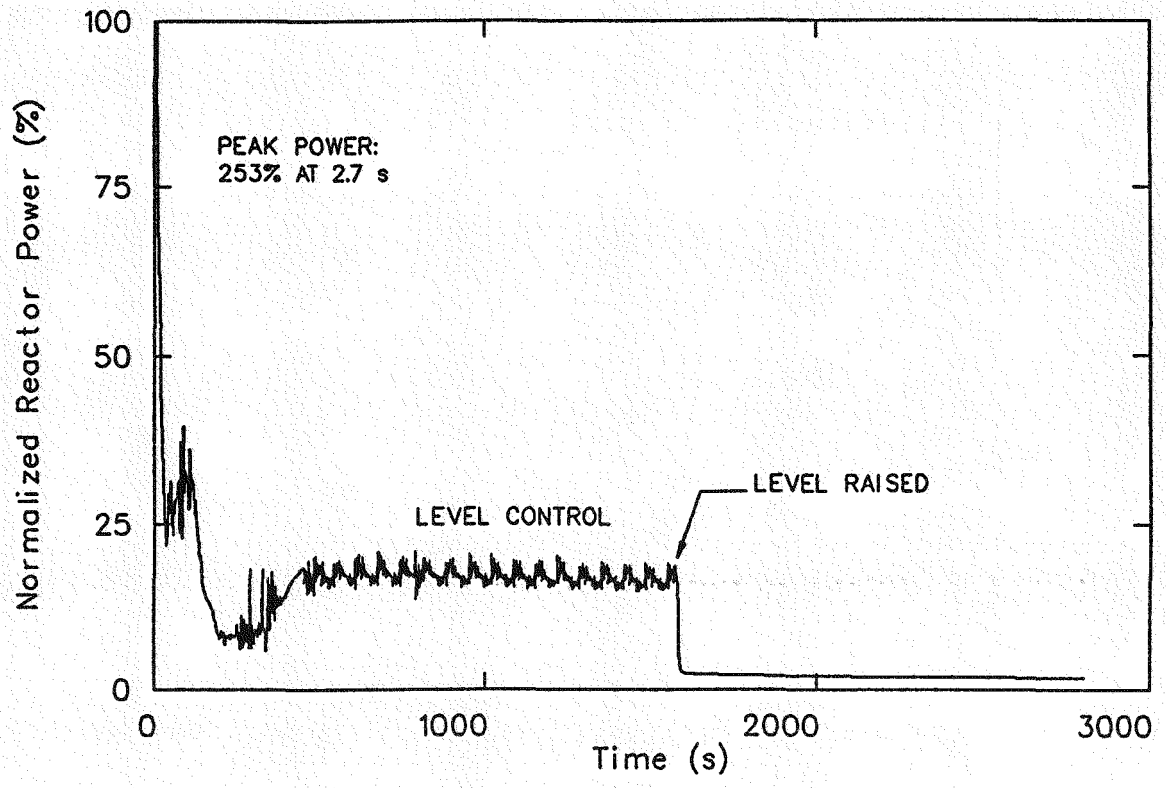

Figure 24. Normalized core power without depressurization.

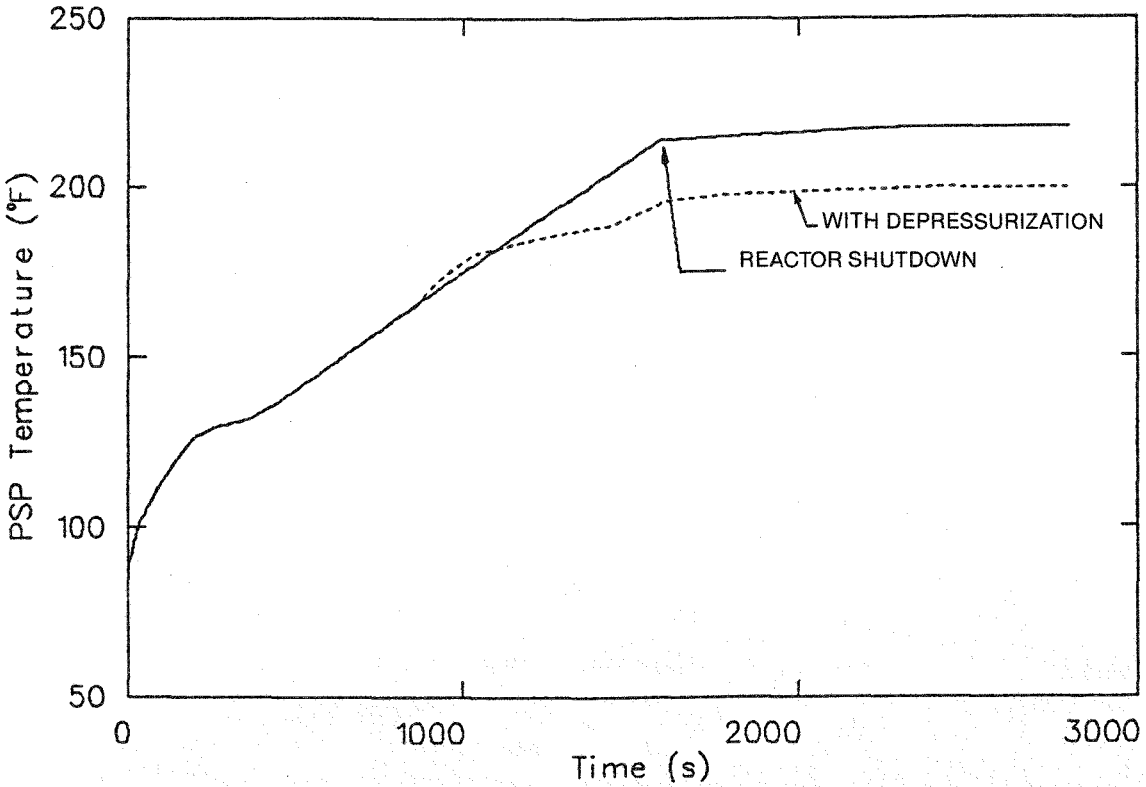

Figure 25. Pressure suppression pool temperature without depressurization.

pool temperature reached 190°F. Because water from the pool is used to cool lube oil for the HPCI turbine bearings, extended operation above that temperature cannot be ensured. If HPCI should fail before the reactor is shutdown, it is unlikely that the remaining high pressure systems would have sufficient capacity to raise downcomer water level to transport boron into the core. Should this be the case, the operator would be required to blowdown the RPV below the low pressure ECC systems injection pressures. This blowdown would occur at a time when there was no condensing capacity left in the PSP.

5.2.4 EPG Nominal—86 gpm SLCS. By bounding the effectiveness of the SLCS, it has been found that PSP pool temperature would range from 140°F to 218°F at hot shutdown. This range is determined by analyzing first, maximum boron effectiveness, and then minimum boron effectiveness. The SLCS capacity used in these analyses was 50 gpm. The NRC's Final Rule[8] for reducing risk from ATWS included the requirement that BWRs have a SLCS with a minimum capacity of 86 gpm of 13% by weight of sodium pentaborate solution. A simulation was performed to assess the effect of this increased flow rate.

For this simulation, it was assumed that the SLCS was initiated at 120 s. The boron solution was modeled to be totally stratified in the lower plenum until 265 lb had been injected. Level control was modeled to begin at 120 s. As before, a core power of ~17% was predicted as a result of level control. At 980 s, RPV water level was raised when 265 lb of boron solution had been injected into the RPV. Figure 26 shows the effect on PSP pool temperature of increased SLCS capacity. With 86 gpm and minimum effectiveness, it is predicted that the reactor would be shutdown in 1000 s. At that time the pool would have reached 173°F, a slight breach of the HCTL. With 50 gpm, shutdown time would be 1600 s with the pool at 218°F. No blowdown was modeled for these two cases. With 50 gpm and a manual depressurization, shutdown occurred at 1600 s, with the PSP at 195°F. The increased SLCS capacity thus resulted in a quicker shutdown and a lower PSP temperature.

5.3 Effectiveness of EPGs

The purpose of this section is to consolidate results from the simulations presented in this report, and illustrate the effectiveness of operator actions in mitigating a MSIV closure ATWS. Because operator actions were modeled from directions given in proposed EPGs, this becomes a partial evaluation of the EPGs.

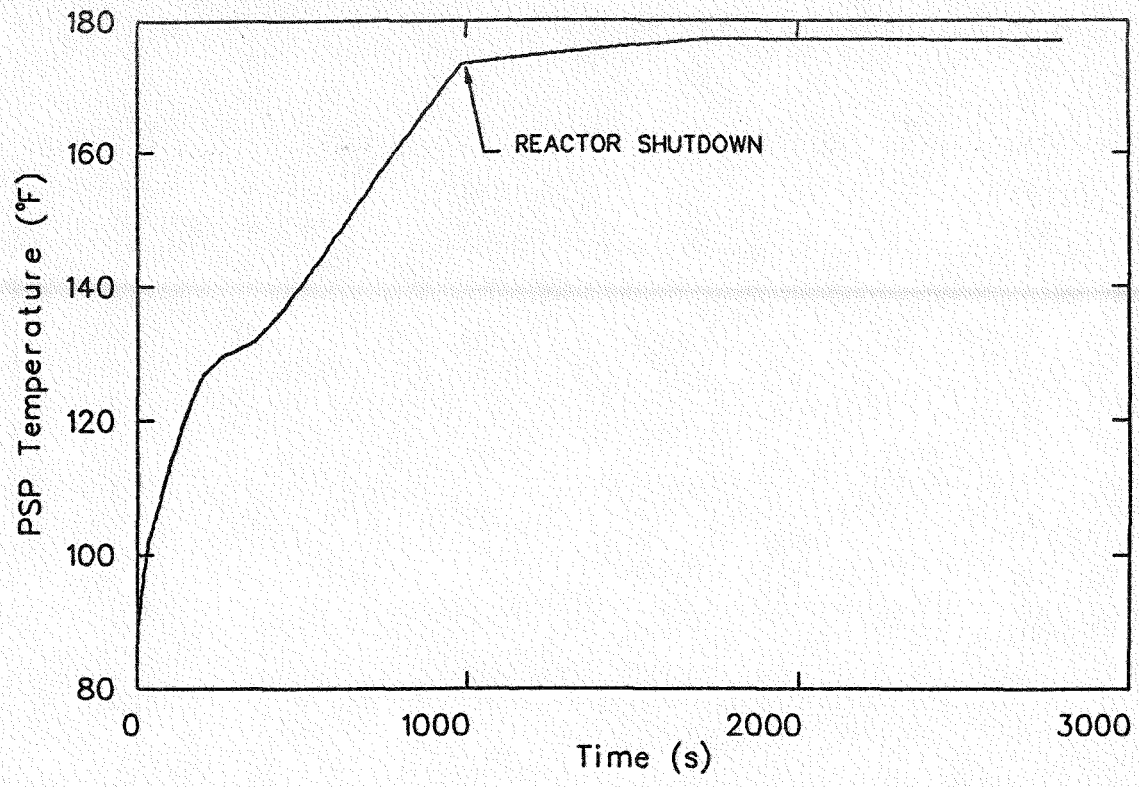

Figure 26. Pressure suppression pool temperature with 86 gpm stratified boron.

Because of the uncertainty involved in modeling the individual rod reactivity, no credit was given for control rod insertion in these analyses. Section 7.3 discusses an approach to allow the modeling of control rod insertion. Because of the potential to reduce power and shutdown the reactor, the EPGs are entirely correct in directing the operator to attempt manual control rod insertion. The effectiveness of that action, however, is not currently quantified.

The EPGs instruct the operator to initiate the SLCS during an ATWS when the PSP temperature reaches 110°F. This is indeed a prudent action, considering the short time frame required for the ATWS progression. The present analysis provides data with which to evaluate boron effectiveness by considering bounding cases. If the operator begins level control procedures at 120 s, and maintains RPV pressure below the HCTL, the following results are predicted. With boron injection at 120 s, assuming isotropic transport (maximum effectiveness), the PSP temperature reached 140°F when the reactor was shutdown. For that case, no RPV depressurization was required because the HCTL was not reached. The other bounding case initiated boron injection at 120 s, but assumed that it totally stratified in the lower plenum until 265 lb was injected (minimum effectiveness). For that case, RPV depressurization was required and low pressure system injections were inhibited. The PSP pool temperature reached 195°F at the time of shutdown. If the RPV was not depressurized, the pool temperature reached 218°F at the time of shutdown. Increasing SLCS flow from 50 to 86 gpm decreased the pool temperature at shutdown from 195 to 173°F, and no depressurization was required.

Level control, as advocated by the EPGs, is predicted to be effective in reducing reactor power from 30 to 17%. This in turn reduces the PSP heatup rate when the MSIV is closed. Reactor power is calculated to be ~17% with level control and the RPV at 1000 psia. At lower pressures, level control is more effective.

Emergency depressurization, as required by the EPGs, may be necessary if the HCTL is violated. This action has been found to be effective in reducing RPV pressure. In addition, depressurization aids in reducing reactor power and PSP heatup rate. It should be noted that operator training may be required to prevent flooding of the RPV by low pressure injection systems following a depressurization. The adverse effects of low pressure power oscillations or unthrottled low pressure ECCS injections could be significant contributors to fuel damage.

Comparisons of predicted PSP temperatures for the five simulations presented in this report are summarized in Table 4. Figure 27 graphically presents the PSP temperature histories for each simulation.

Table 4. Summary of predicted PSP temperatures

Simulation	Description	Time to 200°F in PSP (s)	Time to Saturation Temperature in PSP (s)	PSP Temperature at Shutdown (°F)
1	Plant automatic	924	1220	NA
2	EPG nominal—maximum SLCS effectiveness	NR	NR	140
3	EPG nominal—minimum SLCS effectiveness	NR	NR	195
4	Minimum SLCS effectiveness without depressurization	1380	1585	218
5	EPG nominal—increased SLCS capacity and minimum effectiveness	NR	NR	173

NA: Not applicable.

NR: Not reached.

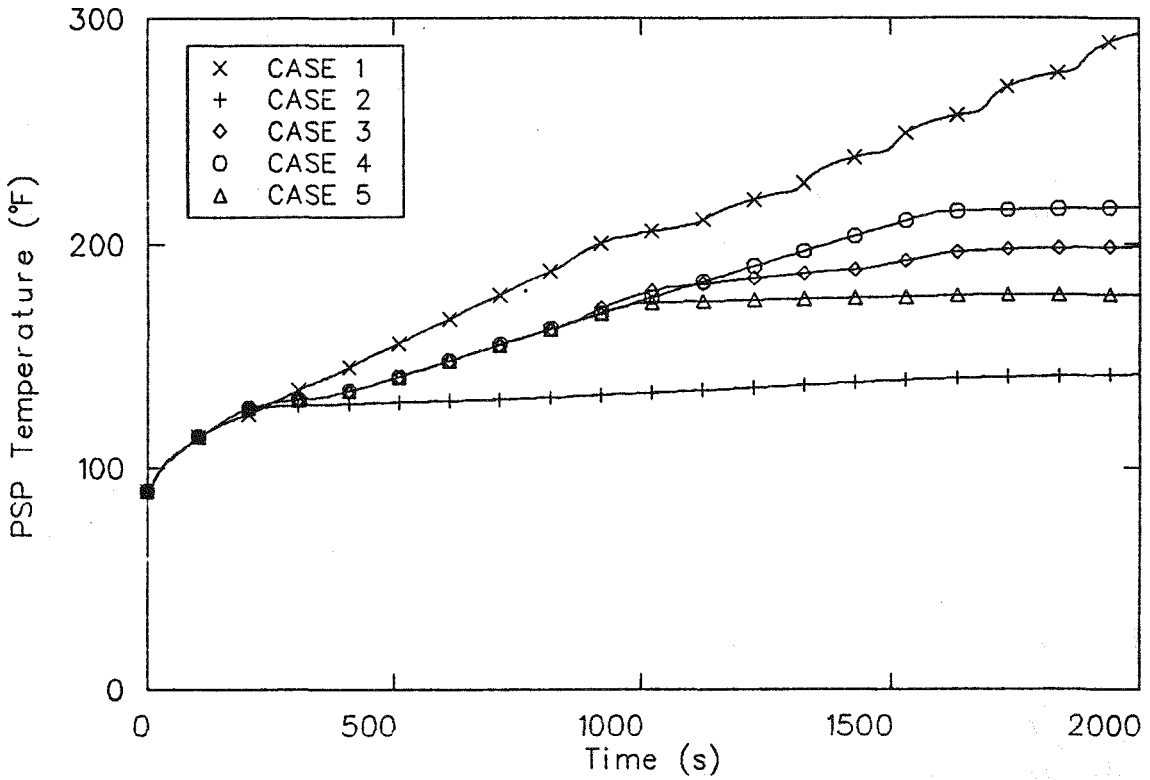

Figure 27. PSP temperature comparisons.

6. FUEL DAMAGE ANALYSIS

During the plant automatic simulation described in Section 5.1, the potential for fuel damage existed in two different portions of the transient. Section 6.1 describes the FRAP-T6[9] analysis of the power excursions caused by low pressure flooding of the RPV. Section 6.2 describes the SCDAP[10] analysis of the high pressure boiloff occurring after ADS isolation. Appendix C contains details of the SCDAP code, and Appendix D presents details of the FRAP-T6 code.

6.1 Power Excursions: FRAP-T6 Results

Between 1275 and 2600 s in the plant automatic simulation (Section 5.1), seven power excursions were predicted. These power spikes (Figure 13) were caused when low pressure injection systems flooded the RPV with highly subcooled water. To examine the possibility of fuel damage during these power spikes, the FRAP-T6 computer code was used. FRAP-T6 is designed to calculate the thermal and mechanical behavior of light water reactor fuel rods during operational transients and hypothetical accidents. Appendix D contains a description of FRAP-T6 and details of its application to this transient.

The modeling approach taken here was to model a single fuel rod and calculate its failure probability. Data from the first power spike (1275-1400 s) were used as a basis for the analysis. The first power spike was calculated by RELAP5, and the actual input used in FRAP-T6 is shown in Figure 28.

FRAP-T6 predicted that 10% of the fuel rods would fail during the first power excursion. Failure is defined here to be a breach of the fuel rod cladding that allows fission products to migrate into the coolant. The failure mechanism was cladding overstress, which is predicted on a comparison of clad hoop stress to the standard deviation of the ultimate hoop stress.[11] Failure was calculated to occur at 1520 s. A small amount of hydrogen generation was predicted during the time that cladding oxidation temperatures were reached. Based on the single fuel rod prediction, approximately 0.003 lb of hydrogen would have been produced by one 8 × 8 bundle.

It should be noted that the prediction of fuel rod failure probability is dependent on the input conditions

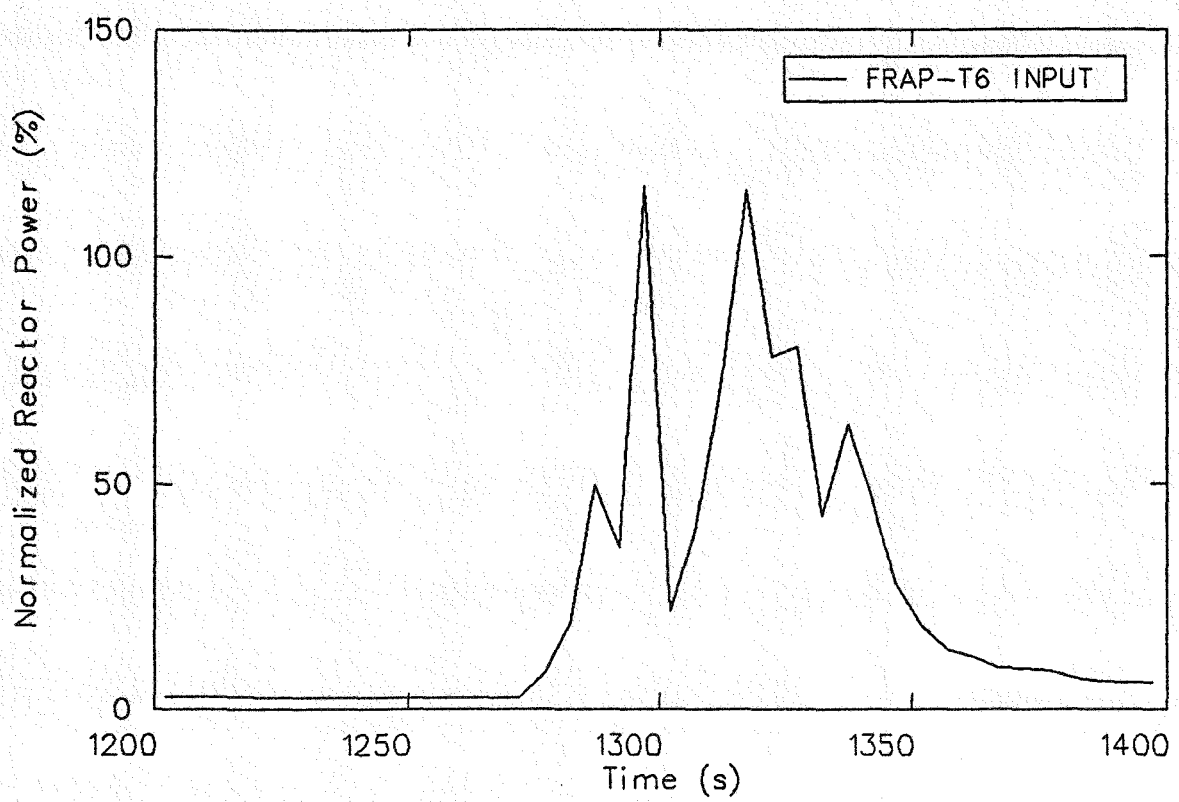

Figure 28. FRAP-T6 input power.

supplied by RELAP5. Since the predicted power oscillated substantially during the excursions, it was averaged every five time steps. The resulting FRAP-T6 input power (Figure 28) had a peak power of 114%. A sensitivity was performed in which a 200% peak power spike was input. That resulted in a prediction that 70% of the fuel rods would fail. Although the integral of power was not held constant, the 200% spike occurred over a very short time frame and had little effect on the integral. Since the rods are near failure, any change in power will cause a much higher failure probability.

6.2 High Pressure Boiloff: SCDAP Results

In the plant automatic transient, the ADS valves close on high containment pressure at 2470 s. This closure keeps the RPV pressure above the low pressure injection systems shutoff heads. The only high pressure injection system available at that time is the CRD system, which injects 112 gpm into the RPV. Even at very low power levels, that flow is insufficient to maintain core cooling. At ~4200 s, the fuel rods began to heat up as a result of the high pressure boiloff. At ~5100 s cladding temperatures were predicted to reach 1350°F, high enough to cause zircaloy oxidation of the cladding and hydrogen production. Using extrapolated boundary conditions from RELAP5, a SCDAP calculation was initiated just before the onset of oxidation. The objective of the calculation was to determine the extent of fuel damage, hydrogen production, and fission product release during a high pressure boiloff. Details of the SCDAP code and its modeling of the high pressure boiloff are presented in Appendix C.

The SCDAP analysis began 5100 s after transient initiation, just prior to the onset of zircaloy oxidation of the cladding. RELAP5 results were used to provide the initial boundary conditions (until 5600 s). Because of the nearly steady state core inlet conditions, the results were extrapolated to 11100 s. At that time the rates of fuel damage and hydrogen production were nearly zero, and the calculation was terminated.

It was realized that the SCDAP core analysis could affect the system response (such as hydrogen generation increasing system pressure and changing core inlet flow). In many cases, extrapolation of the required boundary conditions may not be valid and an iterative approach between RELAP5 and SCDAP would be necessary. In this case, however, the core inlet flow was small, and the enthalpy and pressure were changing very little (pressure was held fairly constant due to SRV actuation). Thus it was judged that the RELAP5 boundary conditions and the SCDAP calculated system conditions were sufficiently decoupled to provide a valid analysis.

A single, high-power fuel bundle was analyzed. The fuel rods were divided into ten axial nodes, each 1.25 ft in length. The temperature histories of the top six axial nodes are shown in Figure 29 (node 10 is the uppermost node). Each of the nodes exhibits temperature excursions due to runaway oxidation. A peak clad temperature of 4300°F was predicted. The temperature excursions in nodes five through ten were terminated by the liquefaction and flow of cladding. The sequential temperature excursions starting at the top of the core are a result of the dropping level in the core during the boiloff. Only minor differences were seen in the radial temperature response across the bundle. CRD flow maintained cooling in the lower three nodes, which prevented temperature excursions there.

Steam mass flow rates in the bundle are shown in Figure 30 at nodes four and ten. The mass flow rate varied between 0.007 and 0.020 lb/s in response to the core inlet flow. The sharp downward spikes in steam flow correspond to the temperature excursions in Figure 29, as steam was consumed by runaway oxidation. Steam starvation was not calculated to occur in the bundle. Cladding temperatures in node 4 exceeded the oxidation threshold temperature of 1350°F, but did not reach the point of enhanced oxidation.

In the regions above the bundle, a significant amount of heatup and subsequent meltdown was calculated. Heated by core exit steam, the top guide, the core shroud head, and standpipes were calculated to experience rapid oxidation and melting. The material in the separator, dryer, and steam dome regions experienced some oxidation, but no melting.

SCDAP calculated that a total of 1.7 lb of hydrogen was produced during the transient by oxidation of the fuel rod cladding, bundle canister, and material in the upper vessel regions. Note that this value is for one 8 x 8 bundle only. A total of 32% of the Xe, I, Cs, and Kr in the fuel was calculated to be released, as a result of the dissolution of fuel by liquefied cladding.

The value calculated for hydrogen production has some uncertainty associated with it because of certain modeling assumptions used in SCDAP. Because SCDAP performs a single bundle thermal-hydraulic analysis, no effect of bundle flow area reduction on steam flow rate is considered. It did predict, however, that the fuel bundle was blocked at 7155 s from liquefied fuel and cladding which solidified near the top of the mixture level. A lower bound on hydrogen production was estimated by assuming that no hydrogen production occurred after blockage was calculated. This reduced the amount of hydrogen produced from 1.7 to 0.8 lb for a single bundle analysis. SCDAP has no model to track the movement of liquefied material in the upper vessel regions. Thus, when this material begins to liquefy, the oxidation

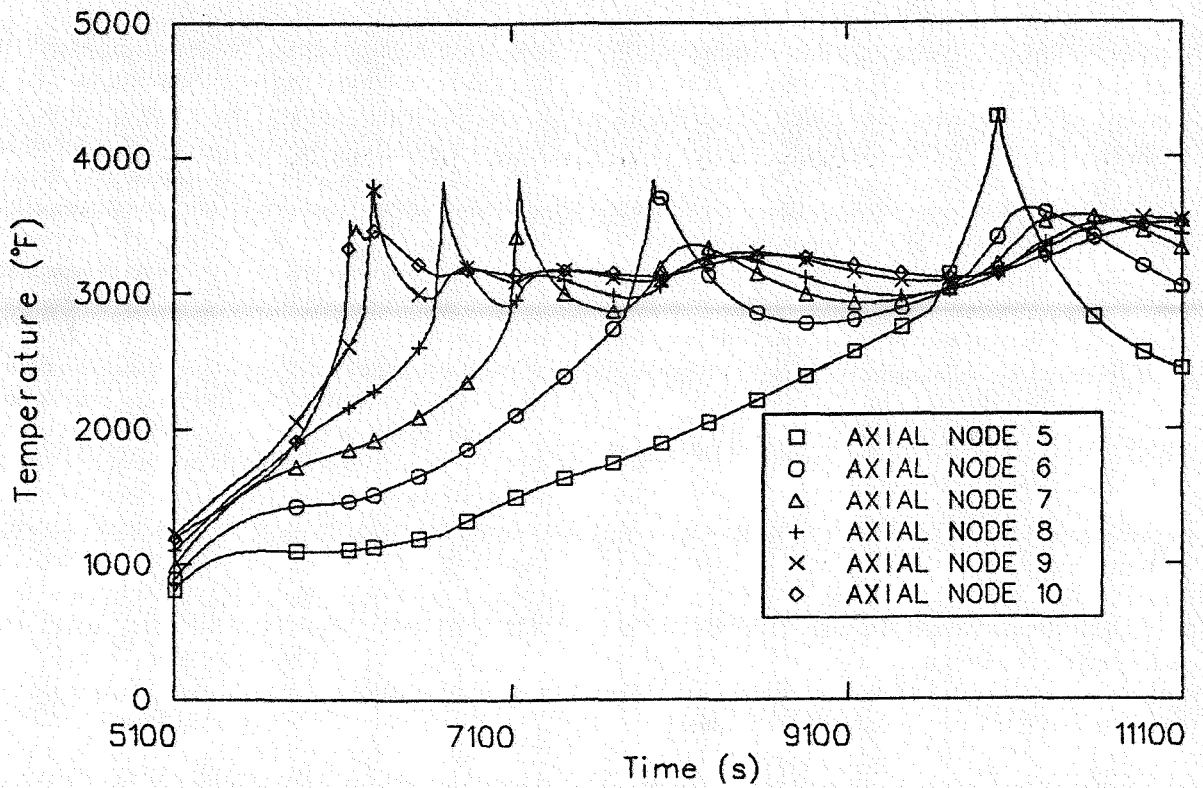

Figure 29. SCDAP fuel rod cladding temperature histories of the top six core axial nodes.

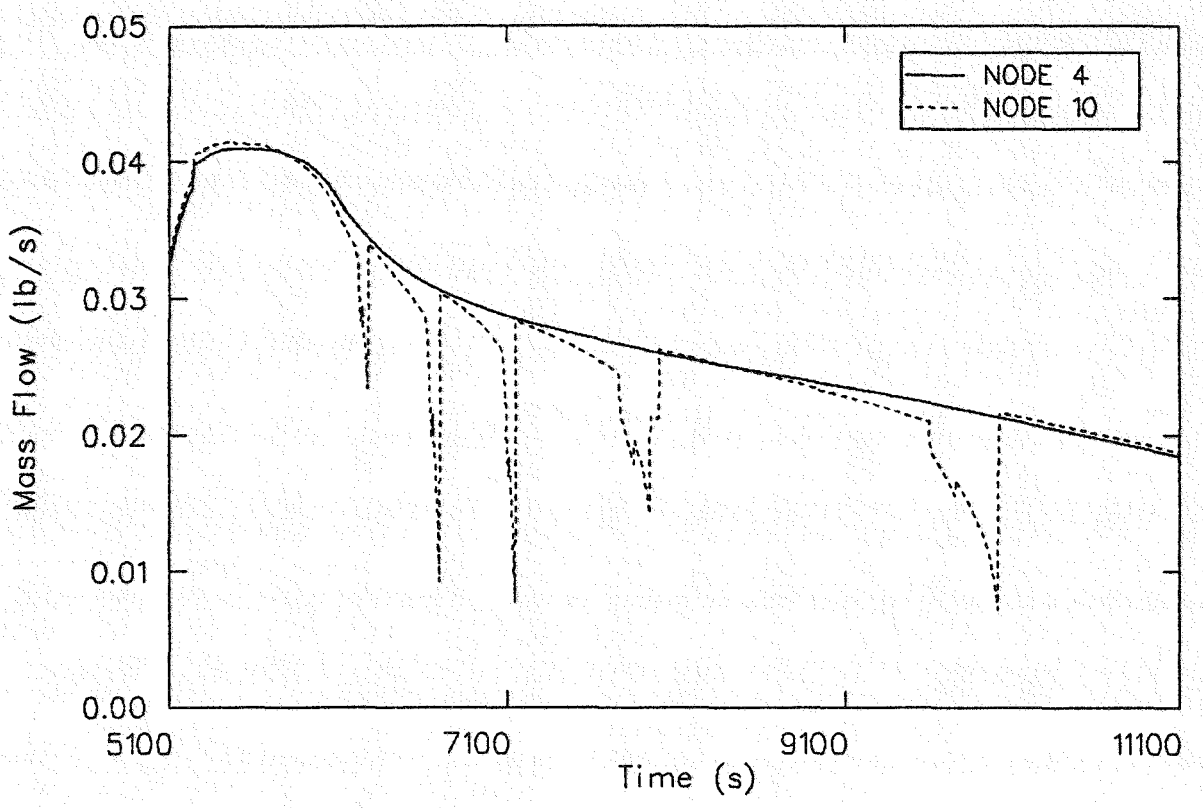

Figure 30. SCDAP mass flow rate of steam in the bundle at nodes four and ten.

and heat transfer from the material is terminated. As a result, the hydrogen production in the upper vessel regions may be underpredicted, although the amount cannot be quantified.

The numbers presented here should be taken as best estimate within the modeling limitations stated above. To obtain more confidence in the results, models for relocation in the upper vessel region are required. Also, an integrated analysis that accounts for blockage and redistribution of coolant to other bundles would reduce the uncertainty in the hydrogen production in the core. Such an analysis capability is currently being developed at the INEL, with the SCDAP/RELAP5/TRAP-MELT computer code.

7. ANALYSIS UNCERTAINTIES

The MSIV closure ATWS simulations analyzed in this report result in predicted plant conditions that exceed the range of available data bases. Uncertainties remain concerning plant systems reliability, effectiveness, and failure modes. Analytical models have been applied in certain areas where data are not available for their proper checkout. This section outlines the significant uncertainties identified by this analysis, and suggests methods for the reduction of the uncertainties.

7.1 SLCS Effectiveness

The SLCS is designed to inject sodium pentaborate in the RPV for the purpose of achieving subcriticality in the event of control rod drive failure. The SLCS is a redundant system, and its reliability is not a major concern. Rather, the question of SLCS effectiveness centers around the mechanism of boron transport in the lower plenum, and the movement of the boron solution into the core.

At BFNP1, injection of the SLCS is through a single sparger located in the lower plenum just below the core plate. This asymmetrical injection raises questions concerning the boron solution being transported uniformly into the core. Because the boron solution has a specific gravity of 1.1 and it is highly subcooled when it enters the RPV, the solution has the potential for settling in the lower plenum particularly during low core flow conditions. In addition, if power is not reduced early in a MSIV closure ATWS, HPCI may fail before sufficient boron has been injected to shutdown the core. This condition becomes more probable if SLCS injection is delayed. The ability of RCIC and CRD flows alone to transport the boron solution into the core is unknown.

The analyses presented in this report used a bounding approach in modeling boron injection. To determine maximum effectiveness, the boron solution was calculated to move isotropically with the liquid in the vessel. This provided results based on ideal conditions. The other bounding solution was obtained by assuming minimum effectiveness. This was done by calculating the boron worth to be zero until an amount sufficient for hot shutdown was injected.

To better analyze the effectiveness of the SLCS, a mechanistic model is required which accounts for density differences between the boron solution and water. Such a model has been developed by the General Electric Company for use in the TRAC-BWR code.[12] However, coefficients needed for the model input are proprietary. Presumably, when coupled with a three-dimensional thermal-hydraulics formulation, the model will accurately predict the mixing of boron for different flow conditions. If the boron is calculated to enter the core symmetrically, a one-dimensional neutronics formulation is then required to calculate core power levels. If entry is calculated to be asymmetric, then a three-dimensional neutronics formulation would be required.

Ultimately, full scale plant data or properly scaled experimental data are required for model verification. In lieu of data, the General Electric model could be incorporated into the INEL version of TRAC-BD1/MOD1. The model could be exercised through the range of conditions expected during a MSIV closure ATWS. If boron is predicted to enter the core symmetrically, the one-dimensional neutronics formulation in TRAC-BD1/MOD1 will accurately predict the neutronics feedback. If the boron is predicted to enter the core asymmetrically, iterations between TRAC-BD1/MOD1 and a three-dimensional neutronics formulation would be required.

7.2 Effectiveness of Level Control

During an ATWS, the reactor power is determined by the energy and mass flow rate of the fluid injected into the RPV. If the injected flow rate and energy are known, the reactor power can be easily calculated by the expression: $Q = W_{jP} (h_g - h_{jP})$, where Q is the reactor power, W_{jP} is the mass flow rate through the jet pump discharge, h_g is the enthalpy of steam leaving the core, and h_{jP} is the enthalpy of the jet pump discharge fluid. The proposed EPGs (discussed in Section 3 of this report) advocate level control for the purpose of reducing core power and the resulting steaming rate to the PSP. The reduction of level to TAF translates to reducing the core inlet flow, and consequently core power. The uncertainties related to this maneuver, particularly the calculation of core power are discussed below.

After the recirculation pumps coast down, the RPV reaches a steady state natural circulation mode of operation. Injected flow maintains a hydrostatic head in the downcomer, which is balanced by the pressure loss in the core flow path. When the downcomer level is lowered to TAF, a new momentum balance is reached. The downcomer hydrostatic head is balanced by the combined hydrostatic, dynamic (flow), and irrecoverable (friction) heads across the core. Since the dynamic head is small, the hydrostatic head in the downcomer is approximately equal to the sum of the

hydrostatic and irrecoverable heads taken across the core.

The downcomer hydrostatic head is easily computed. However, sensitivities arise when trying to compute the individual core pressure drops, even though the sum of them is fixed. The hydrostatic head is linearly dependent on core void. An increase in core void will decrease the hydrostatic head in the core. Because the overall pressure drop is fixed, this will tend to increase the irrecoverable loss in the core.

Irrecoverable losses are dependent on both flow and void content. They are dependent on the flow, at least quadratically, while they exhibit an exponential dependency on void content. Thus, an increase in core void increases flow losses not only by increasing the core flow, but also by exponentially increasing the multipliers associated with wall friction and form losses. These losses are directly related to core power. For example, an increase in power will increase the core void, which would tend to increase the core flow. However, a nonlinear feedback acts to restrain this increase, as irrecoverable losses increase with the void. The algorithm (drift flux formulations, interfacial shear, etc.) by which the core void is calculated is pivotal in the estimation of power during level control.

Further complications arise when the changing thermal-hydraulic conditions feedback to the core neutronics. With saturated core inlet conditions, the axial power profile shifts upward in the core compared with subcooled inlet conditions. The core void profile also shifts as a result of the power profile shift, changing void reactivity. The end result is that as inlet subcooling is lost, core power decreases. However, the shifting axial power profile decreases core voids which limits the power decrease.

Figure 31 illustrates the effects of some of these interactions. Plotted on the figure are predictions of the core thermal power (as a percent of rated) as a function of downcomer level. The curve was generated with RELAP5 through a series of steady-state calculations, and the points on the curve represent asymptotic steady-state values. The model used for these calculations has been previously assessed with natural circulation data from the Full Integral Simulation Test (FIST) facility. An axial power profile typical of a saturated core inlet condition (see Figure A-4) was used.

As the downcomer level is lowered by reducing makeup flow, there is a corresponding reduction in core power. This continues until a plateau is reached where further lowering of the downcomer level results

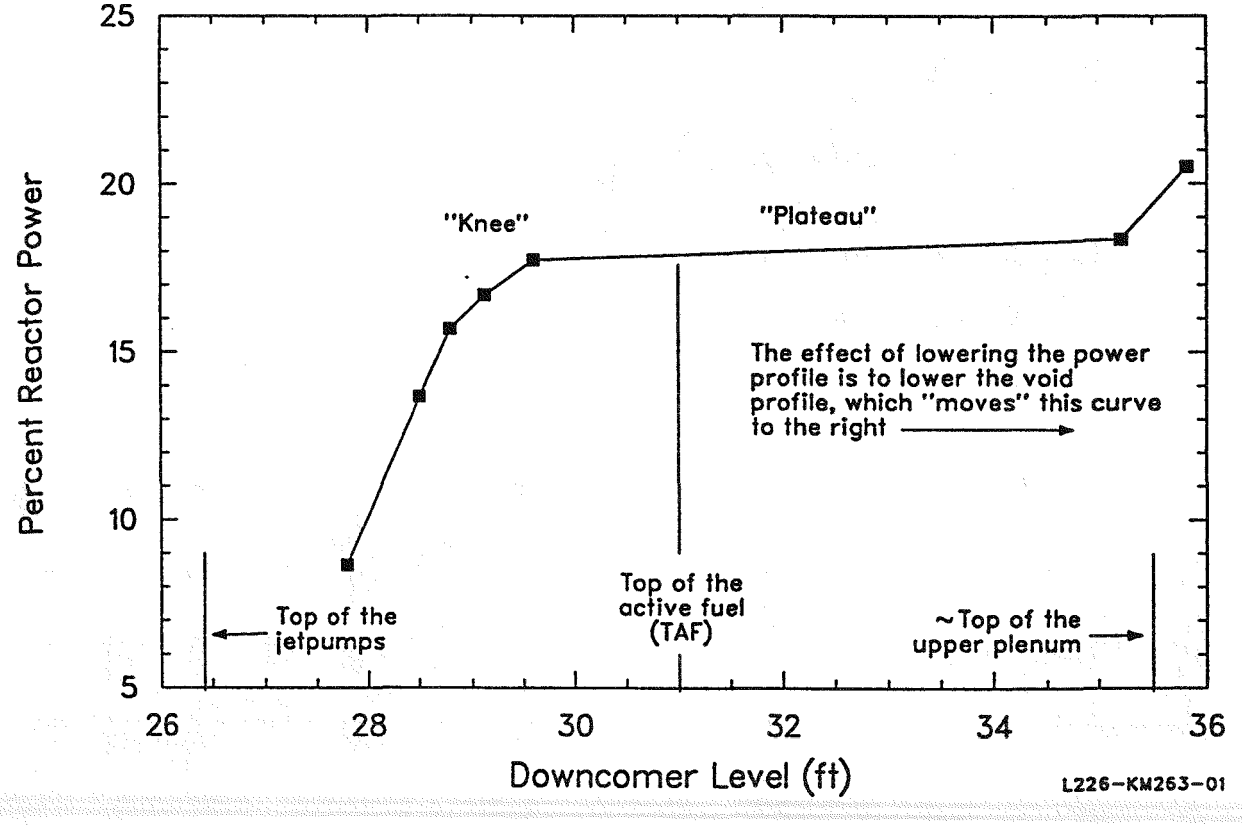

Figure 31. The effect on reactor power of lowering downcomer liquid level in steady-state operations.

in only a small reduction in core power. The plateau exists until the downcomer level reaches slightly below TAF, at which point a cusp (or knee) is seen in the curve. Further lowering of the downcomer level again results in a corresponding power reduction.

Both the plateau and knee in reactor power exist because of a delicate hydrodynamic balance occurring within the core, upper plenum, standpipes, and separator of the reactor. The plateau indicates that a stagnation of the fluid conditions within the core has occurred. In this stagnation condition, the steam exiting the core through the upper plenum and standpipes has insufficient velocity to entrain and transport liquid out of the core, through the separators, and reflux it into the downcomer. That is, the liquid and steam flowing from the core decouple, and the liquid falls back into the core. This differs from the state occurring during normal operation, and during full flow HPCI operation, wherein the phases are strongly coupled.

During normal operation, wherein the phases are strongly coupled, the moderating coolant sweeps through the core at fairly high velocities. The shape of the void profile, which strongly influences both the in-core shape and total magnitude of the reactor power, is strongly influenced by the coolant velocity. As this velocity is decreased, the liquid tends to settle towards the bottom of the core, thus modifying the in-core void profile and content, and the in-core power shape and total reactor power.

On the reactor power plateau, changes in the total void content of the core are compensated for by a rearrangement in the in-core shape of the void profile. At the knee, this compensation can no longer take place. Hence, the core void content increases, and the power again decreases rapidly with level.

The physics dominating the shape of the dependency of reactor power on downcomer level during ATWS mitigation are thermal-hydraulic. However, the shape of the power profile is an important parameter actually projecting what power will occur with level at TAF. Varying the in-core shape of the power will shift the level control curve shown in Figure 31 across the figure. Lowering the power profile (typical of subcooled core inlet conditions) shifts the curve to the right. Thus, a total power of ~8% can be realized if the power profile is sufficiently bottom humped. Using a profile typical of saturated core inlet conditions results in the curve in Figure 31, which indicates a total power of ~18% with level at TAF.

Other factors which are necessary for the prediction of power reduction from level control include core bypass flow characteristics, grid spacer loss coefficients, reactivity coefficients, steam condensation on subcooled makeup water, and xenon poisoning. Using best estimate values in a prototypically assessed model yields the following result. With saturated core inlet conditions, the core power with level at TAF and the RPV at 1000 psia will be approximately 17-20%. This value agrees closely with previously published Electric Power Research Institute (EPRI) results[13] and with RAMONA-3B calculations[14] done at BNL as part of the SASA program. Although these results have converged to a range of several percent, questions remain on their accuracy. A paper[15] discussing the uncertainties in these power predictions claims that the actual power has a 30-35% probability of being more than 5% (of rated power) higher than the predictions. In addition, the paper concludes that an uncertainty of ~5% of rated power is not achievable with the current state-of-the-art.

7.3 Manual Rod Insertion

As explained in Section 3, the proposed EPGs direct the operator to attempt manual insertion of control rods during an ATWS. The effect of this insertion on reducing reactor power was not modeled in the present analysis, because of the uncertainty involved. The worth of an individual control rod could vary considerably depending on its position in the core. Also, the worth is dependent on how many other rods have been inserted and their location. In other words, it is unlikely that an average rod worth (negative reactivity) could be used to model individual control rod insertions.

To determine the effect on power, a detailed three-dimensional neutronics calculation would be required. Using a realistic rod insertion pattern, the effect could be calculated for the expected range of core inlet conditions. When level control is modeled in conjunction with manual rod insertion, the power reduction from rod insertion would have to feedback to the injection required to maintain level. This could be accomplished either by an integrated thermal hydraulic/neutronic analysis or by iterations between three-dimensional neutronics and thermal-hydraulics calculations.

The end product of such an analysis would be a quantification of the effect of individual rod insertions on core power reduction. In addition, a valuable result from the analysis would be a table of control rod reactivity versus time. The table could be used in systems codes to model manual rod insertion (through tabular input of control reactivity) during ATWS simulations. Because of the potential of manual rod insertion to mitigate an ATWS, it is recommended that an effort be undertaken to quantify its effectiveness. It is important that individual control rod effects be separated from other power reducing mechanisms such as level control, pressure control, and SLCS injection.

7.4 Containment Related Uncertainties

The large amount of energy delivered to the PSP during a MSIV closure ATWS causes it to heat up rapidly. The PSP heatup jeopardizes HPCI operation within 13 to 14 min, and it will eventually cause HPCI failure if the plant is not shutdown. With HPCI unavailable, vessel water level will depress below the LLLWL setpoint. Below LLLWL, in the presence of a HDWP signal, the ADS will automatically actuate.

There are some important concerns with respect to the automatic ADS. The timing of the HDWP signal, and thus the automatic ADS timing, is uncertain during a postulated ATWS. An unintentional ADS blowdown is undesirable, because it could lead to very large core power cycles induced by RPV flooding by the low pressure injection systems. Our current estimates range from 16 to 35 min for receipt of the HDWP signal, depending on how well the PSP is mixed and on how effective the T-quenchers are in promoting steam condensation. A large part of the uncertainty in time before steam breakthrough in the PSP is dependent on what the operators are able to do. If, early on, the operators are able to place the RHR system in the torus cooling mode and maintain this alignment as the transient progresses, then the assumption of a well mixed PSP is a good one. In such a case, complete steam condensation could be expected until the pool bulk temperature was nearly saturated. The EPG action of activating the torus cooling mode of RHR when the PSP temperature exceeds 95°F is conclusively appropriate, as it would extend the time the operators would have before it would be necessary to prevent an automatic ADS. The ability of the operator to activate torus cooling is questionable, however, as explained in Section 3. Were the pool not well mixed, extrapolated commercial plant test results[16] indicate that steam breakthrough could be expected at a pool bulk temperature of about 180°F. In either case, mechanistic models to calculate the amount of steam breakthrough to the wetwell atmosphere are not available in todays containment codes.

An automatic ADS blowdown to the PSP would occur at a time when the pool subcooling is significantly diminished. Predicted containment service during the unmitigated ATWS is outside the bounds of known stable condensation for the T-quencher devices.[17] The structural loading of the PSP and drywell during the ADS blowdown was not examined in this work. However, the hydrodynamic loading during a blowdown with low subcooling in the PSP may be of concern.

8. CONCLUSIONS AND RECOMMENDATIONS

A deterministic study was performed that analyzed postulated MSIV closure ATWS scenarios at BFNP1. Conclusions, results, and recommendations resulting from the study are summarized in this section.

1. Mitigative operator actions are required to prevent containment failure and severe fuel damage during a MSIV closure ATWS. During the plant automatic simulation, primary containment failure was predicted from static overpressurization 45 min after transient initiation. In less than four hours, over half of the core was predicted to have liquefied and relocated. Significant hydrogen production and fission product release from the fuel was predicted to occur.

2. It is predicted from these simulations that if all of the actions proposed by the EPGS are completed successfully, then a MSIV closure ATWS would be brought under control. Some of the actions, however, may be very difficult to accomplish.

3. Operator training should be an integral part of the implementation of the EPGs. These simulations indicate that the operator must act properly and promptly to reduce the risk from a MSIV closure ATWS. The process of following the EPGs through their various parts could be very time consuming unless the operators had a thorough understanding of them beforehand.

4. More guidance should be given in the EPGs relative to the injection of low pressure systems to the RPV. The operator is told to "slowly inject" when the RPV is depressurized. More definitive instruction is required, as are measures to prevent automatic injections.

5. Level control as advocated by Contingency #7 is an effective although limited means of reducing reactor power. Lowering RPV water level to TAF at 1000 psia was calculated to reduce reactor power from 30% to approximately 17% of rated. This reduces the PSP heatup rate from 6 to 4°F/min. Although several analyses have converged on the predicted power level range of 17-20%, uncertainties remain and the actual power could be higher.

6. The action of depressurizing the RPV to avoid violation of the HCTL should be evaluated further. RPV depressurization should result in a power reduction during an ATWS, and it may also preclude the need to blowdown the RPV when the PSP has no condensing capacity. However, the potential for low pressure power oscillations and unthrottled low pressure ECCS injections could cause fuel damage.

7. Even with minimum SLCS effectiveness, it is predicted that PSP temperature would be less than 200°F at the time of shutdown. Using 50 gpm of 13% sodium pentaborate solution in conjunction with level and pressure control results in a PSP temperature of 195°F at shutdown. Assuming maximum SLCS effectiveness results in a PSP temperature of 140°F.

8. Increasing SLCS capacity to 86 gpm reduces the predicted PSP temperature at shutdown from 218 to 173°F for minimum effectiveness assumptions and no RPV depressurization. The reduction in temperature is significant in that complete condensation in the PSP should ensure that no steam breakthrough would occur, thus preventing drywell pressurization.

9. The uncertainty of assuming uniform control rod worth is currently too large to allow reliable modeling. It is recommended that the effect of individual rod insertion be quantified in terms of negative reactivity versus time.

10. Use of the torus cooling mode of the RHR system is not assured during a level control transient. Once RPV level is raised back up, torus cooling should be readily accomplished. The importance of torus cooling lies not only in reducing PSP heatup rate but also helping ensure that the torus remains well mixed.

9. REFERENCES

1. S. E. Mays et al., *Interim Reliability Evaluation Program: Analysis of the Browns Ferry, Unit 1, Nuclear Plant*, NUREG/CR-2802, EGG-2199, July 1982.

2. L. B. Claassen and E. C. Eckert, *Studies of BWR Designs for Mitigation of Anticipated Transients Without Scram*, NEDO-20626, 74 Ned 59, GE, October 1974.

3. R. M. Harrington and S. A. Hodge, *ATWS at Browns Ferry Unit One*, NUREG/CR-3470, ORNL/TM-8902, July 1984.

4. S. Z. Bruske and R. E. Wright, *Severe Accident Sequence Analysis (SASA) Program Sequence Event Tree: Boiling Water Reactor Anticipated Transient Without Scram*, NUREG/CR-3596, EGG-2288, April 1984.

5. General Electric Company, *Prepublication Draft, Emergency Procedure Guidelines, BWR 1 through 6, Revision 3*, December 1982.

6. V. H. Ransom et al., *RELAP5/MOD1.5: Models, Developmental Assessment, and User Information*, (Modified for MOD1.6), EGG-NSDM-6035, October 1982.

7. D. W. Hargroves and L. J. Metcalfe, *CONTEMPT-LT/028—A Computer Program for Predicting Containment Pressure-Temperature Response to a Loss-of-Coolant Accident*, NUREG/CR-0255, TREE-1279, EG&G Idaho, Inc., March 1979.

8. Nuclear Regulatory Commission, *Reduction of Risk from Anticipated Transients Without Scram (ATWS) Events for Light-Water-Cooled Nuclear Power Plants*, Final Rule, July 1984.

9. L. J. Siefken et al., *FRAP-T6: A Computer Code for the Transient Analysis of Oxide Fuel Rods*, NUREG/CR-2148, EGG-2104, May 1981.

10. G. A. Berna et al., *SCDAP/MOD1/VO: A Computer Code for the Analysis of LWR Vessel Behavior During Severe Accident Transients*, IS-SAAM-84-002, EG&G Idaho, Inc., January 1984.

11. S. O. Peck, *FRAIL-6: A Fuel Rod Failure Subcode*, WR-CD-025, EG&G Idaho, Inc., September 1980.

12. D. D. Taylor et al., *TRAC-BD1/MOD1: An Advanced Best Estimate Computer Program for Boiling Water Reactor Transient Analysis, Volume 1: Model Description*, NUREG/CR-3633, EGG-2294, April 1984.

13. B. Chexal et al., *Reducing BWR Power by Water Level Control During an ATWS*, NSAC-70, August 1984.

14. P. Saha et al., *RAMONA-3B Calculations for Browns Ferry ATWS Study*, NUREG/CR-4739, BNL-52021, February 1987.

15. D. J. Diamond, "Uncertainty in BWR Power During ATWS Events," *Proceedings of the Topical Meeting on Reactor Physics and Safety, Saratoga Springs, New York, September 17-19, 1986.*

16. B. J. Patterson, *Mark I Containment Program Monticello T-Quencher Thermal Mixing Test Final Report*, NEDO-24542, August 1979.

17. *Supression Pool Temperature Limits for BWR Containments*, NUREG-0783, November 1981.

APPENDIX A

RELAP5/MOD1.6 MODEL OF BFNP1 REACTOR PRESSURE VESSEL

APPENDIX A
RELAP5/MOD1.6 MODEL OF BFNP1 REACTOR PRESSURE VESSEL

This appendix to the report describes the RELAP5/MOD1.6 computer model of the reactor pressure vessel (RPV) of Browns Ferry Nuclear Power Plant Unit 1 (BFNP1), which was used in this analysis, and its qualification against plant transient data.

The BFNP1 model described here was originally transmitted[A-1] to the INEL by the Tennessee Valley Authority (TVA) in the form of a RETRAN-04 input deck. Table A-1 contains plant modeling parameter data. Converted to MOD1.0 of RELAP5, the model was classified as interim and was used in a number of other analyses.[A-2 to A-5] performed at the INEL. Subsequently, the geometry of the model was quality assured by tracing geometric data to plant drawings, and by comparing model performance to plant data, so that the interim label was dropped. The quality assured BFNP1 input deck described here was designed to run on RELAP5/MOD1.6. The steady state for the model described here was run on cycle 018 of RELAP5/MOD1.6.

The model consists of the reactor pressure vessel of BFNP1 and related piping, such as the feedwater and main steamlines, as shown in Figure A-1, and is considered representative of the plant as reloaded through cycle six. This model description segregates RPV regions according to their function. The main steamline is one such region. There are six such regions in the model:

1. Downcomer consisting of the annular region extending downwards from the exterior of the dryers, dryer shroud, standpipes, upper plenum and core shroud, but excluding the jet pumps and their discharge. The downcomer receives feedwater and separator reflux, and provides makeup to the recirculation loop. The downcomer communicates thermally with the environment. The downcomer consists of five components, numbered 415[a] through 475, comprising ten control volumes. RPV level measurements are performed in the downcomer. RPV steam dome pressure measurements are performed in the uppermost downcomer cell.

2. Recirculation loop combining the functional aspects of both plant loops. The loop consists of eight components, numbered 200 through 270 and is comprised of 17 cells.

a. Referring to component serial code CCC on RELAP5 cards CCCOOOOOO.

Table A-1. Plant modeling parameters

Item	Parameter
Plant	Browns Ferry Nuclear Plant
Unit	One
Plant type	BWR/4
Belt line diameter	251 in.
Number of bundles	764
Type of bundles	P8 × 8R
Warranted or rated core power	3293 MW

The recirculation loop has two associated special process models; the recirculation pumps and the jet pumps. Jet pump performance characteristics were set according to available data as shown in Figure A-2.[A-6,A-7]

The recirculation loop also includes the low pressure coolant injection (LPCI) point. Core inlet flow measurements are performed at the jet pump discharge plane.

3. Lower plenum consisting of five components and cells. It communicates thermally with the environment. The lower plenum is penetrated by both the control rod drive (CRD) tubes and CRD efflux and by the standby liquid control system (SLCS) nozzle through which the lower plenum pressure measurements are performed. The lower plenum is numbered 290 through 294, and 350. The pressure tap is taken in volume 294.

4. Nuclear core includes the core inlet piece, channels and fuel rods, bypass and reflector regions inside the core shroud, and upper plenum. The core is numbered 300 through 380. The core models P8 × 8R bundles of 12.5 ft heated length. The core model was developed to meet the following objectives:

   - Accurately predict hydraulic response of the core to various external perturbations, such as a flow coastdown

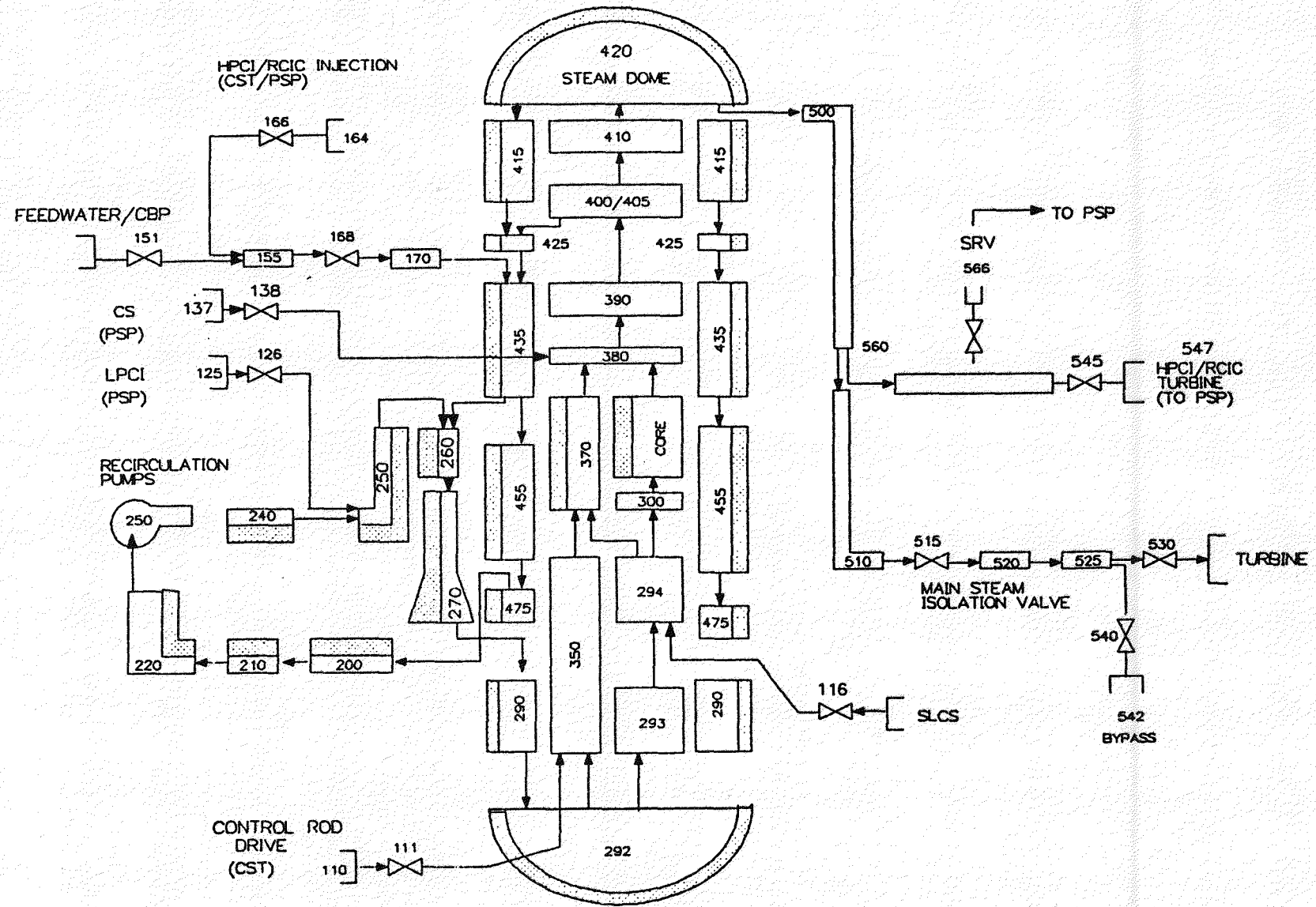

Figure A-1. Vessel nodalization diagram.

EEJ00101

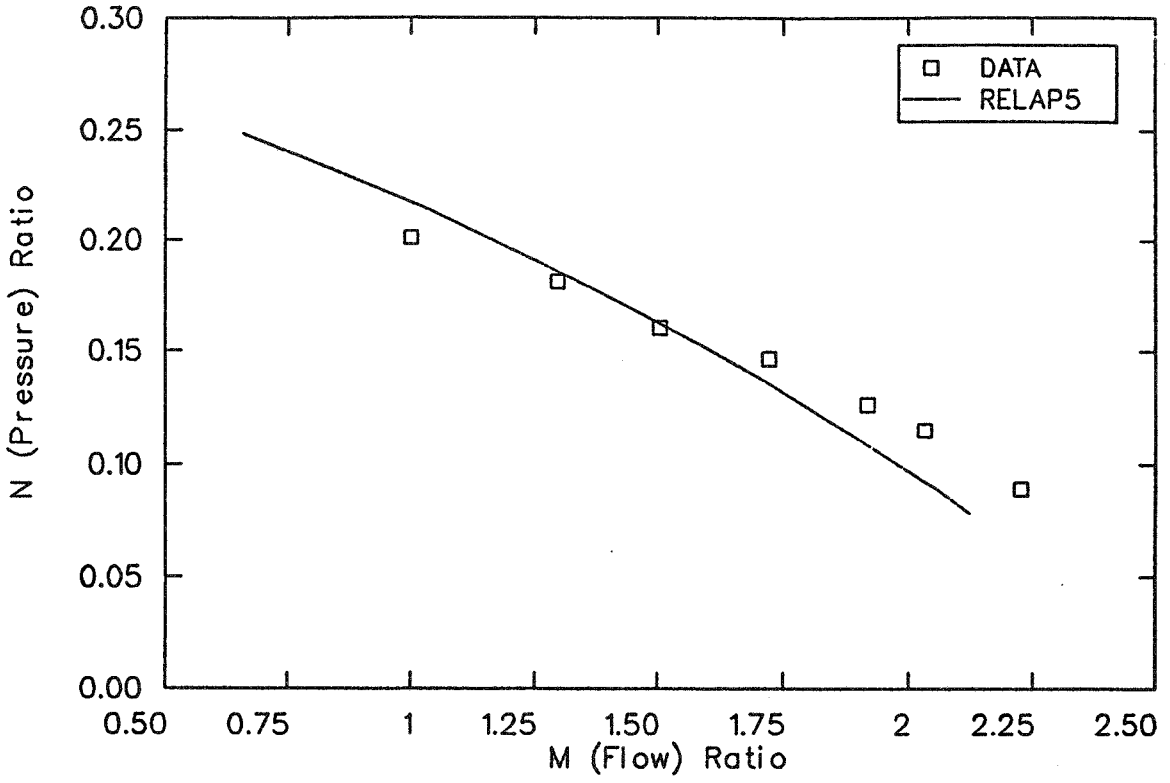

Figure A-2. Jet pump performance curve.

- Accurately predict the thermal response of the fuel, especially in severe accident scenarios under boil-off conditions, and
- Accurately predict the response of the core reactor kinetics to various external perturbations, and the resultant feedback to the thermal-hydraulics.

These technical objectives address SASA program needs. To meet the objectives, the core was divided both radially (across the core) and axially (vertically). The resultant nodalization, as shown in Figure A-3, consists of three axially parallel flow channels. Two of these flow channels represent the interior of fuel assemblies, while the third models the unheated core bypass flow. Axially, the heated length of the fuel assembly channels were divided into 12 control volumes of equal length. This level of detail was required axially to accurately model the nonlinearity associated with the core hydraulics and reactor kinetics.

The core model was designed to model month 11 of cycle 4 at BFNP1. This time of cycle is very near the end of cycle (EOC), when the core is considered to be most reactive. The fuel loading[A-8] is primarily 8 × 8 fuel. Nearly all of the core has been reloaded. Only a few assemblies of the original loading remain in the cycle 4 core. The core is thought to be representative of the loadings of nearly all BWR/4 because of this age factor. Lattice modeling parameters are shown in Table A-2.

Data pertaining to the reactor kinetics are contained in Table A-3. The moderator void reactivity, fuel temperature reactivity, moderator temperature reactivity, boron worth, delayed neutron fraction, and neutron generation time were derived from data presented in References A-9 through A-17.

The fuel loading represents EOC6 at BFNP1. Associated with this loading is a core axial power profile.[A-18] The axial power profile under normal power operation at EOC6 is bottom humped because the control rods are fully withdrawn. Figure A-4 shows this effect in the power profile. The axial peaking factor is 1.23. The power delivered to the fourth axial cell from the bottom of the core receives 123% of the average cell power delivery. Associated with the power profile is an importance profile, which was generated by renormalizing the square of the

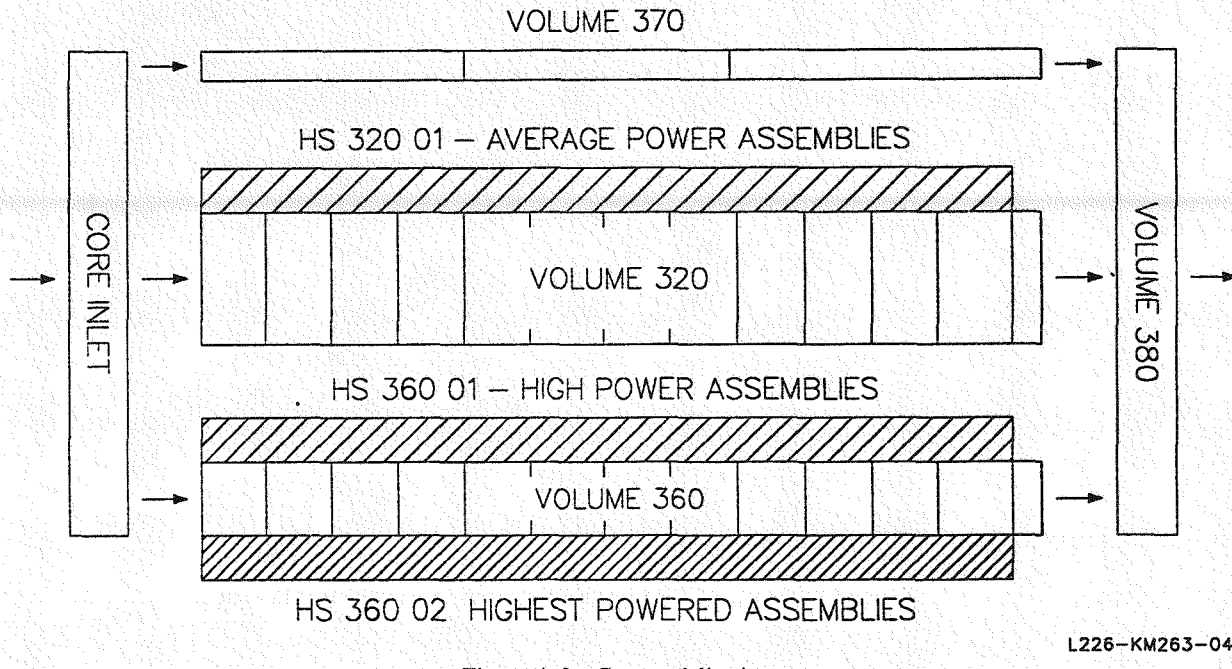

Figure A-3. Core nodalization.

Table A-2. Core lattice modeling parameters

Item	Parameter
Fuel assembly type	P8 × 8R
Number of fuel assemblies	764
Total number of fuel rods	47,368
Active fuel length	150 in.
Total active rod heat transfer area (ft^2)	74,870.5
Direct moderator heating	3%

Table A-3. Reactor kinetics data

Item	Data
Delayed neutron fraction β	0.0054
Delayed fraction to generation time β/Δ	123.7 s^{-1}
Void reactivity function	$\rho_\alpha = (-0.0979 + 0.01\ \Delta\alpha)\ \Delta\alpha$ where α is the void fraction
Doppler reactivity function	$\rho_d = -1.55 \times 10^{-3}\ (\sqrt{T_F} - \sqrt{T_{F0}})$ where T_F is fuel temperature (K)
Moderator temperature function	$\rho_m = -1.38 \times 10^{-4}\ \Delta T_m$ where T_m is moderator temperature (K)
Boron reactivity	$\rho_B = (-3.75 \times 10^{-3} - 5.96 \times 10^{-4}\ \Delta\alpha)\ R_B$ where R_B is the mass of dissolved boron (lb)

Delayed Neutron Constants	1	2	3	4	5	6
Relative yield β_i/β	0.0361	0.2343	0.1974	0.3734	0.1253	0.0335
Decay constant λ_i (1/s)	0.0128	0.0314	0.1242	0.3213	1.3512	3.5802

a. Data obtained primarily from References A-11 and A-14.

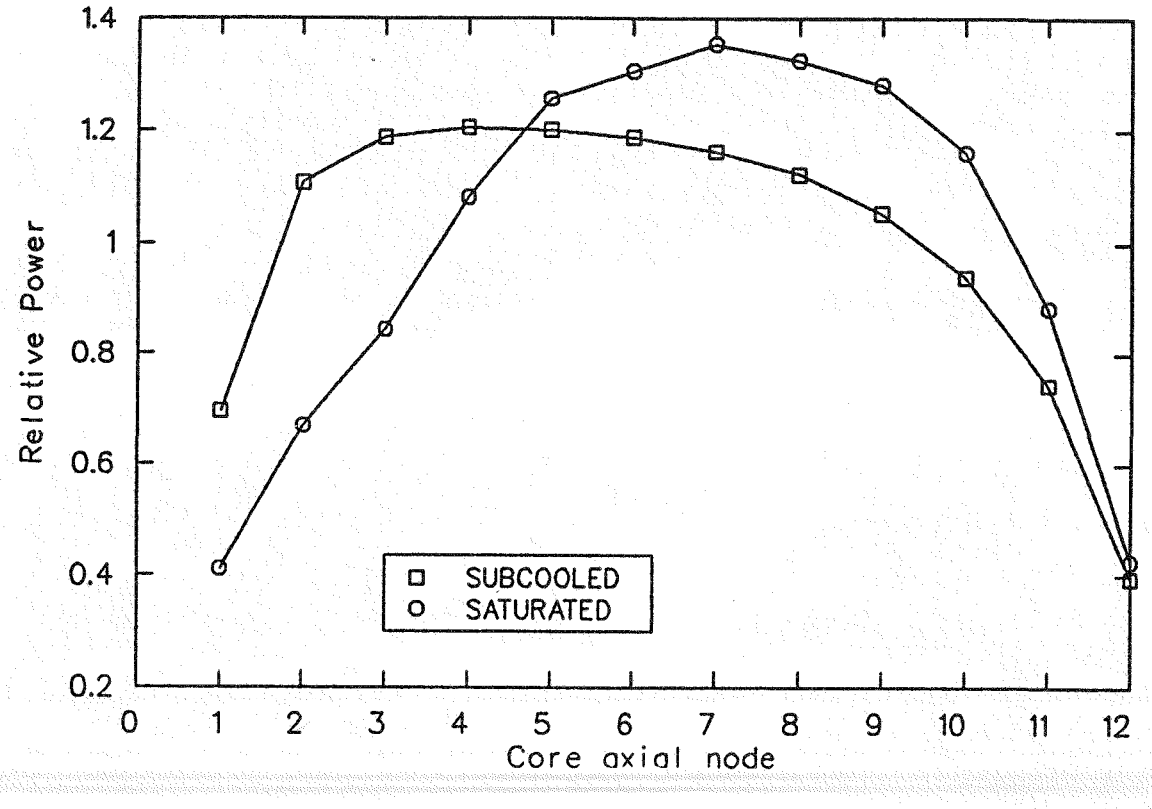

Figure A-4. Core axial power profiles.

power profile. The reactivity importance profile has a relative peak in axial cell four of 140%. The importance profile is used to weigh the relative worth of each axial location to the reactor kinetics.

Under normal power operation, the coolant subcooling at the core inlet is about 20°F. However, under accident conditions, this is not always so. Figure A-4 also shows a power profile, taken from Reference A-19, which was used to simulate core conditions when the inlet of the core is near saturation. Such conditions exist when the operator takes level control, and reduces the downcomer level to the top of the active fuel (TAF).

The core radial power profile is double humped, the peak being located in the third annular ring outwards from the core center. The fifth annular ring, or ring 5, is the location of the secondary hump. According to data derived (see Reference 8) from the core loading, ring 5 contains the eight highest powered fuel assemblies. The eight highest powered fuel assemblies are located in an annular ring of relatively high power.

It is felt that during a severe accident, wherein excessive fuel rod temperatures would be expected to occur, these eight assemblies would be most prone to fail. They were accordingly modeled with a single heat structure. This heat structure was attached to the hydraulic channel representing ring 5. The thermal characteristics of the remaining fuel assemblies in ring 5 were separately modeled and also attached to the single ring 5 hydraulic channel. The remainder of the heated core was modeled using a single channel and heat structure.

Using this approach, the eight hottest fuel assemblies are associated with a relatively hot channel. Thus, hot assembly thermal-hydraulics are modeled while stabilizing the code with a relative large hydraulic impedance in the hot channel. Assembly modeling data are presented in Table A-4.

Corresponding to these core wide variations in power delivery (and exposure) are variations in the thermal (and neutronic) properties of the fuel. Fuel and gap thermal conductivities were calculated for each the three prototypical fuel assemblies modeled. Average core void profiles are shown in Figure A-5 for both power profiles under normal power operation.

5. Separator region consisting of four components and cells (390, 400, 410, and 420). The separator region includes the separator special process model which directs the liquid leaving the nuclear core to the downcomer (reflux) and the steam to the steam dome. The separation process was assumed to occur at the first pick off ring.

6. Feedwater and main steamlines; model the feedwater and main steamlines. The feedwater line consists of two cells, while the steamline has ten. The steamline is numbered 500 through 525, and the feedwater line is numbered 155 and 170.

   Associated with the feedwater line are the reactor water cleanup injection point and the high pressure coolant injection (HPCI) and reactor core isolation coolant (RCIC) injection points.

   The steamline associates with the safety/relief valves (SRV), HPCI and RCIC turbines, and the main turbine and turbine bypass. Turbine steam can be interrupted by the main steam isolation valves (MSIV), or by the turbine stop/control valve. Safety/relief valve characteristics are presented in Table A-5.

Tables A-6 and A-7 contain a summary of RPV geometric and elevational data as modeled, respectively.

Although much labor and care were extended in development of this computer model of BFNP1, it was realized that any plant transient behavior projected by

Table A-4. Fuel assembly data

Assembly Designator	Average Core	Ring 5 Average	Ring 5 Hot
Heat structure number	320-01	360-01	360-02
Number of fuel assemblies	652	104	8
Structure power factor	0.951	1.245	1.358

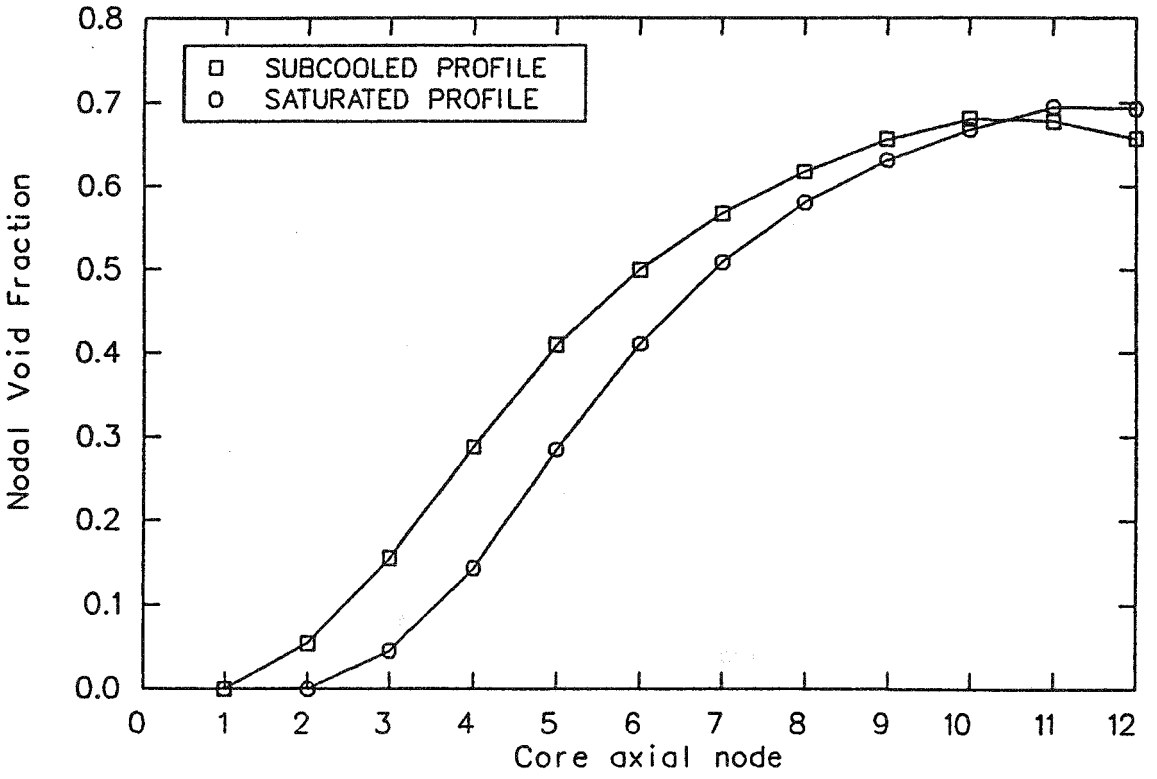

Figure A-5. Core axial void profiles at 20°F subcooling.

Table A-5. Safety/relief valve characteristics

Bank	1	2	3	4	Total
Number of valves	4	4	3	2	13
Set pressure (psia)[a]	1120	1130	1140	1265	N.A.
Valve area (ft^2)	—	—	—	—	1.1154

a. Within each bank, each valve's set pressure differs by 0.1 psi. All valves reclose 50 psi below their set pressure. Valves relieve 3110 lb/s of steam at normal reactor pressure.

Table A-6. RPV geometric data

Volume Component Number	Area, ft^2	Length, ft	Volume, ft^3	ΔElevation, ft
Lower Plenum				
290 01	91.43	5.335	487.78	−5.335
292 01	87.40	5.002	437.16	5.002
293 01	91.71	5.335	489.26	5.335
294 01	92.86	7.163	665.15	7.163
350 01	102.23	12.498	1277.70	12.498
			3357.05	
Core Region				
300 01	80.43	0.526	42.30	0.526
320 01	80.43	2.083	167.55	2.083
320 02	80.43	2.083	167.55	2.083
320 03	80.43	4.167	335.11	4.167
320 04	80.43	4.167	335.11	4.167
320 05	80.43	1.413	113.64	1.413
370 01	65.68	4.672	306.86	4.672
370 02	65.68	4.056	266.40	4.056
370 03	65.68	5.711	375.09	5.711
380 01	264.67	2.363	625.41	2.363
390 01	304.61	1.519	462.86	1.519
			3197.88	
Separator Region				
390 02	42.33	8.720	369.14	8.720
400 01	136.50	4.375	597.18	4.375
410 01	351.34	12.667	4450.31	12.667
420 01	281.63	10.958	2395.78	10.958
			7812.41	
Downcomer				
415 01	11.54	12.667	146.14	−12.667
415 02	207.12	4.375	906.14	−4.375
425 01	293.10	6.208	1819.66	−6.208
435 01	293.11	3.084	903.86	−3.084
435 02	87.86	6.916	607.67	−6.916
435 03	97.04	1.956	189.82	−1.956
455 01	95.21	8.410	800.70	−8.410
455 02	89.88	4.508	405.19	−4.508
475 01	90.28	3.121	281.81	−3.121
			6060.99	

Table A-6. (continued)

Volume Component Number	Area, ft^2	Length, ft	Volume, ft^3	ΔElevation, ft
Recirculation Loop[a]				
200 01	7.80	20.998	163.70	−12.458
210 01	7.80	5.784	45.14	−5.784
220 01	7.80	23.136	180.59	−21.333
220 02	7.80	13.566	105.89	2.534
230 01	7.80	19.561	152.69	2.000
240 01	7.80	31.248	243.91	19.463
250 01	7.80	2.750	21.46	2.750
250 02	16.38	13.729	224.86	1.667
250 03	7.53	16.773	126.30	13.250
250 04	5.47	4.017	21.99	0.833
250 05	5.47	11.879	65.05	11.879
250 06	5.47	2.703	14.80	1.883
260 01	7.30	4.417	32.24	−4.417
270 01	7.30	4.417	32.24	−4.417
270 02	12.53	2.402	30.11	−2.402
270 03	22.28	2.402	53.53	−2.402
270 04	34.87	2.402	83.76	−2.402
			1598.36	
Feedwater Line				
155 01	5.07	129.250	655.61	−18.170
170 01	4.24	99.48	423.870	45.370
			1079.09	
Main Steamline				
500 01	12.20	23.867	291.15	−22.516
500 02	12.20	23.867	291.15	−22.516
507 01	6.09	28.338	172.85	0.00
510 01	12.20	30.462	371.63	−4.394
510 02	12.20	18.878	230.31	−15.500
510 03	12.20	28.719	350.36	0.00
520 01	10.14	33.940	344.31	0.00
520 02	10.14	33.940	344.31	0.00
520 03	10.14	37.960	385.09	35.750
525 01	10.14	13.712	139.20	12.000
			2920.26	

a. Referenced to left loop. This loop lumps both recirculation loops.

Table A-7. RPV vessel elevations

Description	Elevation (ft)	Elevation (in.)
Inside head lower plenum	0.00	0.00
Recirculation suction	13.458	161.50
Core support piece	17.500	210.00
Jet pump suction	26.377	316.52
Top of active fuel	30.526	366.31
Lo-lo-lo level	32.042	384.50
Feedwater line penetration	38.333	460.00
Lo-lo level	39.67	476.00
Normal water level	46.75	561.00
HPCI trip level	48.50	582.00
Main steamline penetration	61.583	739.00

the model could contain significant deviation from actual plant behavior. Without some means of verifying model behavior, verification of plant transient behavior could only be accompanied with extensive qualification because of model uncertainties. A need to verify computer model behavior and to reduce and quantify model uncertainties was identified.

Towards this end, a series of benchmarks was performed. The benchmarks compared model behavior to the best obtainable data. Plant operational transient comparisons were made to identify and reduce deviations from actual plant behavior.

The 100% power steady state or rated conditions of the model are shown in Table A-8. The steady states presented are thought to be representative of plant conditions at 100% power. These steady-state conditions were used as initial conditions for the two plant transient data comparisons that are described here.

Two plant transient simulations were performed. The first was used to compare model performance to plant behavior during a pump coastdown. The transient initiator is the tripping of the recirculation pump motors by interrupting the power to the motors from their associated motor-generator sets. Figure A-6 shows the ensuing recirculation pump coastdown. As shown in the figure, model behavior closely replicates plant data.

The tripping of the recirculation pumps induces a rapid decline in the core inlet flow. Again, data

Table A-8. Steady-state conditions at 100% power[a]

Model Designator	Value
Power, Energy, and Mass	
Total reactor power	3293.0 MWt
Vessel ambient loss	0.134 MWt
System total mass	687,656 lb
Flows	
Feedwater flow	3692.1 lb/s
Steamline flow	3710.0 lb/s
Jet pump discharge	28,468 lb/s
Recirculation pumps	9775.8 lb/s
Core bypass	3383.0 lb/s
Bypass ratio	0.119 : 1
M-ratio	1.91 : 1
Pressures	
Lower plenum (292)[b]	1054.1 psia
Lower plenum (294)	1050.0 psia
Upper plenum (3801)	1024.6 psia
Steam dome (41501)	1014.2 psia
TCV (525)	973.27 psia
Pressure Differences	
Recirculation pump head	233.68 psi
Jet pump suction rise	22.2 psi
Core inlet plate drop (294-370)	21.2 psi
Core drop (294-380)	25.4 psi
Separator drop (380-41501)	10.2 psi
N-ratio	0.11 : 1
Levels	
Downcomer collapsed	46.75 ft
Bundle average void fraction	40.5%
Separator void fraction	81.0%
Thermal Performance	
Feedwater temperature	376.2°F
Jet pump throat subcooling	20.6°F
Core inlet subcooling	22.3°F
Turbine inlet quality, X_s	0.993
Peak centerline fuel temperatures	
Average bundle	1556°F
Ring 5 bundle	1951°F
Hot bundle	2181°F
Recirculation Pumps	
Speed	1623.8 rpm
Head	707.1 ft
Density	47.54 lb/ft^3

a. Conditions obtained with RELAP5/MOD1.6/Cyc 018, and with saturated power profile.

b. Numbers in parenthesis pertain to RELAP5 volume numbers.

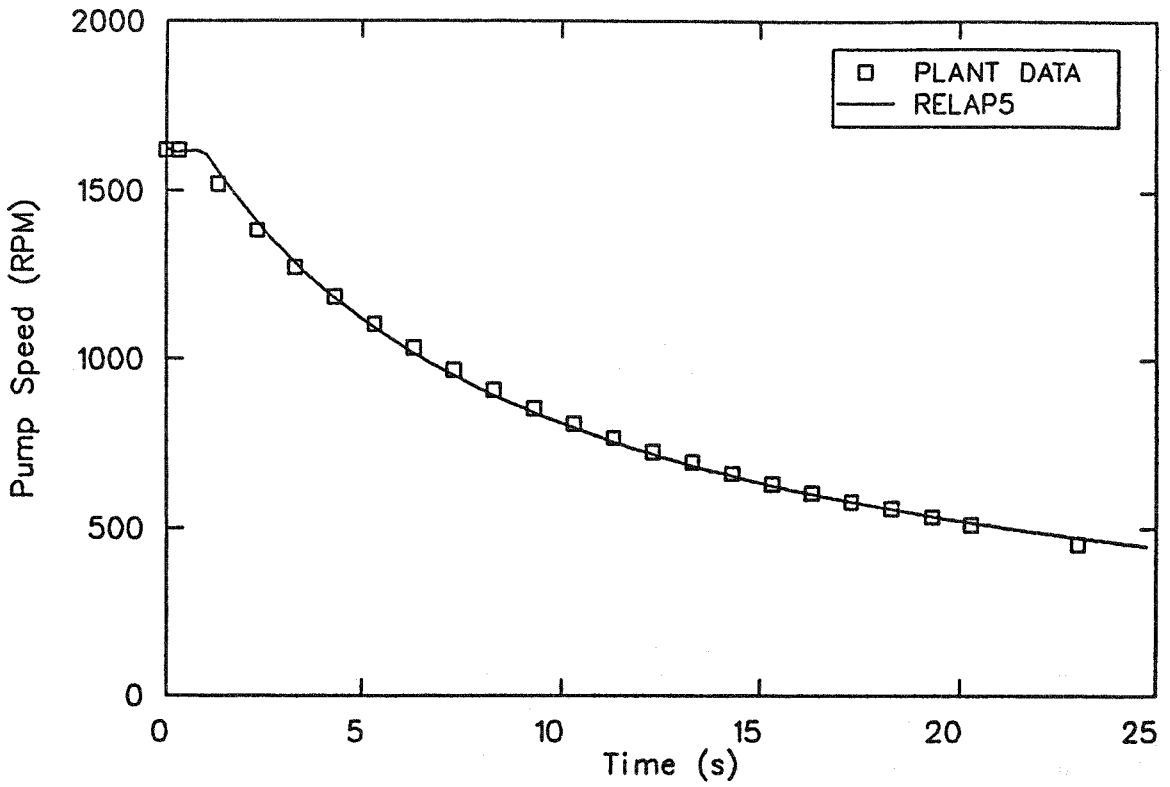

Figure A-6. Pump trip test data comparisons - pump speed.

comparison is favorable, as shown in Figure A-7. The decreasing core inlet flow tends to increase the void content of the core, causing a rapid decrease in the reactor power. Reactor power is shown in Figure A-8. The core responds much more quickly than the inlet flow to the recirculation pump trip. The core flow gradually coast down to about 40% of initial over the 25 s of the transient simulated. The reactor power, however, responds to the external perturbation in approximately 10 s. The power transferred to the core inventory vaporizes a portion of the inventory and causes the reactor to steam. The response of the vessel steaming, Figure A-9, and vessel pressure, Figure A-10, indicate that the response of the main steamline and/or turbine typify the data reasonably well.

Downcomer liquid level is shown compared to plant data in Figure A-11. When considered in the context of the wide range instrumentation, the agreement with plant data is somewhat poor. The collapsed downcomer liquid level is measured in the annular region outside of the dryer shroud. The level signal is used to actuate many important systems such as the HPCI system. This level is strongly affected by the model nodalization. Also shown is a pressure differential signal generated from RELAP5. There exists an uncertainty in this signal which influences transient timings related to level actuated signals.

The second and final plant transient data comparison performed compared the plant and model immediately following a generator load rejection. The generator load rejection transient sequentially clarifies the effect of several events: (a) the effect of increased steam demand on the vessel, (b) the effect of a reactor scram, and (c) the effect of simultaneous MSIV closure, recirculation pump trip, and HPCI/RCIC activation on the reactor vessel.

Transient initiation is induced by the rejection of the electrical load impressed on the main generator (see Reference A-1). This load rejection causes the turbines to overspeed. The turbine control valves begin to close, and the turbine bypass valves open to reduce the turbine overspeed. The overspeed continues, however, the reactor scrams at 1.6 s and the turbine stop valves close.

This sequence of events results in downcomer level depression, and double low level is reached 6 s into the transient. The recirculation pumps trip, the main steamline isolation valves close, and the HPCI and RCIC systems are activated.

Figures A-12 through A-16 show the response of the plant and the model to this sequence of events. In general, the correlation of plant data to the model is good.

In the load rejection transient, the vessel responds to steamline perturbations. Figure A-12 shows the

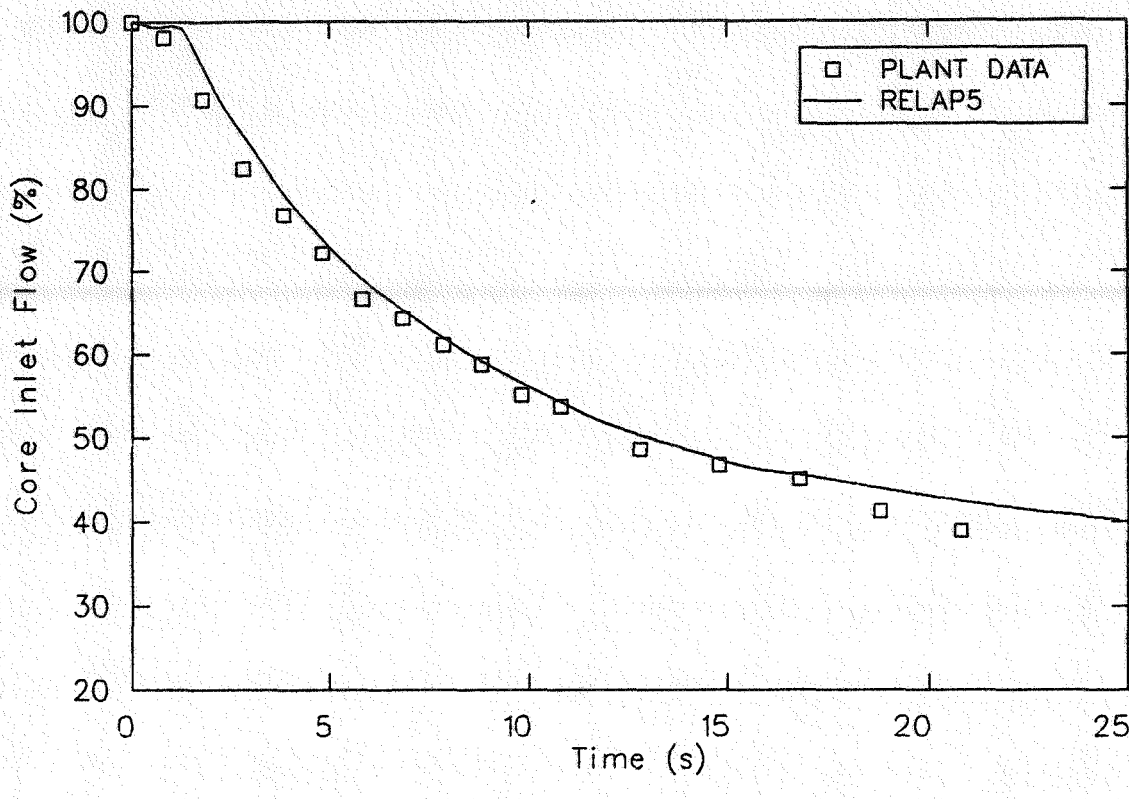

Figure A-7. Pump trip test data comparison - core inlet flow.

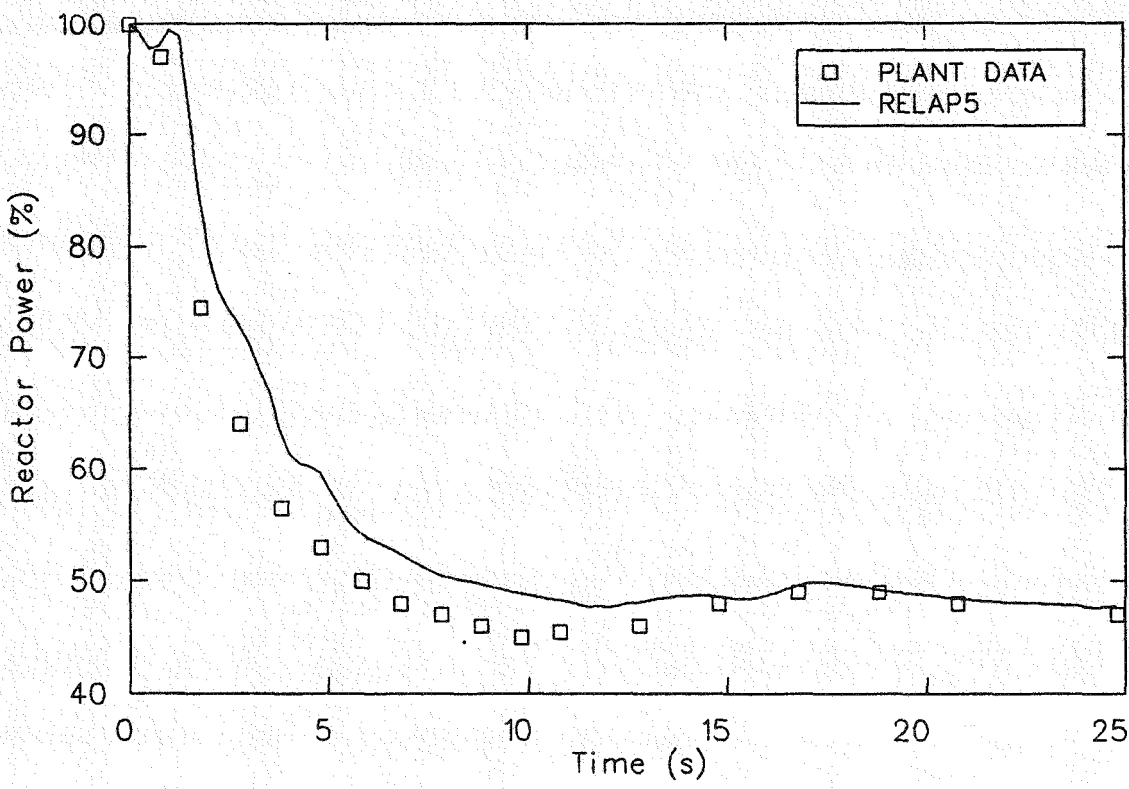

Figure A-8. Pump trip test data comparison - reactor power.

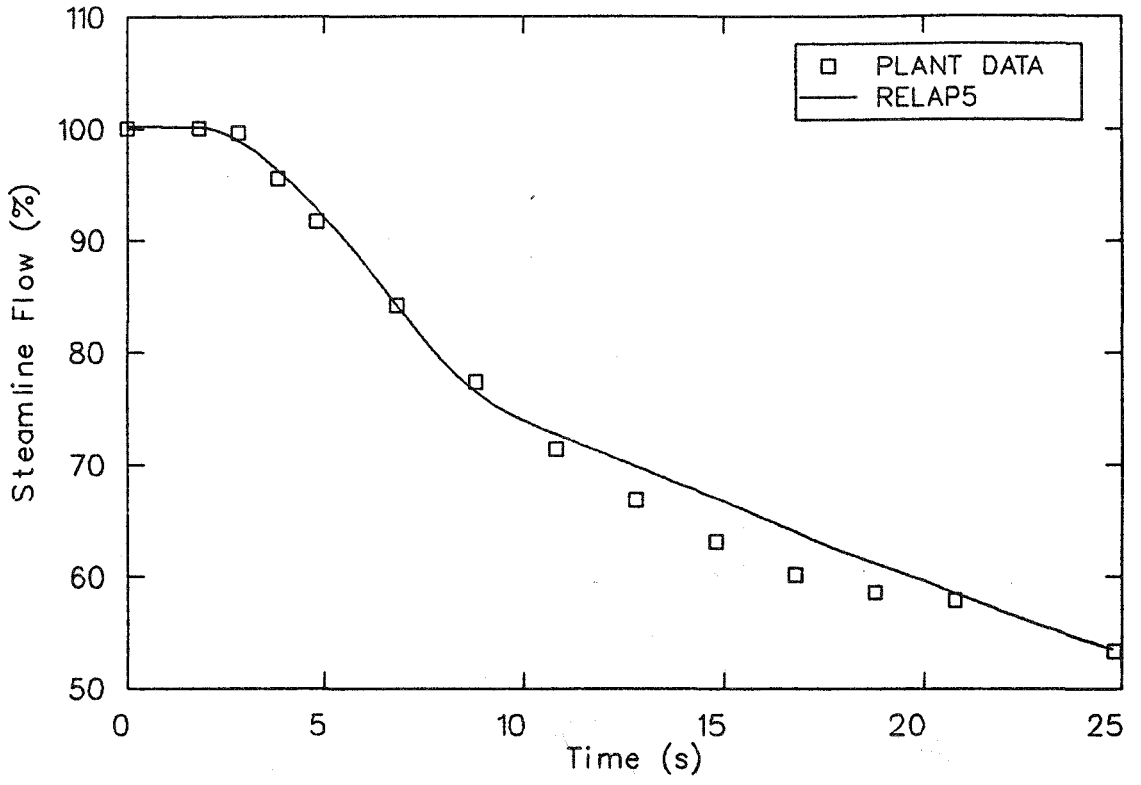

Figure A-9. Pump trip test data comparison - steamline flow.

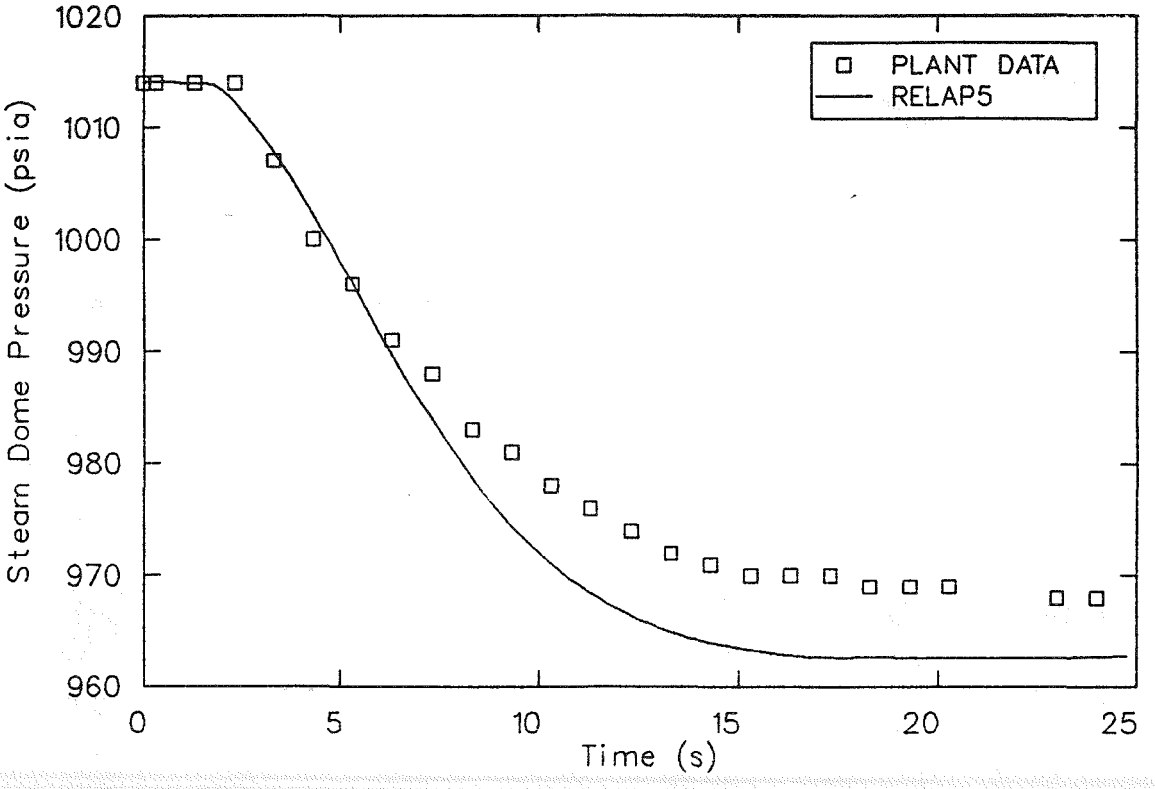

Figure A-10. Pump trip test data comparison - steam dome pressure.

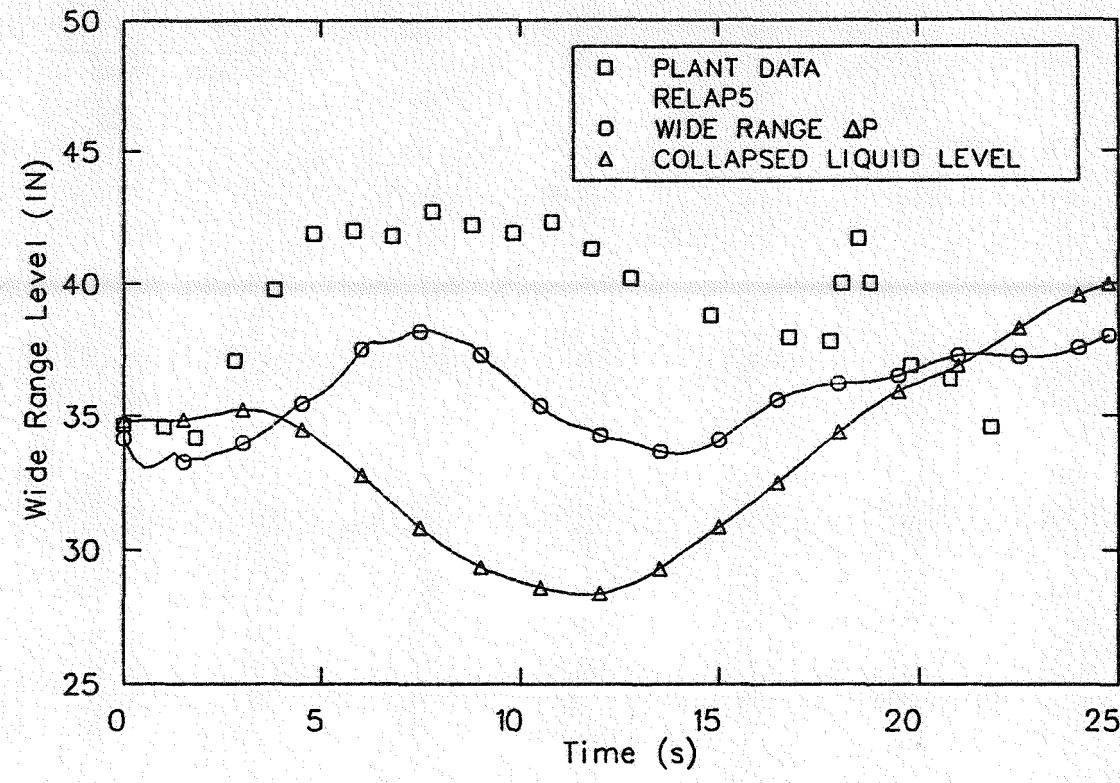

Figure A-11. Pump trip test data comparison - wide range level.

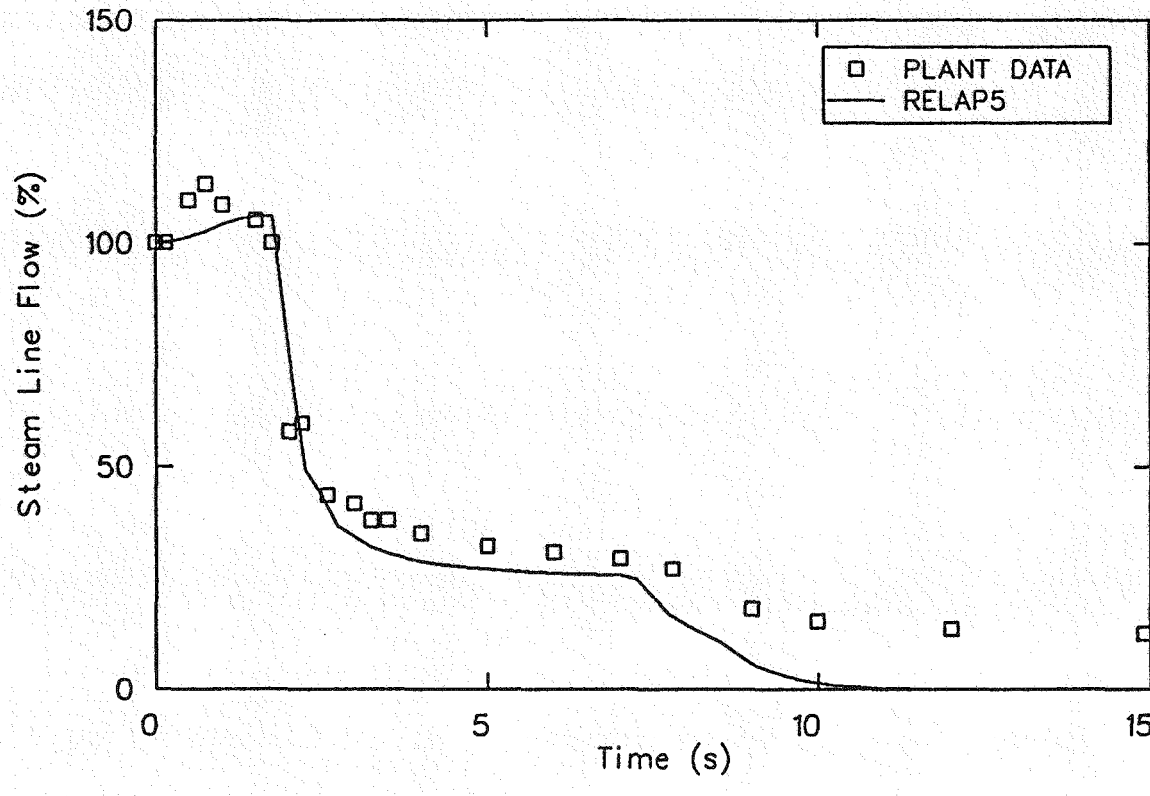

Figure A-12. Generator load rejection data comparison - steamline flow.

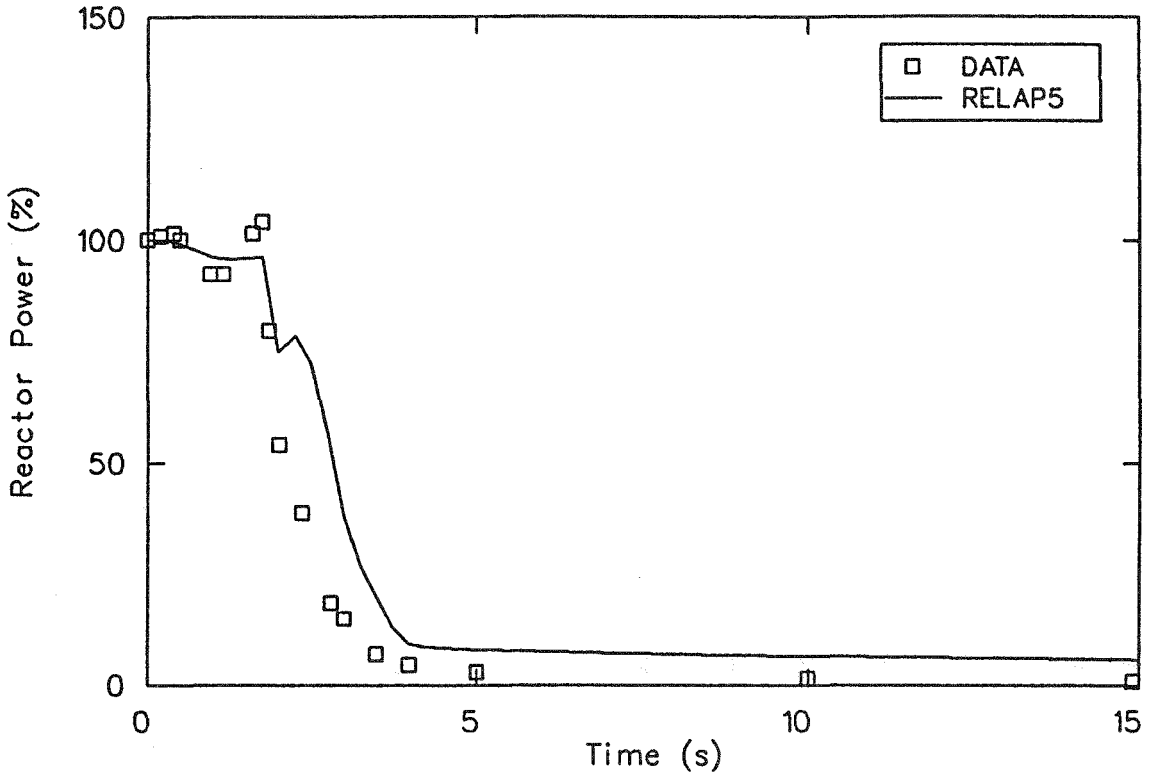

Figure A-13. Generator load rejection data comparison - reactor power.

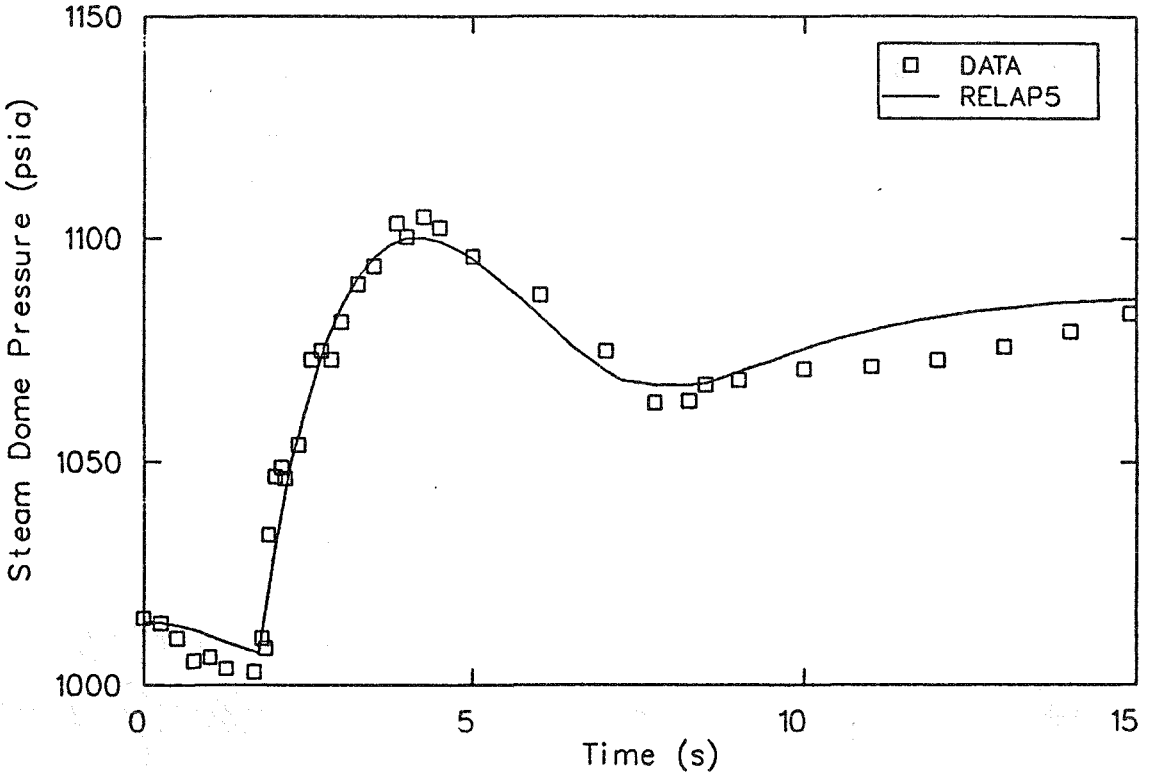

Figure A-14. Generator load rejection data comparison - steam dome pressure.

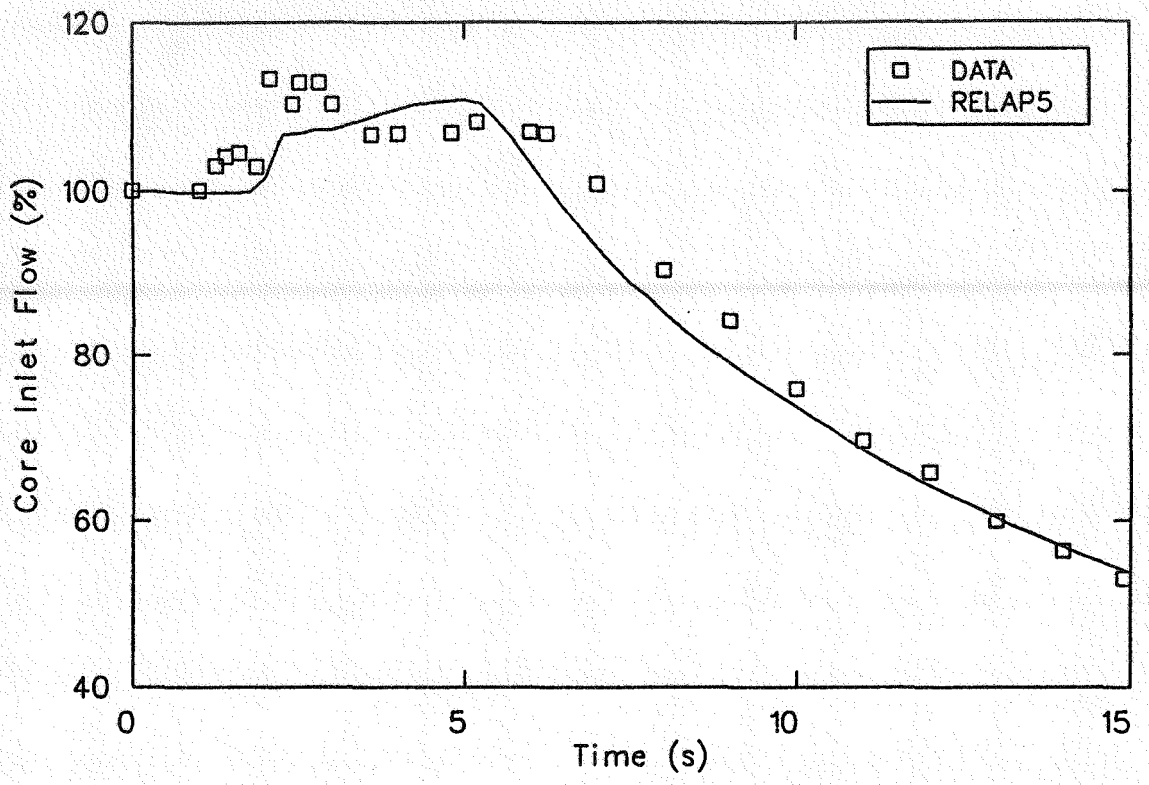

Figure A-15. Generator load rejection data comparison - core inlet flow.

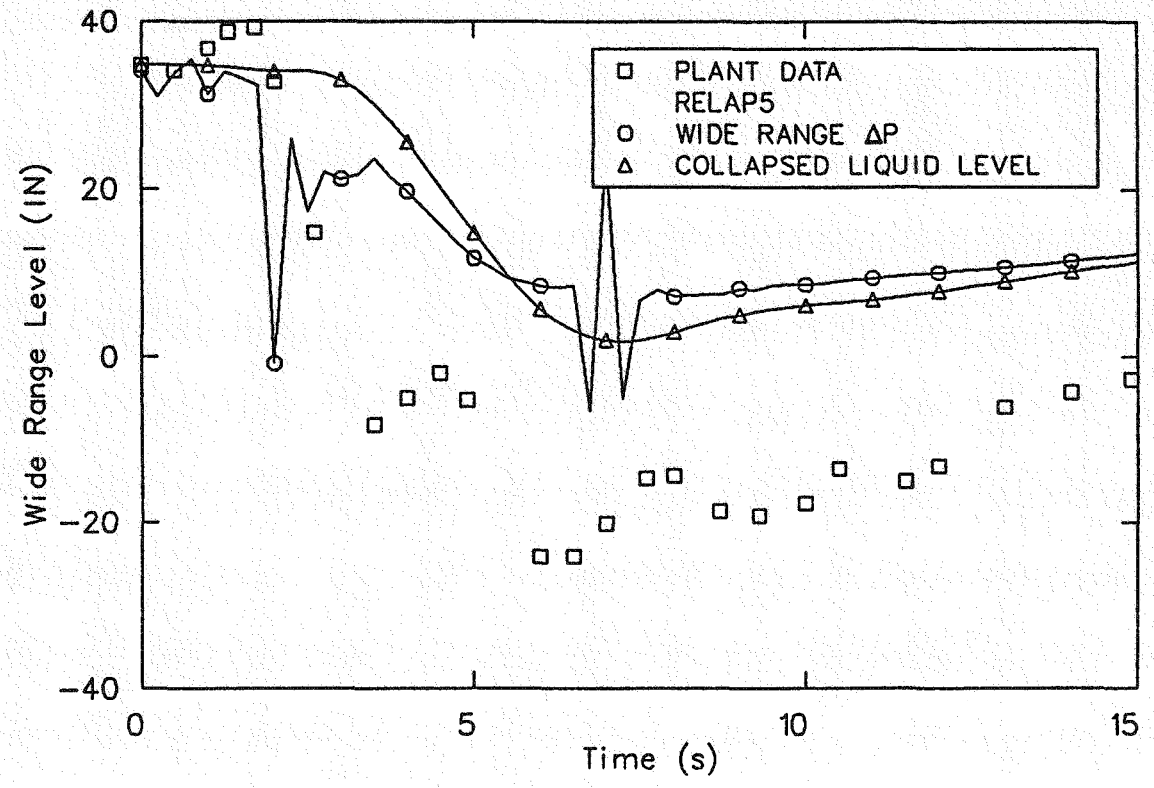

Figure A-16. Generator load rejection data comparison - wide range level.

vessel steam flow as measured at the main steamline flow restrictors. The initial, sharp decline in steam flow is caused by the turbine stop valve closure. This decline is arrested by the action of the turbine bypass valve. The flow rate is relatively constant until 7 s, when the closing action of the MSIVs becomes pronounced. Upon their closure, a no-flow condition is reached. It is thought that the steamline flow described by the data is erroneous after 10 s. Flow cannot reach the flow measuring devices once the MSIVs have closed.

The response of the reactor power to the load rejection is straightforward, as shown in Figure A-13. At 1.6 s, the reactor scrams and power decreases nearly monotonically.

The vessel or steam dome pressure responds to both steam flow and power. The turbine stop valve closure causes a rapid vessel pressurization (Figure A-14). This pressurization is limited by the relieving action of the turbine bypass valve, and by the reactor scram. Vessel pressure declines; but again rises due to the MSIV closure. The rate of subsequent pressure increases is influenced by the relieving action of the HPCI and RCIC steam driven turbines. No safety/relief valves were actuated during the simulation.

Core inlet flow response shows reasonably good data agreement, as is evidenced in Figure A-15. The rapid vessel pressurization induces a sharp increase in core inlet flow. The flow increase is limited by the response of the core thermal-hydraulics. The core thermal-hydraulics respond to the steamline flow perturbation much more rapidly than the pressure of the vessel does. Flow coastdown is induced by the tripping of the recirculation pumps on double lo level.

Because of the poor downcomer level response shown by the model, the timing of the double lo level trip was specified according to plant data. Figure A-16 shows the level response during this transient. For the purposes of this simulation, double lo level was assumed to be reached 6.4 s into the transient.

The results of these plant transient data comparisons are mixed. In general, recirculation pump speed, core inlet flow, and reactor power and pressure show good data agreement. The model is expected to be able to reliably predict these parameters. On the other hand, vessel steaming and downcomer level response are not as well predicted by the model during the transients presented here. The exact cause of the deficiencies in these signals is not well understood, but the significance of the deficiencies to ATWS simulation can be estimated.

It is thought that the deficit and uncertainty accompanying the vessel and/or core steam are of marginal significance when interpretated in terms of ATWS simulation. This deficiency is induced by the short-term transient behavior. Over the typical duration of an ATWS simulation of many hundreds of seconds, this short-term transient behavior will subside. Short-term behavior is governed by the momentum equation. Over a long term, momentum effects will be dominated by the mass and energy balances of the vessel, which are usually independent of the momentum balance.

The level signal is regarded as having large dynamic uncertainties. The significance attached to this signal is attached to operator action. During the normal course of a transient, it is expected that the operator will monitor the downcomer level signal. Thus, simulation timings contingent on proper downcomer simulation will be somewhat in error. However, in the long term, vessel mass and energy balances will dominate momentum induced effects, so that the error in the level signal will not be divergent.

REFERENCES

A-1. Interoffice correspondence, J. A. Raulston (TVA) to R. R. Schultz (INEL), October 24, 1980.

A-2. R. R. Schultz and S. R. Wagoner, *The Station Blackout Transient at the Browns Ferry Unit One Plant: A Severe Accident Sequence Analysis*, EGG-NTAP-6002, September 1982.

A-3. W. C. Jouse and R. R. Schultz, *A RELAP5 Analysis of a Break in the Scram Discharge Volume at the Browns Ferry Unit One Plant*, EGG-NTAP-5993, August 1982.

A-4. W. C. Jouse and R. R. Schultz, *RELAP5/MOD1 6 BWR/4 ATWS Demonstration Calculation on the Browns Ferry Unit 1 Nuclear Plant*, EGG-SAAM-6397, November 1983.

A-5. W. C. Jouse, *Sequence Matrix for the Analysis of an ATWS in a BWR/4; Phenomena, Systems, and Operation of Browns Ferry Nuclear Plant Unit 1*, a draft report for comment, May 1984.

A-6. *Design and Performance of General Electric Boiling Water Reactor Jet Pumps*, APED-5460, GE, September 1968.

A-7. G. E. Wilson, *INEL One-Sixth Scale Jetpump Data Analysis*, EGG-CAAD-5357, February 1981.

A-8. Interoffice correspondence, C. J. Prone (GE) to J. T. Robert (TVA), "Browns Ferry 1, Cycle 6 Reference Loading Map", CJP: 83-047, March 1983.

A-9. R. C. Stirn, *Generation of Void and Doppler Reactivity Feedback for Application to BWR Design*, NEDO-20964, GE, December 1975.

A-10. R. J. Grossenbacker, et al., *BWR/4 and BWR/5 Fuel Design*, Licensing Topical Report, NEDO-20944, GE, October 1976.

A-11. D. J. Diamond, *Generation of BWR Point Reactivity Functions*, BNL-NUREG-32412, September 1982.

A-12. D. J. Diamond and H. S. Cheng, "Higher Order Effects in Calculating Boiling Water Reactor Doppler and Void Reactivity Feedback," Nuc. Tech., 46, 439, December 1979.

A-13. Interoffice correspondence, G. C. Slovik (BNL) to W. C. Jouse (INEL), December 28, 1984.

A-14. S. L. Forkner et al., *BWR Transient Analysis Model Utilizing the RETRAN Program*, TVA-TR81-01, December 1981.

A-15. W. Frisch et al., "The Significance of Fast Moderator Feedback Effects in a Boiling Water Reactor During Severe Pressure Transients," *Nuclear Science and Engineering, 64*, 1977, pp. 843-848.

A-16. Browns Ferry Nuclear Plant Final Safety Analysis Report (FSAR), Tennessee Valley Authority.

A-17. General Electric, *BWR Technology*, NEDO-10260.

A-18. Interoffice correspondence, W. D. Driskell to E. T. Laats, "Power Distribution for the Browns Ferry Cycle 4 Core", WED-1-83, August, 1983.

A-19. B. Chexal et al., *Reducing BWR Power by Water Level Control During an ATWS*, NSAC-70, August 1984.

APPENDIX B

DESCRIPTION OF BFNP1 PRIMARY CONTAINMENT AND CONTEMPT/LT-028 MODEL

APPENDIX B

DESCRIPTION OF BFNP1 PRIMARY CONTAINMENT AND CONTEMPT/LT-028 MODEL

1. BROWNS FERRY CONTAINMENT DESCRIPTION

In this section, the Browns Ferry Nuclear Plant Unit 1 (BFNP1) primary containment is described as an introduction to discussion of the CONTEMPT/LT-028 code model of the containment. For a detailed description of the containment geometry, refer to References B-1 and B-2.

The BFNP1 primary containment is the Mark I General Electric Design. A Mark I containment is composed of essentially two major parts; the drywell and the wetwell. A representation of the lightbulb-shaped drywell/torus wetwell configuration is shown in Figure B-1. The Mark I containment is used in the majority of the operating BWRs in the United States.

The drywell is a steel pressure vessel consisting of a spherical lower section 67 ft in diameter and a cylindrical upper section 38 1/2 ft in diameter. The drywell is enclosed in reinforced concrete for shielding and additional resistance to deformation. The drywell houses the nuclear steam supply system (NSSS), including the reactor pressure vessel, recirculation loops, steamlines, safety/relief valves, feedwater and emergency core coolant systems piping. The drywell is connected to the wetwell by eight large ventilation pipes, each 81 in. in diameter and arranged symmetrically about the periphery of the drywell sphere lower half. These vent pipes protrude into the wetwell and connect to a 57-in. diameter ring header which itself forms a torus within the wetwell proper. Ninety-six downcomer pipes protrude from the ring header, each two feet in diameter, and normally submerged at least three feet into the torus pool (see Figure B-2).

The torus has an inside minor diameter of 31 ft and a major diameter of 111.5 ft. Nominally, it contains about one million gallons of demineralized water and

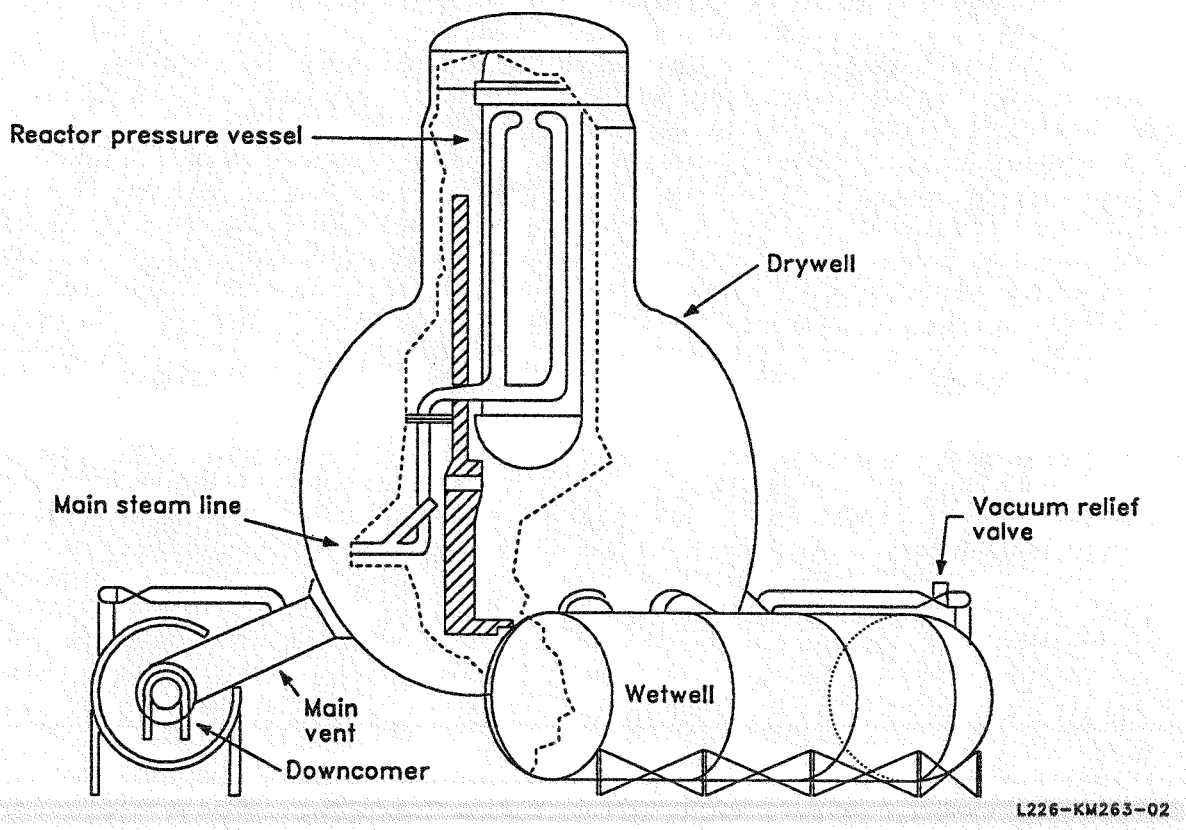

Figure B-1. Mark I drywell/torus configuration.

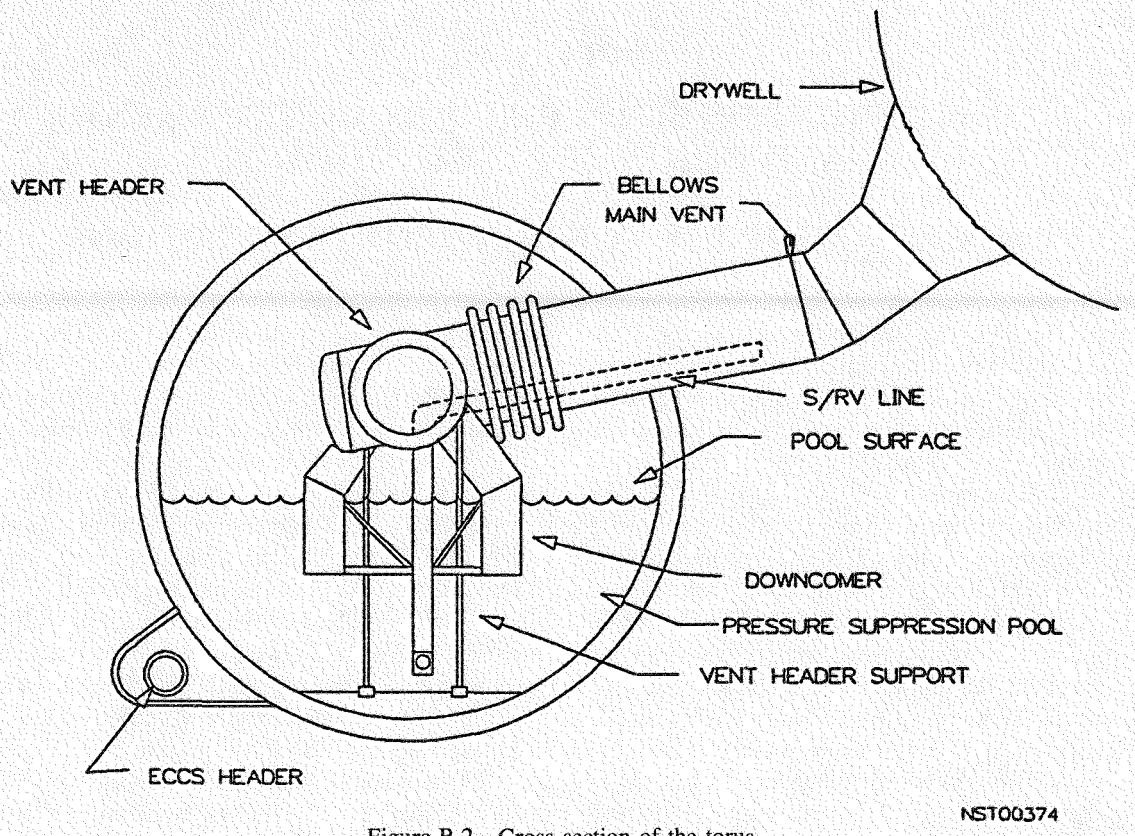

Figure B-2. Cross section of the torus.

is maintained within the normal operating water level range from 14.6 ft to 15.1 ft, nearly half the torus diameter. The torus is designed to contain the initial energy release during a double-ended large break in the 28-in. reactor recirculation pump line, sustaining a 50°F temperature rise in the process. Maximum torus initial water temperature is 95°F per technical specifications constraint.

The torus is one of the distinguishing features of the Mark I containment design, and it performs a number of important functions. It will accept vessel effluent during a loss-of-coolant accident (LOCA) through the drywell/wetwell vent system. The torus condenses steam released from the vessel through the safety/relief valves during off-normal plant operation or an accident. Vessel steam diverted in this manner is discharged to the pressure suppression pool through sparging devices known as the T-quenchers. One purpose of the T-quencher is to maintain local velocities at the discharge point sufficiently high to avoid hydrodynamically induced pressure oscillations in the pool. The T-quencher is also designed to ensure that complete steam condensation occurs in the torus preventing pressurization of the wetwell and drywell. The torus is the primary source of water for the low pressure coolant injection (LPCI) and low pressure core spray (LPCS) emergency systems as well as the containment safety sprays. It serves as a secondary water source for the high pressure coolant injection (HPCI) and reactor core isolation cooling (RCIC) systems. The torus also accepts steam exhaust from the HPCI and RCIC turbines.

The torus has an external design pressure of 2 psid and is protected from collapse by two 18-in. vacuum relief valves, which equalize pressure between the reactor building and the wetwell within one second after a 0.5 psi pressure differential is sensed. Internal design pressure of both the torus and the drywell is 56 psig at 281°F.

During normal operation, the drywell is inerted with nitrogen and positively pressurized with respect to the wetwell by 1.1 to 1.3 psid. System pressure is normally maintained by a compressor and a differential pressure control system between the wetwell and the drywell. The positive pressurization maintains minimal liquid column height inside the downcomer pipes (the drywell side), which would reduce dynamic loads in the torus during an accident in which the drywell is pressurized early and the vents clear. Should the pressure differential reverse and exceed 0.5 psid, there are twelve 18-in. swing check vacuum relief valves (VRV) located at the ends of the 81-in. vent pipes which would relieve pressure from the wetwell to the drywell. One purpose is to prevent a vacuum in the

drywell when the drywell sprays are actuated during a large break LOCA, preventing liquid backflow into the drywell. Another purpose of these VRVs is to alleviate the effects of wetwell pressurization during extended discharge through the SRVs.

The pressure suppression pool temperature can vary considerably depending on the time of year and the status of plant operation. The technical specifications restrict the water temperature to less than 95°F. The water is maintained within plant specifications by the residual heat removal system, whose four heat exchangers combined have a design capacity of 280 million Btu/hr, about 2-1/2% of rated power. The cooling capacity is a function of pool temperature, increasing with increasing temperatures.

Drywell temperature is maintained below 135°F by ten fan cooling units (arranged in two large air handling systems) which exchange heat with the reactor building closed cooling water (RBCCW) system. Eight of these units are normally operational with two spares. The operating load capacity of the drywell cooling system is about 5.2 million Btu/hr. Normal drywell temperature averages about 125°F. Bulk temperatures up to 135°F are acceptable according to design specifications.

The drywell and torus together form the primary safety barrier between the NSSS and the reactor building, the reactor building serving as the secondary containment and the final safeguard between power plant and environment. Detailed discussion of the secondary containment is beyond the scope of this report. However, the reactor building does house a number of systems which could be important to accident management in different situations.

2. MODELING THE BROWNS FERRY CONTAINMENT

In this section, the CONTEMPT/LT-028 computer code and model of the BFNP1 containment are discussed. Section 2.1 gives a brief description of the code and its capabilities. The BFNP1 containment input model is next discussed, and the calculated initial conditions are presented in Section 2.2.

2.1 Code Description

The code used for the analyses documented herein was CONTEMPT/LT-028 (Reference B-3). CONTEMPT is a containment thermal hydraulics code originally developed at the Idaho National Engineering Laboratory (INEL). The code has been used for licensing purposes and was chosen for the ATWS studies because it has been assessed to a greater degree than other containment codes available at the onset of the ATWS calculations (see References B-4 and B-5).

CONTEMPT/LT-028 is a lumped parameter code which was originally designed for LOCA analyses. The code numerics are explicit. Current modeling capability includes BWR Mark I, II, and III plus PWR dry containments. The code has a generalized, lumped volume compartment model that allows liquid and vapor to exist in nonequilibrium. The state of each phase is uniform throughout that phase. Heat and mass transfer provisions exist between the phases, and leakage to and from a compartment can be modeled. Energy additions to a compartment can occur from heat structures, 20 of which are permitted. The heat structure model (for stored energy or heat sink) is distributed, allowing up to 101 mesh points per structure. A heat slab can be either single or double sided. A number of heat transfer options are available for slab boundary conditions. Mass and energy additions to a compartment can also be input as boundary conditions in a tabular format at the user's option.

CONTEMPT/LT-028 has sufficient latitude to enable modeling of fan coolers and various ECC and safety spray systems. There is a vent model which calculates two-phase, two-component flow through the vent system between the drywell and wetwell. This model is basically a series of flow resistances for the purpose of fluid transport between the drywell and wetwell. There is no volume or mass associated with the vent model and it is most suitable for forced convective flow per the LOCA analysis, original design intentions of the code.

Increased tabular data input capacities have been programmed into CONTEMPT/LT-028 to facilitate interfaces with driver codes such as TRAC-BD1 or RELAP5. Such data transfers are done with computer software to minimize the chances of error. Safety/relief valve blowdown to the wetwell pool is treated as a boundary condition in the BFNP1 ATWS modeling, and a tabular input option has been coded to enable this condition. SRV mass flow rate and energy addition rate versus time can be input, with up to 2000 data points allowable for any one problem.

CONTEMPT/LT-028 is an inexpensive, fast running code. Typical one-hour BFNP1 ATWS problems run on a Control Data Corporation CYBER 176 computer for under $30, at a rate approximately 14 times faster than real time.

2.2 Model Description

The BFNP1 containment model used for the reported calculations was based on information from several sources, the Tennessee Valley Authority, the BFNP1 FSAR, etc. It has been constructed with best estimate methods whenever possible. In cases where information was not available, conservative engineering judgment was used. For example, the heat structures between the drywell and reactor building are insulated in the model and no credit is taken for heat loss to the reactor building.

The CONTEMPT/LT-028 model for the BFNP1 is shown in Figure B-3. One compartment each is used for the drywell and wetwell. For the analyses documented herein, it has not yet proved necessary to model the reactor building. Instead, heat structures representing the reactor building provide boundary conditions for heat transfer from the torus. There are 11 heat structures in the model, as detailed in Table B-1. This tabulation lists the heat structures, the compartments to which the structures are connected, and the surface boundary conditions of the heat slabs. Vessel heat slab initial conditions were taken from RELAP5 calculations. Drywell and wetwell slab initial conditions were based on average operating conditions where possible, but these sometimes required engineering judgments where detailed data were unavailable.

As part of the quality assurance program for the input model, steady state calculations were run to generate initial conditions of drywell and wetwell pressure and temperature for the ATWS transients. This procedure was helpful in the isolation of input errors and often suggested modeling improvements. Importantly, it assured that the initial conditions were stable values free of significant numerically induced drifts.

The drywell (DW) and wetwell (WW) initial conditions calculated by CONTEMPT are compared to plant operating specifications in Table B-2. The steady state comparisons are generally good. The wetwell pressure is slightly high, resulting in a calculated DW to WW differential pressure that is too low compared to plant specifications. Because the compressor and pressure control system are not modeled, the drywell and wetwell are driven closer to an equilibrium state at the start of transient calculations than would be the actual case. However, the lower drywell pressure results in a slightly longer time to high drywell pressure (HDWP). The initial DW pressure is within the normal operating range of plant conditions, and the slightly higher than normal wetwell pressure has a negligible effect on the ATWS.

Drywell temperature is controlled by the drywell coolers. These are modeled by a constant heat removal rate from the drywell for these calculations, as CONTEMPT has no mechanistic fan cooler model. For

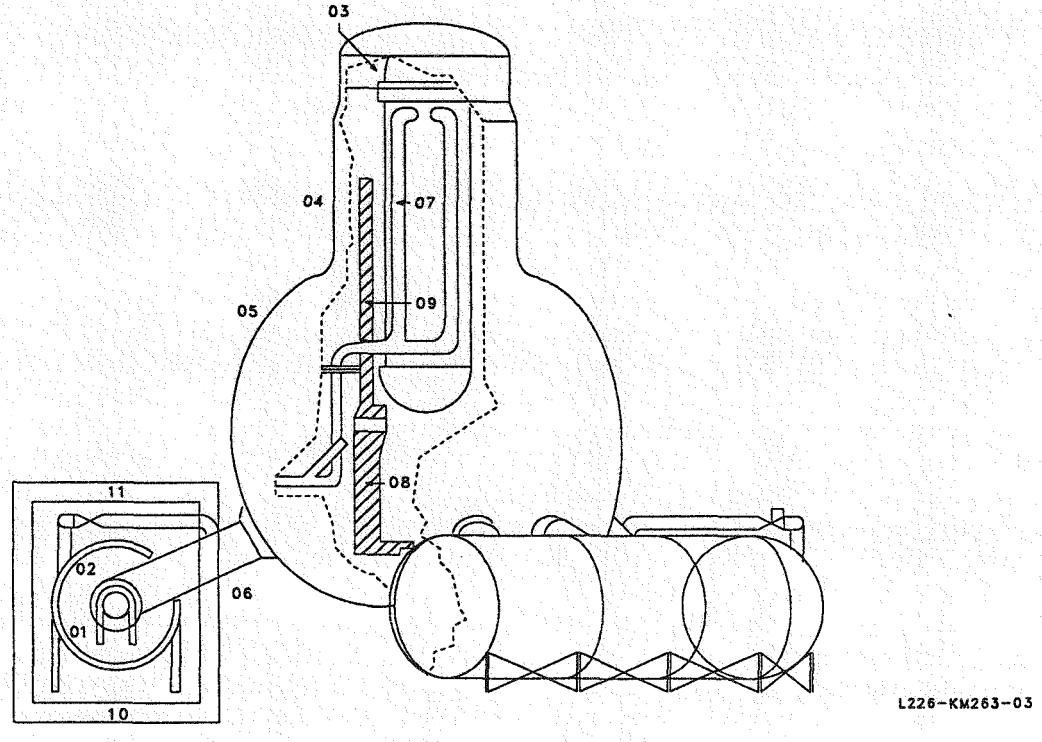

Figure B-3. CONTEMPT Browns Ferry containment model.

Table B-1. CONTEMPT/LT-028 Browns Ferry heat structure modeling

Structure	Description	Steady State (°F)	Connection/Boundary Condition: Left	Connection/Boundary Condition: Right	Steady State (°F)
1	Torus water half	90	WW/Constant HTC	WW/NC & radiation to HS10	82
2	Torus vapor half	90	WW/UCHIDA[a]	WW/NC & radiation to HS11	104
3	Vessel top head	527	Vess/R5 Const. HTC	DW/UCHIDA	135
4	Drywell cylinder	135	DW/UCHIDA	DW/Insulated	—
5	Drywell sphere	135	DW/UCHIDA	DW/Insulated	—
6	Vent system	135	DW/UCHIDA	WW/UCHIDA	90
7	Vessel cyl. shell & bottom head	525	Vess/R5 Const. HTC to HS9	DW/NC & radiation	135
8	Vessel pedestal	135	DW/Turb. NC	DW/UCHIDA	135
9	Biological shield wall	135	DW/NC + radiation to HS7	DW/UCHIDA	135
10	Reactor building foundation	82	WW/NC + radiation to HS1	WW/Insulated	—
11	Torus room overhead	104	WW/NC + radiation to HS2	WW/Insulated	—

a. UCHIDA heat transfer coefficient is a condensing steam value dependent on the mass ratio of water vapor to air. The UCHIDA option defaults to a natural convection boundary condition if the correct conditions for condensation do not exist.

Table B-2. ATWS calculation initial conditions compared to plant specifications

	CONTEMPT/LT-028 Calculated		BFNP1 Specifications	
	Wetwell	Drywell	Wetwell	Drywell
Pressure	+1.14 psig	+1.38 psig	0.5 psig max., −0.5 psig min.,	1.8 psig max.[a] 0.6 psig min.
Temperature	90°F	134.9°F	33°F-95°F	135°F
Humidity	0.97	0.20	—	—
Torus water level	175.8 in.	0.0	175-1/4 in. to 181-1/4 in.	—

a. BFNP1 specification on DW to WW ΔP is 1.1 to 1.3 psid. See discussion in text.

this model, a heat removal rate of 3.75 million Btu/hr (1.1 MW) was used, approximately equivalent to the load capacity of eight drywell cooling units.

The wetwell to drywell vacuum relief system was modeled as twelve 18-in. relief valves, each with a flow area of 1.67 square feet. The relief valve model was programmed to open at a pressure differential (WW to DW) of 0.5 psid. The code assumes that all 12 valves are fully open simultaneously and instantaneously (with no opening delay) when the required differential pressure is reached. This is a limitation of the code, not user specified, but should have very little effect on the results. The CONTEMPT/LT-028 BFNP1 containment model has been reviewed, including a detailed engineering review of the input deck. The model is believed to be an accurate representation of the plant.

REFERENCES

B-1. General Electric Company, "Containment Data", Customer Interface Data Document No. 22A5737, Rev. 1, April 1979.

B-2. General Physics Corporation, *BWR Simulator Training Manual*, Second Edition, Volume 1, 1979.

B-3. D. W. Hargroves and L. J. Metcalfe, *CONTEMPT-LT/028—A Computer Program for Predicting Containment Pressure-Temperature Response to a Loss-of-Coolant Accident*, NUREG/CR-0255, TREE-1279, EG&G Idaho, Inc., March 1979.

B-4. G. J. E. Willcutt, Jr. and R. G. Gido, *Comparison of CONTEMPT-LT Containment Code Calculations with Marviken, LOFT and Battelle-Frankfurt Blowdown Tests*, NUREG/CR-1564, LA-8423-MS Informal Report, July 1980.

B-5. B. S. Anderson, *Comparison of CONTEMPT-LT Predictions to Marviken Experimental Data*, INEL Interim Report I-347-75-02, Aerojet Nuclear Company, June 1975.

APPENDIX C

DESCRIPTION OF THE SCDAP CODE AND THE BFNP1 SCDAP MODEL

APPENDIX C

DESCRIPTION OF THE SCDAP CODE AND THE BFNP1 SCDAP MODEL

During the high pressure boiloff portion of the plant automatic transient, cladding temperatures were predicted to reach the threshold point for cladding oxidation. To obtain information about hydrogen production and fission product release, a SCDAP[C-1] calculation was performed. Results from that analysis were presented in Section 6.2 of this report.

The SCDAP analysis was initiated a short time before the onset of zircaloy oxidation (>1340°F) of the cladding. The calculation was terminated as the rate of hydrogen generation approached zero. SCDAP was used because it was specifically developed to predict core behavior from the onset of zircaloy oxidation through severe core damage. RELAP5 results were used to provide the initial boundary conditions for the SCDAP case and were then extrapolated to provide the boundary conditions for the entire SCDAP analysis. This was possible due to the almost steady-state condition of the plant during the postulated core damage scenario.

The version of the SCDAP code used for the analysis was SCDAP/MOD1/VO subcode SCDVESSEL. SCDVESSEL has simplified boiloff thermal hydraulic models which are fast running. This version also had an upper vessel model to provide information on damage progression in that region of the vessel.

The discussion in this appendix is divided into three parts. A description of the SCDAP code is given in Section 1 Section 2 discusses the model used in the study. Section 3 reviews the boundary conditions used in this part of the study.

1. Code Description

The SCDAP/MOD1/VO computer code models the progression of a postulated event or experiment up to and including core geometry changes and material relocation due to severe overheating and fragmentation of embrittled materials. Important phenomena occurring in both the upper and lower plena are modeled. Cladding and stainless steel oxidation, hydrogen generation, and fission product release are modeled. Cladding ballooning and rupture, material liquefaction and relocation, component fragmentation during reflood, debris formation and thermal-hydraulic behavior are also modeled. Major outputs include:

- Rates of hydrogen generation due to oxidation reactions
- Rates and chemical forms of released fission gases
- Rates and characteristics of debris formation
- Coolability of the disrupted core geometry and/or debris
- Vessel internal state up to loss of the core support structure integrity.

SCDAP/MOD1/VO is a modular computer code and has been designed so that either all of the code or individual subcodes and models can be readily used to perform calculations. This modularity allows the user and code developer (a) to tailor calculations for particular problems or experiments, (b) to test individual parts or all of the code, and (c) to test alternative models or subcodes to establish the sensitivity of different modeling assumptions. For this case the subcode, SCDVESSEL, was used. SCDVESSEL will compute the behavior of a single fuel rod, control rod, shroud, an individual bundle, or a reactor vessel consisting of core, upper and lower plena, and layered outer shroud. The simplified boiloff thermal-hydraulics model, developed for the fast running version of SCDAP/MOD0 (designated SCDSIMP) was used. SCDVESSEL is a pilot capability designed to test the models which treat plenum behavior and radiation heat transfer in arbitrary geometries. SCDVESSEL can be used for analysis up to the point of debris formation through quench-induced fragmentation. SCDVESSEL consists of SCDSIMP, and pilot plenum and radiation models.

SCDAP/MOD1/VO simulates disruption within the vessel through a detailed analysis of representative vessel components. The code can analyze a boiling water reactor (BWR) vessel and components, a pressurized water reactor (PWR) vessel and components, and experimental bundles through a user defined description of the components, bundle, and vessel. The code consists of detailed physical models for uranium dioxide (UO_2)-zircaloy fuel rods, thermal models for one-dimensional cylinders and slabs, plenum structure models, and general one-dimensional thermal-hydraulics models for both the core and plena. Models are provided to describe the formation and thermal-hydraulic behavior of the plena and any core debris which may form as the vessel components are disrupted through either a material liquefaction and redistribution process or a quench induced material fragmentation process.

2. SCDAP Model Description

The SCDAP model used for the analysis consisted of a core model and an upper vessel model. The core inlet conditions were provided by the RELAP5 studies. The core outlet flow provided the inlet condition of the upper vessel regions.

The core model used for this analysis consisted of one fuel bundle including the canister, typical of those in the BFNP1 plant. The fuel rods were in an 8 × 8 configuration. The bundle was divided into five regions, called components. The fuel rods were divided into three rod components, describing the radial power distribution. One component was used to model the two water rods in the bundle and one component was used to model the canister.

Information for the model was obtained from the Final Safety Analysis Report (FSAR),[C-2] or was provided by the Tennessee Valley Authority (TVA).[C-3,C-4,C-5] In accordance with the available data, the bundle was assumed to be in the eleventh month of the sixth cycle. The hot bundle from ring five was modeled. The bundle burnup was 10064 MWD/MTU. The control rods were assumed to be completely withdrawn at the time of the transient and were not modeled.

The fuel was divided into 10 equally spaced axial regions of 1.25 ft. Ten regions is the maximum allowed by SCDAP. Radially each rod group was modeled with six nodes, four in the fuel and two in the cladding. Other input variables are listed in Table C-1.

The vessel above the core was modeled to describe seven distinct regions associated with the reactor design. The seven regions are:

1. The area from the top of the active fuel length to the top of the canister,
2. Upper core grid,
3. The region from the top of the canister to the top of the core shroud head,
4. The region from the top of the core shroud head to the top of the stand pipe,
5. The separator region,
6. The dryer region, and
7. The steam dome region.

In the upper vessel region, SCDAP only models zircaloy and stainless steel. Since the first two regions were mostly zircaloy and the other five mostly stainless steel, the upper vessel region could be adequately modeled. The upper vessel models used inlet coolant conditions from the core and are able to describe the processes of oxidation and melting of upper vessel structures. The structures were scaled by the number of bundles in the core.

Table C-1. SCDAP input parameters

Parameter	Units	Value
Active fuel length	ft	12.5
Fuel pellet radius	ft	0.0171
Cladding outside radius	ft	0.02012
Cladding inside radius	ft	0.01746
Axial node heights	ft	1.25
Pitch	ft	0.0535
Coolant pressure (transient initiation)	psia	1040

3. Boundary Conditions

The SCDAP study was an extension of the RELAP5/MOD1.6 analysis. The SCDAP calculation was initiated a short time before the onset of zircaloy oxidation. The required boundary conditions taken from the RELAP5 analysis were enthalpy and mass flow of the fluid entering the core, coolant pressure at the inlet to the core, and core power. Enthalpy, pressure and flow boundary conditions were required during the entire SCDAP calculation. The boundary conditions from RELAP5, were in a quasi steady-state condition during the time that the SCDAP calculation was conducted. Therefore these conditions were extrapolated where necessary to provide the necessary input for SCDAP. It was realized that the SCDAP core analysis could affect the system response (such as hydrogen generation increasing system pressure and changing inlet flow) and in many cases extrapolation of the required boundary conditions may not be valid and an iterative approach between RELAP5 and SCDAP would be necessary. In this case, however, the core inlet flow was very small and the enthalpy and pressure were changing slowly (pressure was held fairly constant due to SRV actuation) and consistently. Thus it was judged that the RELAP5 boundary conditions and the SCDAP calculated system conditions were sufficiently decoupled to provide a valid analysis, as described.

REFERENCES

C-1. G. A. Berna et al., *SCDAP/MOD1/VO: A Computer Code for the Analysis of LWR Vessel Behavior During Severe Accident Transients*, IS-SAAM-4-002, January 1984.

C-2. Browns Ferry Nuclear Plant Final Safety Analysis Report (FSAR), Tennessee Valley Authority.

C-3. R. J. Grossenbacker et al., *BWR/4 and BWR/5 Fuel Design*, Licensing Topical Report, NEDO-20944, Rev. 1, October 1976.

C-4. Systems Manual, Boiling Water Reactor, USNRC Inspection and Enforcement Reactor Training Center, Volume 1, Chapter 2, February 1980.

C-5. Supplemental Reload Licensing Submittal for Browns Ferry Nuclear Plant Unit 1 Reload No. 4, Y 1003J1A19 Rev. 0, March 1981.

APPENDIX D
FRAP-T6 CODE AND MODEL DESCRIPTION

APPENDIX D
FRAP-T6 CODE AND MODEL DESCRIPTION

During the plant automatic simulation described in Section 5.1, large power excursions were predicted. These excursions were caused by unthrottled flooding of the RPV by low pressure injection systems. In all, seven power spikes were predicted between 1275 and 2600 s in the transient. To determine the probability and extent of fuel damage during the power spikes, the FRAP-T6[D-1] code was used. Results of the code analysis were presented in Section 6.1.

This appendix presents a description of the FRAP-T6 code and input model. Also described are the boundary conditions used in the FRAP-T6 analysis.

1. FRAP-T6 Code Description

The FRAP-T6 computer code calculates the thermal and mechanical behavior of light water reactor fuel rods during a wide range of operational transients and hypothetical accidents. Models in the code calculate fuel and cladding temperature distributions, rod internal pressure, and elastic and plastic fuel and cladding deformation. These rod behavior areas are treated both as interdependent parameters and as functions of power, rod design, burnup, gap and surface heat transfer, and changes in material properties. In addition, such parameters as cladding oxidation, CHF, and conditions at cladding failure are calculated.

The user must input the initial rod geometry, coolant channel geometry and boundary conditions, and power history. If the rod has experienced prior burnup, initial conditions for a transient may be supplied through a data file from FRAPCON-2, the companion steady state fuel rod analysis program.

Several options are available to the user. The FRAP-T6 code is dimensioned to handle rod arrays of limited size, but currently no feedback is provided to account for subchannel interactions occurring as a result of coolant flow redistribution, cladding deformation, or fuel rod failure. An option is available by which uncertainties in fuel rod behavior are calculated due to uncertainties in fuel rod design, power, coolant, and material properties. In addition, choices can be made among several deformation, film boiling, and critical heat flux correlations. Also available is an option that calculates fission gas release.

2. FRAP-T6 Model

The FRAP-T6 model consisted of a single fuel rod, divided into 12 evenly spaced axial regions. Radially the rod was divided into 11 radial nodes, 9 in the fuel and 2 in the cladding. The radial power profile was obtained from the FLXDP[D-2] subcode and the axial power profile was obtained from Reference D-3. The fuel was UO_2, with a 95% theoretical density. The fill gas was helium. The rod was pre-pressurized to 44.0 psia (see Reference D-3).

For this calculation, the FRAP-T6 code was used with the FRACAS I cladding deformation model. With FRACAS I the stress induced deformation of the fuel pellet is ignored. This feature is more conservative than the FRACAS II model which allows for stress induced deformation of the cladding. FRACAS I was used due to convergence problems found in FRACAS II, when the cladding temperature exceeds 1000°F.

The following assumptions are found in the FRACAS I model:

- Increment theory of plasticity
- Prandtl-Reuss flow rule
- Isotropic work-hardening
- No low temperature creep deformation of cladding
- Thin wall cladding (stress, strain, and temperature uniform through cladding thickness)
- No axial slippage occurs at fuel cladding interface when fuel and cladding are in contact
- Bending strains and stresses in cladding are negligible
- Axisymmetric loading and deformation of cladding.

Deformation and stresses in the cladding in the open gap regime are calculated using a model which considers the cladding to be a thin cylindrical shell with specified internal and external pressures and a prescribed uniform temperature. Fuel cladding mechanical response is important since this mechanism effects heat transfer across the gap as well as providing information on cladding ballooning and failure. FRAPCON-2 (Reference D-4) provided the fuel conditions at the start of the transient. To be consistent with the SCDAP analysis, burnup was assumed to be one year.

The Carthcart oxidation model was used to predict cladding oxidation when cladding temperatures exceeded 1340°F. The no balloon and relocation options were used. The no balloon option based cladding failure on effective cladding plastic strain exceeding

instability strain. The relocation model used the FRACAS II fuel relocation and fuel thermal conductivity models with FRACAS I.

Additional input variables are shown on Table D-1.

3. Boundary Conditions

Power and thermal hydraulic boundary conditions are required as input to FRAP-T6. All of these boundary conditions were supplied by the RELAP5 analysis.

The specific thermal hydraulic conditions required were; heat transfer coefficient, system pressure, and coolant temperatures along the axial length of the rod. These conditions were available to the FRAP-T6 analysis from a data file at every RELAP5 time step.

Since rod failure was predicted during the first power excursion, only the first excursion was analyzed. The emphasis of this analysis was on qualitative rather than quantitative results, i.e., did these excursions cause rod failure and roughly to what extent. The first excursion was also the lowest power excursion, and if this excursion would cause failure any of the subsequent excursions would. The power input used in FRAP-T6 is shown in Figure D-1.

Table D-1. Additional input for the FRAP-T6 analysis

Parameter	Value
Pellet O.D., ft	0.03417
Clad thickness, ft	2.1×10^{-3}
Clad O.D., ft	0.0402
Pellet height, ft	0.03417
Fill gas	Helium
Burnup, MWD/MTU	10064
Plenum spring data:	
Number of coils	90
Spring height, ft	0.78
Coil diameter, ft	3.7×10^{-3}
Rod height, ft	12.5

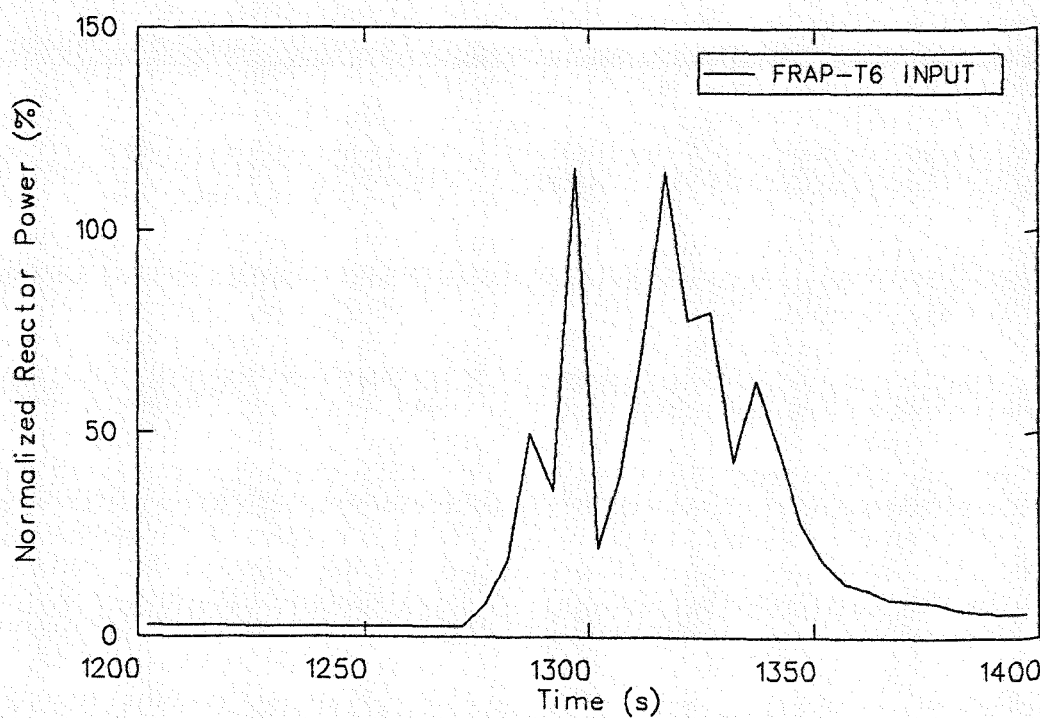

Figure D-1. FRAP-T6 input power.

REFERENCES

D-1. L. J. Siefken et al., *FRAP-T6: A Computer Code for the Transient Analysis of Oxide Fuel Rods*, NUREG/CR-2148, EGG-2104, May 1981.

D-2. J. A. Dearien et al., *FRAP-S: A Computer Code for Steady State Analysis of Oxide Fuel Rods, Vol. 1 - FRAP-S2 Analytical Models and Input Manual*, SRD-S2-76, January 1976.

D-3. R. J. Grossenbacker et al., *BWR/4 and BWR/5 Fuel Design*, NEDO-20944, Rev. 1, October 1976.

D-4. G. A. Berna et al., *FRAPCON-2: A Computer Code for the Calculation of Steady State Thermal-Mechanical Behavior of Oxide Fuel Rods*, NUREG/CR-1845, December 1980.